



Biochronology and evolution of *Pulleniatina* (planktonic foraminifera)

Paul N. Pearson, Jeremy Young, David J. King, and Bridget S. Wade

Department of Earth Sciences, University College London, Gower Street, London WC1E 6BT, UK

Correspondence: Paul N. Pearson (p.pearson@ucl.ac.uk)

Received: 13 May 2023 – Revised: 5 September 2023 – Accepted: 22 September 2023 – Published: 22 November 2023

Abstract. *Pulleniatina* is an extant genus of planktonic foraminifera that evolved in the late Miocene. The bottom and top occurrences of its six constituent morphospecies (*P. primalis*, *P. praespectabilis*, *P. spectabilis*, *P. praecursor*, *P. obliquiloculata*, *P. finalis*) provide a series of more or less useful constraints for correlating tropical and subtropical deep-sea deposits, as do some prominent changes in its dominant coiling direction and a substantial gap in its record in the Atlantic Ocean. Biostratigraphic information about these events has accumulated over many decades since the development of systematic deep-sea drilling in the 1960s, during which time the geochronological framework has evolved substantially, as have taxonomic concepts. Here we present new data on the biochronology of *Pulleniatina* from International Ocean Discovery Program Site U1488, which has a record of its entire evolutionary history from the centre of its geographic range in the Western Pacific Warm Pool. We then present and compare revised calibrations of 183 published *Pulleniatina* bioevents worldwide, with stated sampling errors as far as they are known, using a consistent methodology and in the context of an updated evolutionary model for the genus. We comment on the reliability of the various bioevents; their likely level of diachrony; and the processes of evolution, dispersal, and extinction that produced them.

1 Introduction

The history of life contains a series of events that have left traces in sedimentary successions which can be used for their correlation (biostratigraphy) and age dating (biochronology) (Bown et al., 2022). Planktonic foraminifera are one of the most widely used of all fossil groups for this purpose because of their exceptional fossil record, which also makes them model organisms for the study of evolution. Taxonomic and biostratigraphic studies developed in the early and mid-twentieth century (e.g. Subbotina, 1953; Bolli et al., 1957), after which the acceleration of scientific deep-sea drilling in the 1960s initiated a rapid and ongoing accumulation of information during which time biostratigraphic schemes were constantly tested, validated, modified and extended (see, for example, Blow, 1969, 1979; Kennett and Srinivasan, 1983; Bolli et al., 1985; Berggren et al., 1985a, b, 1995a, b; Wade et al., 2011). Such schemes undoubtedly work very well in practice, but when anomalies are encountered it can be challenging to trace data back to their source and to evaluate uncertainties, for example those arising from changing taxo-

nomic concepts and the reliability of calibrations to the geological timescale as understood at the time a biostratigraphic study was undertaken. Evaluating such uncertainties is necessary for improved biochronology and assessing the usefulness of individual events and the extent of their diachrony and for the study of evolution, dispersal and extinction. In this contribution we focus on *Pulleniatina*, one of several extremely abundant genera that are routinely used in planktonic foraminiferal biostratigraphic schemes for the Miocene to the Recent period. We have re-evaluated its biochronology as a prelude to a fundamental taxonomic review and revision of the genus. The current work consists of two parts, (1) an update of the biostratigraphic record of *Pulleniatina* from International Ocean Discovery Program (IODP) Site U1488 and (2) recalibration of *Pulleniatina* bioevents worldwide using a consistent methodology and timescale.

Living *Pulleniatina* is widely thought to consist of a single biospecies, *P. obliquiloculata* (Schiebel and Hemleben, 2017; Brummer and Kučera, 2022), albeit with several morphologically cryptic genotypes (Ujiié et al., 2012; André

et al., 2014; Ujiie and Ishitani, 2016). Plankton tow, sediment trap and geochemical data indicate that *P. obliquiloculata* tends to live in subsurface thermocline environments throughout the tropical oceans and in warm boundary currents where it can also be hugely abundant (e.g. Bé and Hutson, 1977; Jonkers and Kučera, 2015; Schiebel and Hemleben, 2017; Dang et al., 2018). It appears to be herbivorous, feeding on phytodetritus (Toué et al., 2022). It is comparatively rare outside the tropics and does not occur in the Red Sea or Mediterranean Sea (Thunell, 1979; Azibeiro et al., 2023), although there is a single record from the Aegean Sea, where it is regarded as invasive (Zenetos et al., 2008), and there are occasional documented occurrences in Mediterranean sediments (Serrano et al., 2007; Casalbore et al., 2010). Its failure to thrive in the Mediterranean and Red seas cannot be temperature-related because these are within its tolerance range; more likely it is related to the anomalous vertical salinity profile, stratification and deep plankton ecology that similarly affect several other deep-dwelling species (Azibeiro et al., 2023). The environmental sensitivity of the species is further underlined by the fact that it declined in abundance and then effectively disappeared from across the equatorial Atlantic and Caribbean during the last glacial cycle, reappearing in the Holocene (Prell and Damuth, 1978). Similar cold-climate-related *Pulleniatina minima* have been recorded in peripheral areas of its geographic range in the Pacific (Kuroshio Current region; Lin et al., 2006, and South China Sea; An and Jian, 2009) and Indian Ocean (Andaman Sea; Sijinkumar et al., 2011).

Like other planktonic foraminifera, *Pulleniatina* individuals secrete chambered shells made of calcium carbonate that sink through the water column and can accumulate in large numbers on the seafloor, along with other terrigenous and biogenic matter, forming thick deposits of gradually accumulating sediment. Its geographic distribution in seafloor sediments is similar to that in the water column except that it is not found in large areas of deep ocean because of carbonate dissolution (Siccha and Kucera, 2017; Fig. 1). Note that the map in Fig. 1 was plotted using software developed for the mikrotax website, and an interactive version is available online (https://www.mikrotax.org/system/ranges-ForCenSbiogeog.php?search=Pulleniatina_obliquiloculata&plotorder=ASC&scale=1&basemap=Gplatesbathymetry, last access: 14 November 2023).

After its origin, *Pulleniatina* populations evolved through areas of morphospace that taxonomists have broken down into a series of six named morphospecies (according to the taxonomy preferred here). These appear to belong to two separate lineages, one of which, the *P. primalis* – *P. praespectabilis* – *P. spectabilis* lineage, became extinct in the mid-Pliocene. The main lineage (comprising the morphospecies *P. primalis* – *P. praecursor* – *P. obliquiloculata* – *P. finalis*) is characterized by a tendency for relatively abrupt switches in the dominant coiling direction (e.g. Brönnimann

and Resig, 1971; Saito, 1976; Resig et al., 2001; Pearson and Penny, 2021), a phenomenon that can be traced back to its ancestor *Neogloboquadrina acostaensis* and beyond that to *N. continuosa* in the middle Miocene (e.g. King et al., 2023). The morphological succession and coiling direction history together constitute a series of bioevents with potential for stratigraphy and geochronology.

Pulleniatina species have frequently been used as formal index species in biozonation schemes. Banner and Blow (1965) described a *Globorotalia* (*G.*) *multicamerata* – *Pulleniatina obliquiloculata* (s.s.) Partial-Range Zone (“Zone N20”) for the stratigraphic interval characterized by the nominate species between the Top of *Dentoglobigerina altispira* and Bottom of *Globorotalia tosaensis*. This zone, modified by Blow (1969), was used quite frequently in the 1970s and 1980s. Lamb and Beard (1972) defined their *Pulleniatina obliquiloculata* Zone as the biostratigraphic interval in the Pliocene between the Top of *Globorotalia margaritae* and the Top of *Dentoglobigerina altispira*, and the *Pulleniatina finalis* Subzone as the interval from the Bottom of *Pulleniatina finalis* to the Bottom of “large forms of *Globorotalia tumida* sensu stricto”. Neither of these biozones has gained widespread use and the latter in particular is only locally applicable to the Caribbean Sea. Jenkins and Orr (1972) proposed an alternative *P. obliquiloculata* Zone defined as the biostratigraphic interval typified by the nominate taxon from the Top of “*Globigerinoides fistulosus*” (now *Globigerinoidesella fistulosa*) to the Recent period (see also Orr and Jenkins, 1980). This biozone is essentially the same as the “*Globigerinoides fistulosus* – *Globorotalia truncatulinoides* Interval Zone” of Berggren et al. (1995a, b), who gave it the alphanumeric designation “PT1” (for Pleistocene Zone 1), which was renamed the “*Globigerinoides ruber* Partial-Range Zone” (PT1) by Wade et al. (2011). Srinivasan and Kennett (1981) proposed a *Pulleniatina primalis* subzone (labelled “N17b” by them) between the Bottom of *P. primalis* and the Bottom of *Globorotalia tumida* (see also Perembo, 1994; Nathan and Leckie, 2003; Sinha and Singh, 2008). This is a viable biostratigraphic unit, at least for the tropical Indo-Pacific and could be revived in future to subdivide the long *Globorotalia plesiotumida*/*Globorotalia linguaensis* Concurrent Range Subzone (Subzone M13b) of Wade et al. (2011).

1.1 Biostratigraphic and biochronological principles

We follow the International Stratigraphic Guide (Salvador, 1994) in recognizing a fundamental distinction between the domains of rock and time, wherein biostratigraphy is essentially the science of what can be observed at the present day and biochronology is about what happened in the past. Accordingly, we distinguish between the observable Bottom and Top occurrence of a species in biostratigraphy and can only infer past bioevents such as the First Appearance Datum and Last Appearance Datum (FAD and LAD, respectively)

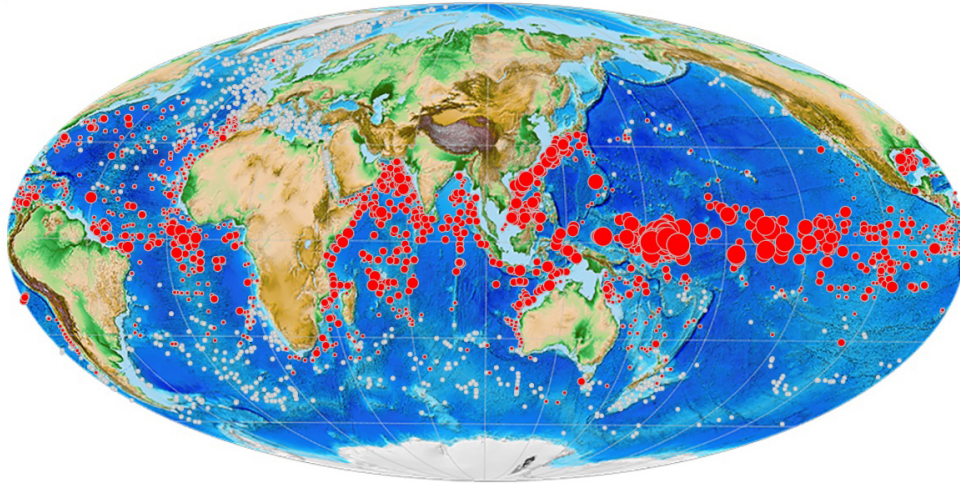


Figure 1. Global distribution of *Pulleniatina obliquiloculata* in modern seafloor sediments from the ForCenS database (Siccha and Kucera, 2017). Red circles indicate samples containing the species; diameter indicates abundance relative to other species. The smallest red circles indicate $< 1\%$ of the assemblage, while larger circles are scaled according to frequency. White circles indicate samples with planktonic foraminifer assemblages that lack *Pulleniatina*. Large blank areas in the subtropical oceans are areas where the seafloor is too deep and seawater too corrosive to preserve foraminifer shells.

of a species. To develop a deeper understanding of any individual bioevent and its potential diachrony, it is necessary to consider the evolutionary processes that gave rise to it, how long they may have operated and over what geographical area. Romer (1959) put this well when he remarked that fossils would be just as useful for biostratigraphers if they were distinctive assortments of nuts and bolts rather than organic remains but that an evolutionary context allows us to question the mechanisms that underlie their utility (see also Pearson, 1998, for discussion). For instance, the first global appearance of a named taxon may be caused by a gradual evolutionary transition from a pre-existing form (sometimes called a “pseudospeciation”) or a relatively sudden punctuated event; locally the appearance of the same taxon may be caused by dispersal and hence immigration. A species may start off rare and localized and only later become abundant and widespread. Similarly, the final disappearance of a named taxon may be the result of the evolution of one named form into another (“pseudoextinction”), which may be a slow or rapid process, or its lineage may have been completely extinguished (true extinction). In any single location, the disappearance may be a geographic range contraction (local extinction) that precedes the Last Appearance Datum elsewhere.

Fossils are unlike Romer’s nuts and bolts because they are not exact machine-tooled copies of one another. Foraminifer species may be extremely variable in form, through ontogeny, and because of genetic or ecophenotypic variability. They may vary along a spatial gradient (a “geographical cline”) and through time because of accumulated evolutionary changes (a “chronocline”). This makes cases of pseudospeciation and pseudoextinction especially problematic to

delimit and define in a consistent way. On a practical level, the taxonomy of planktonic foraminifera is guided by the principles of the International Code of Zoological Nomenclature (Ride et al., 2000) in which every “species”, with its formal Linnaean binomial, is typified by a unique name-bearing specimen that is set aside and curated as a prime exemplar. Taxonomic discovery is itself a historical and contingent process that involves principles of seniority and rules of objective or subjective synonymy. Biostratigraphers at work rarely have the luxury of fully describing the range of variation they see, so the subjective act of grouping specimens into named “species” based on similarity to type specimens can impose artificial divisions on what may be a morphological continuum. Fossil “species” are really morphospecies, often with rather arbitrary bounds, and cannot be assumed to represent objective biological or evolutionary entities (Pearson, 1998; Poole and Wade, 2019).

2 The *Pulleniatina* record at Site U1488

International Ocean Discovery Program (IODP) Site U1488 ($02^{\circ}02.59' N$, $141^{\circ}45.29' E$) is on the Eauripik Rise in the western equatorial Pacific at 2603 m water depth (Rosenthal et al., 2018e). A succession consisting mainly of clay-bearing foraminifer-rich nannofossil ooze was recovered during IODP Expedition 363 using the Advanced Piston Corer in multiple holes, penetrating over 300 m to upper Miocene sediments deposited around 10 million years ago. A high quality palaeomagnetic record exists back to the Matuyama/Gauss boundary at 2.610 Ma, below which the age model is based on planktonic foraminifer and nannofossil biostratigraphy (Rosenthal et al., 2018e). The siliciclastic component

of the lithology is strongly cyclic, and the site is expected to have an astronomically tuned timescale, although at the time of writing this work has yet to be completed. The site encompasses the entire evolutionary history of *Pulleniatina* with no known hiatuses. Its position in the core of the Western Pacific Warm Pool is in the centre of the geographic range of the genus, which occurs continuously in the sediment at high abundance. The site is just ~ 28 km northwest of Deep Sea Drilling Project (DSDP) Site 62 (Shipboard Scientific Party, 1971) where pioneering work on the taxonomy and biostratigraphy of *Pulleniatina* was previously conducted (Brönnimann and Resig, 1971; Brönnimann et al., 1971). For these reasons we have re-studied the site to improve on the shipboard biostratigraphy.

Shipboard planktonic foraminifer studies were conducted in Hole U1488A with a sampling density of four samples per core (approximately 3 m intervals or less) (Rosenthal et al., 2018e). We have re-studied the samples taken shipboard to record qualitative abundance variations of the six *Pulleniatina* morphospecies for the first time at the site and to complete the coiling ratio record for parts of the succession that were not originally studied. Biochronological ages are based on calibrations between a series of palaeomagnetic and biostratigraphic levels; these are considered preliminary because an astronomically tuned age model is to be expected in the future when detailed isotope records become available. All data are presented as a supplementary dataset available at the NERC Geoscience data centre (Pearson, 2023). Qualitative abundance fluctuations and stratigraphic ranges of the various morphospecies and the ancestral form *Neogloboquadrina acostaensis* alongside a record of the coiling direction ratios of *Neogloboquadrina* and *Pulleniatina* spanning the last ~ 9.5 Myr are shown in Fig. 2. Four prominent coiling ratio changes are highlighted by asterisks. This record provides a general picture of evolution in the genus over the whole time of its existence, albeit at relatively low sampling resolution that could be greatly improved with more detailed sampling of the succession. It reveals the picture at one site, but to establish how representative it is it is necessary to synthesize data from many other sites that has been produced over many years.

3 Recalibration of *Pulleniatina* bioevents from the published literature

3.1 Recalibration method

In this section, we focus on each biohorizon or bioevent in turn, recalibrating previously published biostratigraphic data to a common timescale (Raffi et al., 2020) taking into account the original sampling errors where known, and discuss the evolutionary mechanism that may have produced them. Calibrations from “rock” to “time” are of three types: astrochronological, magnetostratigraphical or biochronological (or occasionally a combination of the latter two).

Magnetostratigraphical calibrations are based on historical changes in the polarity (or, in principle, intensity) of the Earth’s magnetic field that can be recorded in sedimentary records via the alignment of magnetic mineral grains. Changes in polarity are generally quite rapid (lasting a few thousand years) and their expression in the sediment is potentially instantaneous, albeit subject to bioturbation and other sedimentary and diagenetic effects. Magnetic reversal timescales for the Neogene were previously based on seafloor magnetic anomalies arising from ocean ridge spreading, with the ages provided by radiometric dating of rocks of known stratigraphic position (e.g. Cande and Kent, 1995). Biohorizons are calibrated to magnetostratigraphy with reference to their known relative position in a given sedimentary succession, usually linear interpolation by depth between magnetic anomalies. This method has been used to date foraminiferal bioevents since the 1960s (e.g. Hays et al., 1969).

Astrochronological calibrations are based on estimating the age of an event from its depth in a sedimentary succession that has been “tuned” directly to a long-term orbital solution for Earth’s insolation. The current standard tuning target for the Neogene is the numerical solution of Laskar et al. (2004), which encompasses precession, obliquity and eccentricity variations (or, for longer intervals including the Paleogene, its improvement for eccentricity only by Laskar et al., 2011). The former was used to calibrate the Neogene period by Lourens et al. (2004). The tuning process is based on a statistical fit of cyclic signals in a sedimentary record that generally starts with the selection of a series of tie points that link distinctive cyclic features to the insolation target. The accuracy of an astronomically tuned age model obviously depends on judicious selection of tie points and the nature and fidelity of the cyclic signal as expressed in the sediment. The most stable orbital component is generally the long-term (~ 405 kyr) eccentricity cycle, but in many successions it is possible to tune to the shorter-term precession and obliquity signals (~ 21 and ~ 41 kyr). Any such age estimate may involve lags in the Earth system from the insolation forcing to its expression in a given sediment record, which may in turn be affected by bioturbation and other sedimentary variations such as short-term changes in sedimentation rate and hiatuses. It may also depend on the accuracy of high-precision inter-hole splicing as is commonly used to create composite depth scales at those sites recovered by overlapping hydraulic piston coring. For these reasons, historical astronomical age estimates are subject to revision that may result from changes in the inter-hole splice, the local astronomical tuning, or the orbital solution used. More recently, efforts have been made to align the magnetic reversal record to orbital chronology based on the identification of magnetic anomalies within orbitally tuned sedimentary records (e.g. Drury et al., 2017). The current Neogene magnetostratigraphy (Raffi et al., 2020) is the latest iteration of this approach, wherein its ages are in principle aligned to the orbital solution of Laskar

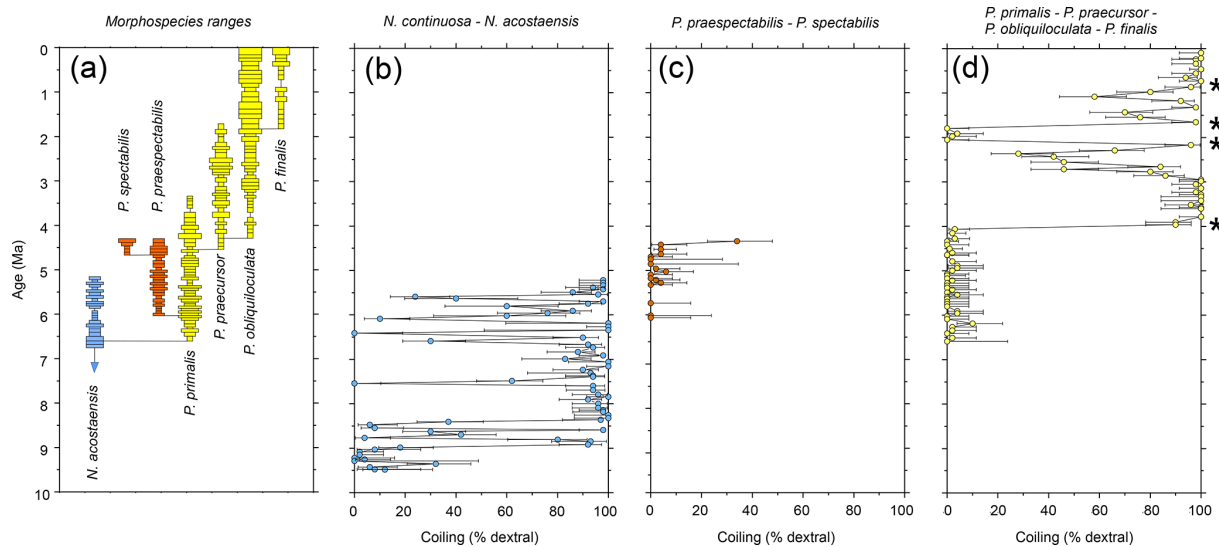


Figure 2. Biochronological and coiling record of the *Neogloboquadrina continuosa* – *acostaensis* lineage and the two *Pulleniatina* lineages at IODP Hole U1488A, western tropical Pacific Ocean. **(a)** Morphospecies range chart. Bars on spindle plots represent qualitative abundance by visual estimation relative to the whole planktonic foraminifer assemblage indicating, in order of decreasing width, “abundant” (> 20 % of the assemblage), “common” (> 10 %–20 %), “few” (> 5 %–10 %) and “rare” (< 5 %). **(b)** Coiling proportions of the ancestral *Neogloboquadrina continuosa* – *N. acostaensis* lineage. **(c)** Coiling proportions of the *Pulleniatina praespectabilis* – *P. spectabilis* lineage. **(d)** Coiling proportions of the *Pulleniatina primalis* – *P. praecursor* – *P. obliquiloculata*– *P. finalis* lineage. Asterisks represent coiling bioevents that are discussed further in the text. Error bars on coiling proportions are 95 % confidence intervals according to the modified Wald method. Timescale of Raffi et al. (2020).

et al. (2004). Because many updates and refinements to the magnetic polarity timescale have been made over the years, historical numerical age estimates obviously need to be interpreted with reference to the timescale then in use and updated accordingly.

The majority of deep-sea successions lack both an orbital age model and magnetostratigraphy and so need to be dated by biostratigraphy alone. Biochronological calibrations are those in which a given bioevent is dated with reference to other bioevents of known or assumed age in the same sedimentary succession, generally by linear interpolation. Major compilations of (sub)tropical planktonic foraminifer biochronologies have been published by Berggren et al. (1985a, 1995a, b), Wade et al. (2011) and Raffi et al. (2020), aligned against successively updated timescales. King et al. (2020) also included a table of age calibrations, some of which are updated from Raffi et al. (2020) following revisions of the inter-hole splices in several astronomically calibrated successions. Many of the age estimates within the compilations listed above are themselves indirect calibrations of this type, often with complex histories of their own, as will be discussed on a case-by-case basis for *Pulleniatina* below.

In principle, astrochronology is to be preferred over magnetostratigraphy, which is to be preferred over biochronology. This is because astrochronologies directly calibrate a sediment sample to time, whereas the other methods rely on

interpolations between events assuming sediment rate constancy (if the interpolations are linear) or smoothly changing sedimentation rates (if the age model is a spline fit, for example). Biochronologies are always secondary and indirect, in that in addition to making similar assumptions about sedimentation rate, they also assume known ages for adjacent bioevents separately calibrated elsewhere and that there is no diachrony between the sites of interest. In practice, however, an astrochronological calibration can easily be misaligned if the cyclic signal is weak or ambiguous. Similarly, it is quite possible that the sequence of magnetochrons is wrongly identified in a given section. Although in principle a cyclic signal in a given sedimentary sections may provide a unique astrochronological fingerprint, and the pattern of magnetic reversal durations over a long sedimentary succession might also be uniquely aligned to the global history, in practice most astrochronological or magnetostratigraphical age models begin with knowledge of biostratigraphy and are cross-checked against it.

In this contribution we review each bioevent in the most important successions where it has been recognized and recalibrate those data to the current timescale of Raffi et al. (2020) using a consistent and transparent methodology. Apart from the relatively few astrochronological calibrations, our method is to calibrate the age of the “target” bioevent by linear interpolation between (or occasionally extrapolation from) two selected “bracketing” magnetostratigraphical

or biochronological events of assumed age. In doing so we have reviewed the published stratigraphy of each site, avoiding intervals with severe reworking, dissolution, coring gaps, or other obvious issues that might obviously compromise the interpretation. We have incorporated the known sampling errors of the biostratigraphic data from the original study, even if it was not used in the original source (for instance, a Top occurrence is taken to be the midpoint between two samples, where known, not the topmost sample containing a particular morphospecies, as is sometimes reported). This applies to both the target event and the two bracketing events, producing a combined estimate of error. If the depth error on a magnetostratigraphic reversal is known, that is also incorporated in our calculation (see Wade et al., 2012, fig. 3, for a graphical representation of the linear calibration method which propagates the full errors from both bracketing events). Our method also allows in principle, and occasionally in practice, for age uncertainties in the bracketing events themselves to be propagated into secondary calibrations, although current timescales generally do not quote such errors. Wherever possible we have revisited the original data as tabulated in the source publications, and for those DSDP or Ocean Drilling Program (ODP) samples known only from their sample identification codes, the depths were determined from the online Laboratory Information Management System (LIMS) database (<https://web.iodp.tamu.edu/LORE/>, last access: 14 November 2023). For the older literature it has sometimes been necessary to measure data manually from published illustrations of stratigraphic ranges on which sampling errors are not indicated. Such calibrations have no quoted errors but may still be useful.

The various local calibrations of each bioevent are tabulated and then compared in summary correlation plots, generally ordered geographically by longitude or latitude as is deemed most informative. Such plots are then used to discuss the biochronology of each event. When calibrations align well within error between sites it is evidence of relative synchrony. Apparent misalignment on correlation plots is not sufficient evidence of diachrony, as is sometimes implicitly assumed in the literature, because it may have a variety of other causes, the most difficult being due to taxonomic issues in which different workers have applied different criteria for separating closely related morphospecies. This is a pertinent issue in the *Pulleniatina* group, in which morphospecies frequently intergrade, and which workers have subdivided in different ways, as is discussed on a case-by-case basis below. We applied a consistent approach to discriminating the various morphospecies when re-interpreting taxonomic subdivisions that differ from our own. Misalignment of bioevents may also be a sampling issue related to the identification of taxa that may only be present in low abundance in volumetrically limited samples, or that first or last occur as rare outliers on a broad morphological spectrum, or have spotty stratigraphic distributions where the “true” Top or Bottom occurrences could easily be missed. Simple misidentifica-

tion is also possible – for instance, members of the *Globocanella* group can be mistaken for *Pulleniatina* (Fenton et al., 2018). There are also a raft of issues relating to local preservation fidelity that may be sources of error such as dissolution, recrystallization, reworking, bioturbation, infiltration, and down-hole or laboratory contamination. And of course there are multiple potential problems with age models relating to changes in sedimentation rate, cryptic hiatuses, condensation, the bulking out of sedimentary sequences by ash bands or turbidites, and so on. Finally, for biochronologic calibrations, apparent misalignment or diachrony may just as well be a problem for one or other bracketing bioevent rather than the target. For these reasons, sites with anomalous calibrations were investigated with additional care and sometimes rejected or revised.

Mindful of the many sources of error, the possibility of diachrony in a bioevent can be considered. This is a subjective process because it requires weighing evidence of different quality and reproducibility from multiple sites in which there is an obvious preference for sedimentary successions with well-explained and well-illustrated taxonomies, good core recovery, and high-resolution sampling. Diachrony is most plausibly demonstrated when there is a clear geographic pattern, for instance, a progression in ages across latitudes or a clear difference between ocean basins or marginal seas. Sites which are local to one another or that sample the same overlying water mass are much less likely to be genuinely diachronous than those in different ocean basins or latitudinal provinces. Although this approach is time-consuming, we prefer it to a blind reliance on large databases or multivariate “optimization” methods because it is important to be able to track and critically evaluate all the constituent data. The correlation plots will be useful for guiding future investigators faced with curious or anomalous occurrences toward those published records where new primary observations or sampling are most desirable for improving the biochronology.

The final step in our investigation is to discuss the likely mechanisms behind each bioevent, attempting to distinguish genuine speciations and extinctions from taxonomic pseudospeciations and pseudoextinctions, dispersal events, range contractions, and global or regional genetic sweeps. Although biohorizons are generally encountered from top to bottom working down the hole, we here present the bioevents in the order they occurred from oldest to youngest because it makes most sense in an evolutionary context and for discussing the processes involved. We conclude with a revised interpretation of the evolutionary history of the genus and a top-down summary table.

3.2 FAD of *Pulleniatina primalis*

3.2.1 Biochronology

We report 27 recalibrations of this bioevent (Table 1, Fig. 3).

Table 1. Recalibrations of the FAD of *Pulleniatina primalis*. Note that Pacific (Pac.), Atlantic (Atl.) and Indian (Ind.) ocean samples are labelled as such in all relevant tables.

Reference	Location			Upper calibration event				Lower calibration event				Target event					
	Site	Physiographic feature	Grid reference	Event	Age (Ma)	Top constraint (m)	Bottom constraint (m)	Event	Age (Ma)	Top constraint (m)	Bottom constraint (m)	Top constraint (m)	Bottom constraint (m)	Age (Ma)	Calculated error + (Ma)	Calculated error - (Ma)	Plotted?
Chaisson and Pearson (1997)	ODP 925B	Ceara Rise, Atl.	04°12.25' N, 43°29.35' W	–	–	–	–	–	–	–	–	144.15	153.65	5.33	0.25	0.25	Y
Norris (1998)	ODP 959B	Ivorian Basin, Atl.	03°37.70' N, 02°44.10' W	Top <i>G. nepenthes</i>	4.38	59.09	60.59	Bottom <i>G. tumida</i> (Atl.)	5.82	86.09	87.59	62.59	64.09	4.567	0.080	0.080	–
Jenkins (1978)	DSDP 360	Cape Basin, Atl.	35°50.75' S, 18°05.79' E	Bottom <i>G. puncticulata</i>	5.15	98.50	102.38	Bottom <i>G. contomiozea</i>	7.89	150.08	165.00	123.09	127	6.331	0.333	0.275	Y
Routledge et al. (2020)	U1457D	Arabian Sea, Ind.	17°9.95' N, 67°55.80' E	Top <i>N. ampliflicus</i>	5.98	610.05	610.36	Bottom <i>N. ampliflicus</i>	6.82	628.34	629.53	615.500	621.360	6.349	0.151	0.144	Y
Routledge et al. (2020)	U1456D	Arabian Sea, Ind.	16°37.28' N, 68°50.22' E	Top <i>N. ampliflicus</i>	5.98	526.60	520.18	Bottom <i>N. ampliflicus</i>	6.82	552.55	555.47	520.18	534.05	6.082	0.139	0.102	Y
Podder et al. (2021); Farrell and Janecek (1991)	ODP 758A	Ninety East Ridge, Ind.	05°23.05' N, 90°21.67' E	C3n.4n	5.235	77.11	77.11	C3r	6.023	91.080	91.080	84.060	84.880	5.650	0.023	0.023	Y
Van Gorsel and Troelstra (1981)	Java	Solo River, Ind.	06°55' N, 111°14' E	Bottom <i>G. tumida</i> (Pac.)	5.57	510	520	S to D coiling in <i>N. acostaensis</i>	6.37	655.0	665.0	575	590	5.942	0.069	0.069	Y
Sinha and Singh (2008)	ODP 763A	Exmouth Plateau, Ind.	20°35.20' S, 112°12.50' E	C3n.4n	5.235	99.50	99.50	C3r	6.02	107.97	107.97	106.66	108.15	5.970	0.069	0.069	Y
Rosenthal et al. (2018a)	IODP U1482B	NW Australian Margin, Ind.	15°3.32' S, 120°26.10' E	Bottom <i>G. tumida</i> (Pac.)	5.57	260.01	262.90	N. <i>acostaensis</i> dex. To sin.	6.76	313.39	315.84	298.02	300.93	6.421	0.061	0.062	–
Nathan and Leckie (2003)	ODP 1143	South China Sea, Pac.	09°21.72' N, 113°17.11' E	Bottom <i>G. tumida</i> (Pac.)	5.57	224.07	228.30	Bottom <i>G. plesiotumida</i>	8.77	453.060	454.560	238.520	241.050	5.761	0.046	0.047	Y
Nathan and Leckie (2003)	ODP 1146A	South China Sea, Pac.	19°27.40' N, 116°16.37' E	Bottom <i>G. tumida</i> (Pac.)	5.57	321.41	322.88	Bottom <i>G. plesiotumida</i>	8.77	406.630	408.130	337.560	338.520	6.167	0.046	0.046	Y
Wang et al. (2020)	DSDP 296	Kyushu-Palau Ridge, Pac.	29°20.41' N, 133°31.52' E	Top <i>G. margaritae</i>	3.85	108.02	108.02	Top <i>G. nepenthes</i>	4.38	121.320	121.320	109.000	109.000	3.889	0.000	0.000	–
Rosenthal et al. (2018e); this study	IODP U1488A	Eauripik Rise, Pac.	02°02.59' N, 141°45.29' E	Top <i>N. ampliflicus</i>	5.98	174.99	177.15	Bottom <i>D. quinqueramus</i>	8.12	242.02	243.79	193.99	196.29	6.591	0.069	0.070	Y
Krashennikov and Hoskins (1973)	DSDP 200	Caroline Abyssal Plain, Pac.	12°50.2' N, 156°47.0' E	Bottom <i>G. tumida</i> (Pac.)	5.57	33.00	38.00	Bottom <i>G. plesiotumida</i>	8.77	47.5	49.000	39.500	47.700	7.603	1.211	1.597	–
Lam et al. (2022)	DSDP 586B	Ontong Java Plateau, Pac.	00°29.84' S, 158°29' E	Top <i>D. quinqueramus</i>	5.53	163.81	163.50	Bottom <i>A. primus</i>	7.45	197.100	198.600	189.210	190.710	7.007	0.074	0.071	Y

Table 1. Continued.

Reference	Site	Location		Upper calibration event				Lower calibration event				Target event		Plotted?			
		Physiographic feature	Grid reference	Event	Age (Ma)	Top con-straint (m)	Bottom con-straint (m)	Event	Age (Ma)	Top con-straint (m)	Bottom con-straint (m)	Top con-straint (m)	Bottom con-straint (m)		Age (Ma)	Calculated error + (Ma)	Calculated error - (Ma)
Chaiasson and Leckie (1993)	ODP 806B	Ontong Java Plateau, Pac.	00°19.1'N, 159°21.7'E	Bottom G. <i>lunida</i> (Pac.)	5.57	171.29	172.79	Bottom G. <i>plestonioida</i> (Pac.)	8.77	296	297.500	206.00	206.30	6.445	0.023	0.023	Y
Jenkins and Semivasan (1986); Barton and Bioemerdal (1986); this study	DSDP 587	Lansdowne Bank, Pac.	21°11.08'S, 161°19.99'E	C3n.1n	6.272	59.60	61.30	C3An.1r	6.386	65.450	67.080	65.905	67.405	6.394	0.030	0.031	Y
Expedition 320/321 Scientists (2010a); Wilkens et al. (2013); Tian et al. (2018)	IODP U1337A	Central equatorial Pac.	03°50.01'N, 123°12.36'W	Top tie	6.262	118.34	118.34	Bottom tie	6.742	129.210	129.210	122.220	127.150	6.542	0.109	0.109	Y
Expedition 320/321 Scientists (2010b); Wilkens et al. (2013); Drury et al. (2018)	IODP U1338A	Eastern equatorial Pac.	02°30.47'N, 117°58.16'W	Top tie	6.024	106.15	106.15	Bottom tie	6.098	108.510	108.510	106.130	108.240	6.056	0.033	0.033	Y
Keigwin (1982)	DSDP 503	Colombian Basin, Pac.	4°04.04'N, 95°38.21'W	C2Ar	4.180	94.00	94.00	Bottom G. <i>lunida</i> (Pac.)	5.57	134.550	139.700	160.20	167.75	6.435	0.273	0.242	Y
Lam et al. (2022)	DSDP 588	Lord Howe Rise, Pac.	26°06.7'S, 161°13.6'E	C3n.4n	5.235	96.25	97.75	C3An.1r	6.386	133.650	134.650	120.830	130.350	6.121	0.164	0.166	Y
Lam et al. (2022)	DSDP 590A	Lord Howe Rise, Pac.	31°10.02'S, 163°21.51'E	Bottom C. <i>rugosus</i>	5.08	171.76	173.26	Top D. <i>quinqueremus</i>	5.53	195.460	196.960	193.305	194.805	5.489	0.028	0.028	Y
Premoli Silva et al. (1993); Sager et al. (1993)	ODP 810C	Shatsky Rise, Pac.	32°25.40'N, 157°50.74'E	C3n.3r	4.997	70.4	70.4	C3n.4n	5.235	73.600	73.600	71.5	73	5.135	0.056	0.056	Y
Lam et al. (2022)	DSDP 591	Lord Howe Rise, Pac.	31°35.06'S, 164°26.92'E	Bottom C. <i>rugosus</i>	5.08	189.84	193.30	Top D. <i>quinqueremus</i>	5.53	212.140	215.140	212.020	220.450	5.583	0.115	0.117	Y
Lam and Leckie (2020)	ODP 1209A	Shatsky Rise, Pac.	32°39.10'N, 158°30.36'E	C1r.1n	1.076	14.22	14.22	C1r.3r	1.775	25.28	25.28	22.47	23.72	1.637	0.040	0.040	-
Lam and Leckie (2020)	ODP 1208A	Shatsky Rise, Pac.	36°07.63'N, 158°12.09'E	C2r.1n	2.155	101.01	101.01	C2r.2r	2.610	119.45	119.45	107.96	108.96	2.339	0.012	0.012	-
Lam and Leckie (2020)	ODP 1207A	Shatsky Rise, Pac.	37°47.43'N, 162°45.05'E	C3n.3r	4.997	96.84	96.84	C3n.4n	5.235	99.95	99.950	95.58	100.01	5.070	0.170	0.170	Y

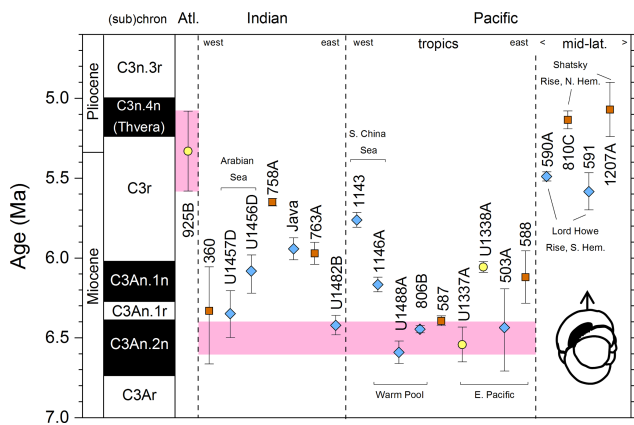


Figure 3. Biochronological constraints on the FAD of *Pulleniatina primalis*: gold circles are astrochronological, brown squares are magnetostratigraphical and blue diamonds are biochronological. Some anomalously young and old calibrations are omitted (see Table 1). DSDP Site 360 is grouped with the Indian Ocean because it samples the Agulhas outflow. The pink bands show the suggested Atlantic (5.33 ± 0.25 Ma) and tropical Indo-Pacific (6.50 ± 0.10 Ma) summary calibrations. The cartoon is a key to graphically illustrate the bioevent; in this instance the up arrow represents a FAD and the line diagram represents *P. primalis*.

Based mainly on its record in the Caribbean Sea and adjacent areas, *Pulleniatina* was initially thought to have a fossil record that extended down to the lower Pliocene as a single species, *P. obliquiloculata* (e.g. Bolli et al., 1957). Bandy (1963) extended the range into the upper Miocene in the Pacific sector. Banner and Blow (1967, p. 151) differentiated the genus into a series of morphospecies or subspecies including the first to evolve, *P. primalis*. They proposed that *P. primalis* was descended from “*Globorotalia (Turborotalia) acostaensis*” (now *Neogloboquadrina acostaensis*) because of similarities in morphology between the two species and their co-occurrence in sediments, as well as the existence of supposedly intermediate specimens from outcrops in Papua New Guinea. These samples were assigned biostratigraphically to the lower part of the Messinian stage of the upper Miocene, although the holotype specimen is from Pliocene sediments from Buff Bay, Jamaica (see King et al., 2020, for discussion of that section), and other figured specimens are from outcrop and exploration wells from the Pliocene of Venezuela. Although Banner and Blow (1967, p. 153) published a range chart showing the biostratigraphic distributions of the various morphospecies they recognized, those occurrences are not supported by sufficiently detailed sampling information to attempt a modern biochronological calibration. Nevertheless, their suggestion of a late Miocene origination of *Pulleniatina* from *Neogloboquadrina acostaensis* in the Indo-Pacific sector has received support from many subsequent studies.

In their study of DSDP Site 62 on Eauripik Rise in the western equatorial Pacific, Brönnimann and Resig (1971)

proposed a formal name for morphotypes intermediate between *acostaensis* and *primalis* of “*Pulleniatina praepulleniatina*”. Given that the holotype of *P. primalis* is a relatively “advanced” form, there is indeed scope to apply this taxonomic split, but we have not elected to do that because almost all subsequent workers have included such forms within a broad concept of *P. primalis*. Brönnimann and Resig’s (1971) study is very well documented, but unfortunately the timing of the evolutionary transition is difficult to constrain because of uncertainty in dating the lower part of the record at Site 62.

Belyea and Thunell (1984) performed the only morphometric study so far published of the *N. acostaensis* – *P. primalis* transition, an outline shape analysis of populations from below and above the Bottom of *P. primalis* at DSDP Site 214 on the Ninety East Ridge in the Indian Ocean. That study supports the close relationship between *N. acostaensis* and *P. primalis* but the stratigraphic control is insufficient to date the transition with precision. An additional problem is that the level of the reported biohorizon differs substantially between Belyea and Thunell (1984) and the subsequent record of Srinivasan and Chaturvedi (1992). The relevant interval at Site 214 requires more study before firm conclusions can be reached.

The earliest geochronological calibration for the Bottom of *P. primalis* to have propagated through the literature is from Keigwin (1982), who located the event in the extended stratigraphic interval between the Bottoms of *G. plesiotumida* and *G. tumida* (i.e. the combined interval of Subzone M13b and M14 as currently understood; Wade et al., 2011) at DSDP Hole 503A in the eastern equatorial Pacific. Unfortunately, the succession in Hole 503A is problematic because the palaeomagnetic record is uninterpretable in the lower part of the succession (Kent and Spariosu, 1982b) and there is little independent biostratigraphic control. Berggren et al. (1985a) cited Keigwin’s data as yielding a calibrated age of 5.8 Ma. Our own recalibration suggests it provides only a very broad constraint at a considerably older age (~ 6.4 Ma; see Table 1 and Fig. 3) because of subsequent changes to the timescale discussed below.

A series of sites was drilled on DSDP Leg 21 in the western Pacific, several of which contained *P. primalis* (Kennett, 1973). The Bottom of *P. primalis* at DSDP Sites 206 and 209 are in hiatuses. The best of these records is at DSDP Site 208 where it falls within the upper Miocene *Globorotalia conomiozea* Zone as then understood. However, it is difficult to provide a reliable biochronological calibration for that occurrence because of taxonomic uncertainties relating to *G. conomiozea* and *G. miotumida* as understood then and now, and their various calibration ages for those morphospecies in Northern Hemisphere and Southern Hemisphere temperate regions (discussed in Raffi et al., 2020). For that reason we have not attempted to recalibrate it here. Another transect was recovered in the same region during DSDP legs 89 and 90, which recorded the Bottom of *P. primalis* at several more sites (Jenkins and Srinivasan, 1986), two of which

(DSDP Sites 586 and 587) were in tropical latitudes. Srinivasan and Sinha (1991) used graphic correlation techniques to suggest an age of 5.80 Ma for the FAD of *P. primalis* at Sites 586 and 587, but the age control is difficult to interpret. Lam et al. (2022) recently provided updated age models and biostratigraphic data for these sites. Hole 586B on the Ontong Java Plateau provides a calibration (revised here from Lam and Leckie, 2020, to the timescale of Raffi et al., 2020) of 7.01 Ma based on nannofossil biostratigraphy, but this is affected by sedimentary complications in the lower part of the record and anomalous stratigraphic ranges. Hence, it is regarded as unreliable, especially as the age is much older than that reported at neighbouring Site 806 by Chaisson and Leckie (1993) (see Fig. 3), as discussed further below. At Site 587 on the Lansdowne Bank, Lam et al. (2022) offered a palaeomagnetic calibration of 7.14 Ma based on combining the biostratigraphy of Jenkins and Srinivasan (1986) with the palaeomagnetic record of Barton and Bloemendal (1986) on the timescale of Ogg et al. (2016). However, Barton and Bloemendal (1986) described the palaeomagnetic record at that site as poorly defined and their interpretation as being of low confidence. In particular, Barton and Bloemendal (1986, fig. 10) were not able to resolve the full magnetic reversal sequence in the Gilbert interval. An alternative interpretation of the anomaly sequence can be made by the simple expedient of shifting it one step younger such that the Base of Subchron C3An.2n becomes the base of C3An.1n and so on. This brings the record into much better agreement with biostratigraphy at the site and yields a revised calibration (preferred here) of 6.39 Ma (see Table 1, Fig. 3).

Chaisson and Leckie (1993) provided high-resolution biostratigraphic data across the Bottom of *P. primalis* at ODP Hole 806B (Ontong Java Plateau, western Pacific Ocean). Assuming an age of 5.80 Ma based on Berggren et al. (1985a), they found the event to be at approximately the expected level relative to other bioevents. However, the same data were recalibrated to 6.40 Ma by Berggren et al. (1995b). This large change in apparent age was the result of substantial revisions to the timescale, especially changes to the accepted ages of magnetochrons around the Miocene–Pliocene transition that arose from improved orbital chronology (Shackleton et al., 1990, 1995; see discussion in Berggren et al., 1995b). Berggren et al. (1995b) claimed simultaneous appearances for *P. primalis* in the tropical Indian and western Pacific oceans at 6.40 Ma based on the combined data of Srinivasan and Sinha (1992) and Chaisson and Leckie (1993). They also located the biohorizon to within Chron C3An.2n, but that was a secondary inference because no reliable magnetostratigraphy exists for the cited calibrations. This age estimate of Berggren et al. (1995b) was subsequently amended to 6.60 Ma by Wade et al. (2011) and 6.57 Ma by King et al. (2020) because of successive changes to the astronomical timescale by Lourens et al. (2004) and Drury et al. (2017).

Two relevant sites (ODP Sites 1143 and 1146) were drilled during ODP Leg 184 in the South China Sea, an area that is peripheral to what appears to be the main centre of evolution in the tropical Pacific. *Pulleniatina* is comparatively rare and discontinuous in the Miocene of that area in comparison to the central western Pacific (Li et al., 2005). These two sites produce younger and quite divergent ages, as recalibrated here from Nathan and Leckie (2003), suggesting that *Pulleniatina* may have been slow to disperse and thrive in the South China Sea.

Two more significant tropical Pacific sites were drilled during IODP Expedition 321. Shipboard data (Expedition 320/321 Scientists, 2010a, b) for these sites has been amended according to the revised composite depth scale by Wilkens et al. (2013) and astronomically tuned age models have been published by Tian et al. (2018) for IODP Site U1337 and Drury et al. (2018) for the relevant part of Site U1338. We recalibrated the shipboard biostratigraphic data to these age models using adjacent tie points. Site U1337, which is in the central Pacific, yields a tuned age consistent with the data in the western Pacific Warm Pool including Site U1488 discussed in Sect. 2 of this paper, but the sampling interval is relatively wide. Site U1338, on the other hand, yields a much younger age, as do other sites in the eastern Pacific (Fig. 3), where in general the stratigraphic record of *Pulleniatina* is patchy and at low relative abundance. It is noteworthy that the eastern tropical Pacific environment in the modern day is much more affected by equatorial upwelling and high productivity, with a less well-stratified water column, at least outside of El Niño events.

To summarize the situation in the tropical Pacific, the biochronological calibration at Site 586B is anomalous and can probably be discounted because of stratigraphic complications. The calibrations at Sites U1488 (see Sect. 2 above), 806, U1337 and 503 (the latter providing only a very broad constraint) are within error of each other. The palaeomagnetic calibration at Site 587 can be brought into line with these records by the reinterpretation of the anomaly sequence proposed herein. From these combined data we suggest a tropical Pacific calibration of 6.50 ± 0.10 Ma, which places the bioevent in Subchron C3An.2n. The best prospect for improved calibration is at Site U1488 where *Pulleniatina* is relatively abundant near the beginning of its range, an astrochronology is to be expected in due course and high-resolution sampling could be conducted.

Although the FAD of *P. primalis* may be more or less synchronous in the western tropical Pacific, it is evidently highly diachronous in the subtropics and mid-latitudes. Srinivasan and Sinha (1991) originally suggested this based on their interpretation of DSDP Leg 90 sites (DSDP Sites 588, 590 and 592), some of which were recalibrated by Lam et al. (2022) and are recalibrated again here using the same data to the timescale of Raffi et al. (2020). Wang et al. (2020) recorded a late FAD at DSDP Site 296 in the Kuroshio Current south of Japan, where *P. primalis* appears around 3.9 Ma

and then rapidly disappears (not plotted in Fig. 3). Additionally, Lam and Leckie (2020) produced three palaeomagnetic calibrations for FO *P. primalis* at sites on Shatsky Rise in the mid-latitude northern Pacific (ODP Holes 1207A, 1208A and 1209A). Two of those are anomalously young (see Table 1 and Fig. 3), and given that major diachrony across the area of Shatsky Rise is unlikely, they may indicate reworking or taxonomic issues relating to the distinction between *P. primalis* and sub-adult *P. obliquiloculata*, but that at ODP Hole 1207A in the Thvera subchron (C3n.4n) at 5.07 Ma may represent a local influx of the species into the area in the early Pliocene. This is supported by our recalibration of the biohorizon from ODP Hole 810C, also on Shatsky Rise, using the data of Premoli Silva et al. (1993) in combination with the palaeomagnetic record of Sager et al. (1993) which is also in the Thvera subchron (C3n.4n) at 5.14 Ma.

It is also possible that the FAD of *P. primalis* was diachronous into the Indian Ocean, despite earlier suggestions of synchrony with the Pacific (e.g. Berggren et al., 1995b; Singh, 1995). Sinha and Singh (2008) produced a new palaeomagnetic calibration based on their study at ODP Hole 763A (Exmouth Plateau off northwestern Australia at $\sim 20^\circ$ S) that placed the bioevent in the lower part of Subchron C3r (lower Gilbert), a significantly higher level than the tropical Pacific Ocean records discussed above. Site 763 is in a frontal region affected by the northward Western Australian Current, and it is possible that dispersal of *P. primalis* into the southern Indian Ocean was delayed, similar to peripheral and mid-latitude areas of the Pacific. We also note that the palaeomagnetic age interpretation for the lower part of the succession in Hole 763A (Tang, 1992) is questionable because of complications arising from at least one hiatus. Data from IODP Expedition 363 provided another calibration with reasonably tight constraints at tropical Indian Ocean IODP Hole U1482B (Rosenthal et al., 2018a). Routledge et al. (2020) have provided two calibrations for IODP Holes U1457D and U1456D in the eastern Arabian Sea and Podder et al. (2021) recorded the FAD at ODP Hole 758A in the eastern tropical Indian Ocean which is calibrated here against the magnetic reversal record of Farrell and Janacek (1991). Based on this combined information (Fig. 3), we suggest the tropical Indian Ocean may have been virtually synchronous with the Pacific but with the likelihood that there was diachrony to cooler water locations.

Various studies have recorded *Pulleniatina primalis* in the Atlantic sector, but its Bottom occurrence is always within the Pliocene at a much higher correlative level than the Indo-Pacific (e.g. Beckmann, 1972; Jenkins, 1978; Keigwin, 1982; Romine, 1986). Unfortunately, almost none of the Atlantic Ocean sites offer good opportunities for geochronological calibration because of site-specific issues such as hiatuses and incomplete recovery; hence, the bioevent has rarely been used for correlation there. The astronomical calibration of Chaisson and Pearson (1997, p. 28) of 5.33 ± 0.25 Ma (see Table 1 and Fig. 3) provides a very broad constraint but the

original low-resolution sampling could easily be improved in future. The calibration of Norris (1998) at ODP Site 959 is considerably younger, but *Pulleniatina* is rare there, probably because the site is affected by coastal upwelling.

3.2.2 Evolution

The distributions of *Neogloboquadrina acostaensis* and *Pulleniatina primalis* for 6–7 and 3–6 Ma in the Triton database (Fenton et al., 2021; Dunhill et al., 2021) are shown in Fig. 4, as plotted using software developed for this study and implemented at the mikrotax website, <https://www.mikrotax.org/system/ranges-tritonbiogeog.php> (last access: 11 November 2023). The ancestral species *Neogloboquadrina acostaensis* has a cosmopolitan distribution that spans all the ocean basins and extends into moderately high latitudes in both hemispheres but not the Southern Ocean (Fig. 4a and c). The evidence published to date indicates that *Pulleniatina primalis* speciated either as a peripheral isolate that re-established itself across the tropical Indo-Pacific (allopatric speciation) or in sub-populations spanning that area but certainly not across the entire geographic range of *N. acostaensis* (a form of parapatric speciation) (Fig. 4d). Our interpretation, based on our observations at IODP Site U1488, is that once established, *P. primalis* underwent rapid evolutionary change and that so-called “transitional” specimens between *N. acostaensis* and *P. primalis* that have occasionally been reported are more likely to be the earliest representatives of the *P. primalis* lineage, which Brönnimann and Resig (1971) referred to as *P. praepulleniatina*. Evidence for this is that such forms in the lowermost sample at Site U1488 containing *P. primalis* are predominantly sinistral but occur beside predominantly dextral *N. acostaensis* in the same samples, which appear morphologically unchanged in comparison to lower samples. This pattern suggests that a sub-population of *N. acostaensis* invaded a new ecological niche and quickly evolved to take advantage of it, transmuting into the form we call *P. primalis*. This change involved a marked increase in test size and the development of a more subspherical shape with chambers overhanging the umbilicus, as well as a shiny cortex that was distributed over most of the adult surface. The cortex, which is a relatively thin but compact layer of platy crystals that covers the pores (Lastam et al., 2023), is the defining feature of the genus *Pulleniatina*. The cortex was often only partially covering the external surface to begin with (Kennett and Srinivasan, 1983). The evident success of this new group seems not to have impacted the remaining *N. acostaensis*, which continued to thrive independently and apparently unchanged for over a million years. There is no evidence that the time of FAD *P. primalis* was in any way unusual climatically; for instance it postdates the late Miocene carbon isotope shift that occurs between 7 and 8 Ma.

Although new studies of historic Pacific DSDP Sites 200 and 586 would be required to confirm that the occurrences

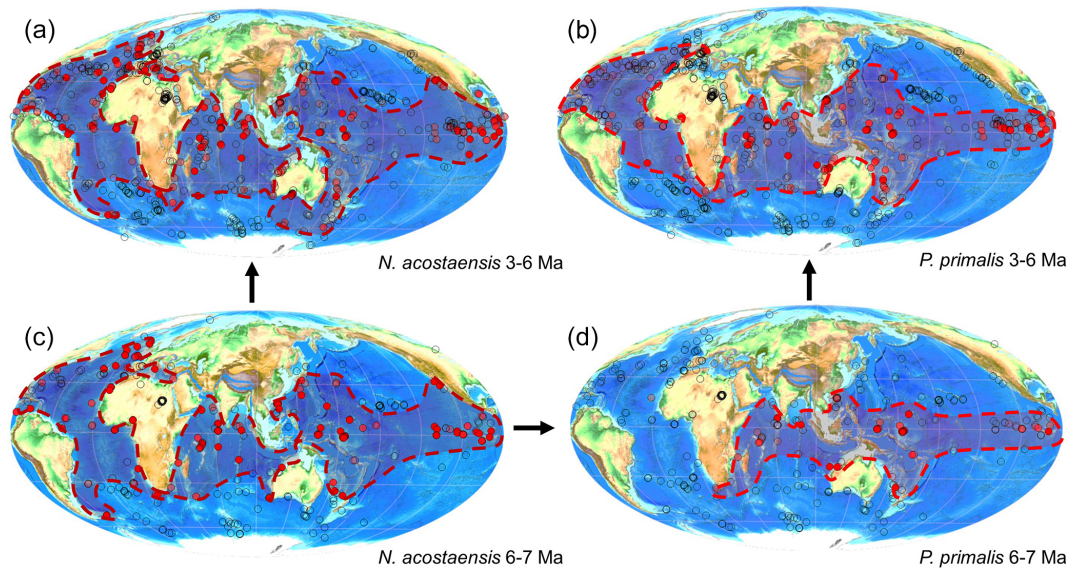


Figure 4. Geographic distribution of *Neogloboquadrina acostaensis* and *Pulleniatina primalis* according to the Triton database: (a) *N. acostaensis* 3–6 Ma, (b) *P. primalis* 3–6 Ma, (c) *N. acostaensis* 6–7 Ma and (d) *P. primalis* 6–7 Ma. Red circles indicate documented occurrences shaded according to the relative abundance of the species at the site. Dashed lines enclosing shaded areas are manually drawn around the known occurrences.

there are anomalous (see Table 1), *Pulleniatina primalis* probably evolved in the Western Pacific Warm Pool, the hottest area of the open ocean, around 6.55 Ma. This remains the area where *Pulleniatina* occurs at highest abundance (see Fig. 1). Its migration into peripheral basins and the middle southern and middle northern latitudes of the Pacific was diachronous and in low abundance (Srinivasan and Sinha, 1991; Li et al., 2005; Lam et al., 2022). The delayed appearance at Shatsky Rise (Premoli Silva et al., 1993; Lam and Leckie, 2020) may be related to an expansion of its geographic range along the Kuroshio Current extension. Its appearance in the Indian Ocean may have been rapid in favourable areas such as at IODP Site U1482, which samples the Indonesian Throughflow, but diachronous elsewhere.

Entry of the species into the Atlantic Ocean was certainly much delayed (Fig. 4b). An interesting exception is the record at DSDP Site 360 in the Cape Basin off South Africa, which is technically in the southern Atlantic, being west of Cape Agulhas, where Jenkins (1978) recorded discontinuous upper Miocene occurrences of *P. primalis*. It is likely that these populations were carried from the Indian Ocean by eddies originating in the warm Agulhas Current, but failed to thrive in the Atlantic. The only other Atlantic occurrence in the Triton database > 6 Ma is from DSDP Site 141 off western Africa (Beckmann, 1971), but this appears to be a database error because Beckmann's occurrences are all Pliocene. After 6 Ma, *P. primalis* became widely distributed across both the North and South Atlantic, including as far north as the southern United Kingdom (Jenkins et al., 1986) although it did not extend quite as far north and south as *N.*

acostaensis. Like modern *Pulleniatina* it was absent from the Mediterranean Sea where *N. acostaensis* is fairly common (Lirer et al., 2019). The factors that impeded the expansion of *Pulleniatina* into the Indian and Atlantic oceans, and the mid-latitudes, are as yet unknown, but may have related to stratification and food supply at depth. Detailed sampling and geochemical investigation may yield further insights into the pattern and process of speciation and dispersal.

3.3 FAD of *Pulleniatina praespectabilis*

3.3.1 Biochronology

We report five recalibrations of this bioevent (Table 2, Fig. 5).

Pulleniatina was regarded as monospecific (*P. obliquiloculata*) for several decades after being described by Cushman (1927). The first significant taxonomic change was made by Parker (1965), who described a form with an acute periphery as *P. spectabilis* from three Pacific cores taken by Scripps Institution of Oceanography. Parker suggested that *P. spectabilis* first appeared around the Miocene–Pliocene boundary, as then understood, and was a useful marker for the lower part of the Pliocene, at least in the Pacific Ocean. Banner and Blow (1967, p. 143) further noted that *P. spectabilis* had apparently become extinct within the Pliocene (see Sect. 3.8 below) and also described and illustrated morphological variants from New Guinea as transitional between *P. spectabilis* and its supposed ancestor, *P. primalis*. Brönnimann and Resig (1971) described the evolutionary transition from *P. primalis* to *P. spectabilis* at DSDP Site 62 on Eauripik Rise, western equatorial Pacific Ocean,

Table 2. Recalibrations of the FAD of *Pulleniatina praespectabilis*.

Reference	Location			Upper calibration event			Lower calibration event			Target event					
	Site	Physiographic feature	Grid reference	Event	Age (Ma)	Top con-straint (m)	Bottom con-straint (m)	Event	Age (Ma)	Top con-straint (m)	Bottom con-straint (m)	Age (Ma)	Calculated error + (Ma)	Calculated error - (Ma)	Plotted?
This study	IODP U1488A	Eauripik Rise, Pac.	02°02.59'N, 141°45.29'E	Top C. <i>armatus</i>	5.04	131.70	134.70	Top N. <i>am-plicifcus</i>	5.98	175	177.09	5.981	0.046	0.047	Y
Brönnimann et al. (1971)	DSDP 62	Eauripik Rise, Pac.	01°52.2'N, 141°56.3'E	Bottom G. <i>tumida</i> (Pac.)	5.57	143.99	145.49	Bottom P. <i>primalis</i>	6.43	212.08	213.58	5.901	0.039	0.037	Y
Kaushik et al. (2020)	ODP 807A	Ontong Java Plateau, Pac.	03°36.42'N, 156°37.49'E	Bottom G. <i>fitulosa</i>	3.85	66.00	66.00	Top G. <i>nepenthes</i>	4.38	92.91	93.22	5.227	0.011	0.011	Y
Chassignon and Leckie (1993)	ODP 806B	Ontong Java Plateau, Pac.	00°19.1'N, 159°21.7'E	Top G. <i>nepenthes</i>	4.38	111.00	112.80	Bottom G. <i>tumida</i> (Pac.)	5.57	171.29	172.79	5.436	0.030	0.030	Y
Expedition 320/321 Scientists (2010b); Wilkens et al. (2013); Drury et al. (2018)	IODP U1338A	Eastern equatorial Pac.	02°30.47'N, 117°58.16'W	Top tie	5.237	82.200	82.200	Bottom tie	5.539	91.140	91.140	5.318	0.092	0.092	Y

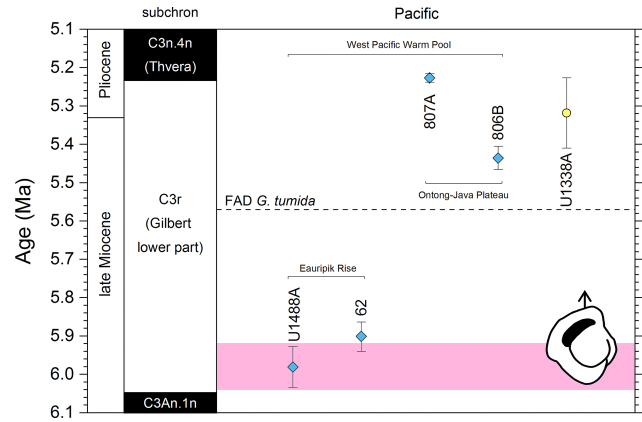


Figure 5. Biochronological constraints on the FAD of *Pulleniatina praespectabilis* in the Pacific Ocean, sites ordered west to east: the gold circle is astrochronological, and blue diamonds are biochronological. The pink band shows the suggested summary calibration of 5.98 ± 0.05 Ma.

and in the process named a new morphospecies, *P. praespectabilis*, to encompass intermediate forms that extended down well into the upper Miocene. Hence, in their taxonomy, which has become widely adopted, the evolutionary lineage spans the origin of two morphospecies at different times, first the transitional *P. praespectabilis* and then “fully developed” *P. spectabilis*.

In the relatively few studies that have recorded a Bottom occurrence for *P. praespectabilis* there is little agreement as to the stratigraphic level (see Table 2). In the type location, DSDP Site 62, Brönnimann and Resig (1971) and Brönnimann et al. (1971) recorded a level below the Bottom occurrence of *Globorotalia tumida*, which has been dated to 5.57 Ma in the Pacific (Raffi et al., 2020; King et al., 2020). Both Chassignon and Leckie (1993) at ODP Site 806 and Kaushik et al. (2020) at ODP Site 807 found the biohorizon at a higher level on the Ontong Java Plateau, within the range of *G. tumida*. Another site where the biohorizon was found is IODP Site U1338 in the eastern equatorial Pacific. Here we use the shipboard biostratigraphy (Expedition 320/321 Scientists, 2010b) and the modified splice of Wilkens et al. (2013) to produce an astronomical calibration based on the tuning of Drury et al. (2018). This provides a relatively broad constraint similar to the levels recorded on the Ontong Java Plateau.

Our study of the bioevent at IODP Site U1488 (Sect. 2 above) is on the Eauripik Rise close to (~ 28 km) the location of DSDP Site 62 where the morphospecies was first described (Brönnimann and Resig, 1971). The site benefits from excellent recovery with the Advanced Piston Corer, as opposed to DSDP Site 62, which was rotary cored and suffered drilling disturbance and incomplete recovery. Qualitatively, we find the transition from *P. primalis* to *P. praespectabilis* to involve two kinds of shape change that occur

at different stratigraphic levels: first, (going up core) an increasing acuteness of the periphery in some specimens, creating a subtriangular morphology in edge view and, second, a tendency for biconvexity associated with further peripheral acuteness. The distinction between the morphospecies could be made at either level but would be equally subjective in that populations always show a wide range of morphology and the characters of interest vary from chamber to chamber through ontogeny. Only by adopting a broad concept of *P. praespectabilis* can we find a Bottom occurrence close to (in fact slightly lower than) the equivalent stratigraphic level recorded by the authors of the species (Brönnimann and Resig, 1971). Both the Eauripik Rise and Ontong Java Plateau are in the Western Pacific Warm Pool and sampled similar water masses, and hence the reason for the discrepancy is likely taxonomic (i.e. where to draw a distinction between *P. primalis* and *P. praespectabilis*) and possibly preservational as the tests are susceptible to dissolution and fragmentation. In such instances the older calibration is preferred for a Bottom occurrence. Taking into account this consideration we propose a “global” calibration of 5.98 ± 0.05 Ma for the FO of *P. praespectabilis* (pink band in Fig. 5) based on the record at Site U1488, but we express low confidence in the biohorizon for accurate correlation.

3.3.2 Evolution

The FAD of *Pulleniatina praespectabilis* appears to be a gradual evolutionary transition, that is, a pseudospeciation. The morphological trend involved the gradual development of a more acutely curved periphery and biconvex shape among populations of *P. primalis*. Only at higher stratigraphic levels is it possible to observe a clear morphological separation between *P. primalis* and the *P. praespectabilis* – *spectabilis* lineage, implying that cladogenesis must have occurred sometime earlier. It is very difficult to pin down the timing of this separation – which is different in principle from the first occurrence of the morphospecies – without detailed morphometric studies that have yet to be conducted. Qualitatively, according to our own observations, the divergence of the lineages seems to follow a slowly bifurcating pattern, in contrast to the more discrete budding pattern of *P. primalis* from *N. acostaensis*. It is as if populations of *P. primalis* initially diversified in their new ecological niche and became quite variable in form and function before separating into two clearly distinct groups, one of which (the *P. praespectabilis* – *P. spectabilis* lineage) initiated a trend towards more angular morphologies. The fossil record of planktonic foraminifera contains many instances of evolutionary lineages which evolved more angular peripheries that led to anguloconical or flattened biconvex shapes with peripheral rims or keels (Cifelli, 1969; Norris, 1991). It may be that such trends are related to changes in the structure of the external pseudopodial network for feeding. In some instances the transitions seem to be associated with an increase

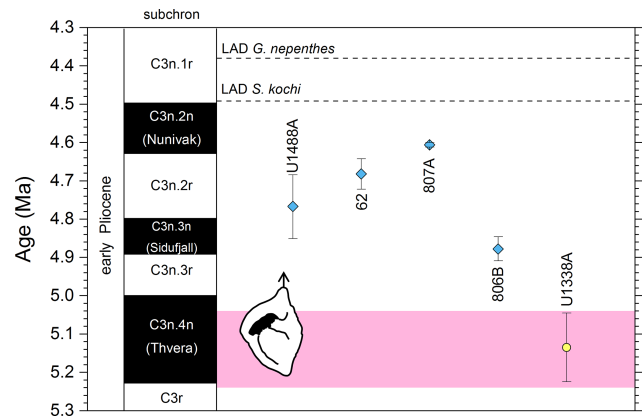


Figure 6. Chronological constraints on the FAD of *Pulleniatina spectabilis* in the Pacific Ocean arranged west to east: the gold circle is astrochronological, and the blue diamonds are biochronological. The pink band shows the suggested summary calibration of 5.14 ± 0.1 Ma.

in depth habitat, so changes in buoyancy related to shape, aspect ratio or shell volume may have been involved in driving such trends. Single-shell stable isotope analyses may eventually help test such hypotheses in the case of *P. praespectabilis* – *spectabilis*.

3.4 FAD of *Pulleniatina spectabilis*

3.4.1 Biochronology

We report five recalibrations of this bioevent (Table 3, Fig. 6).

As discussed in the previous section, the morphospecies *Pulleniatina praespectabilis* and *P. spectabilis* fully intergrade as part of a chronocline, the two being distinguished by apparently arbitrary criteria relating to the flattening of the spiral side and pinching of the periphery (Brönnimann and Resig, 1971). Nevertheless, *Pulleniatina spectabilis* is a very distinctive marker for a restricted stratigraphic interval in the lower Pliocene in the Pacific. Any attempt to date the FO of *P. spectabilis* must be from a study that also recognizes *P. praespectabilis* (which rules out, for instance, the records of Jenkins and Orr, 1972, and Orr and Jenkins, 1980, at DSDP Sites 77 and 83 in the eastern equatorial Pacific) and ideally it should be accompanied by an indication of how the taxa were separated. We follow Brönnimann and Resig (1971) by restricting our concept of *P. spectabilis* to forms with a distinctly pinched periphery. Useful biochronological markers in the interval are the LAD of the zone fossil *Globoturbotalita nepenthes*, which has been astronomically dated to 4.37 Ma (Chaisson and Pearson, 1997; King et al., 2020), and the LAD of *Sphaeroidinellopsis kochi*, astronomically dated to 4.53 Ma (Chaisson and Pearson, 1997; King et al., 2020).

In our new investigation in IODP Hole U1488A on the Eauripik Rise (Sect. 2 above) we locate the bioevent in a coring gap at a level that is consistent with neighbouring Site 62

Table 3. Recalibrations of the FAD of *Pulleniatina spectabilis*.

Reference	Location			Upper calibration event			Lower calibration event			Target event					
	Site	Physiographic feature	Grid reference	Event	Age (Ma)	Top constraint (m)	Bottom constraint (m)	Event	Age (Ma)	Top constraint (m)	Bottom constraint (m)	Age (Ma)	Calculated error + (Ma)	Calculated error - (Ma)	Plotted?
This study	IODP U1488A	Eauripik Rise, Pac.	02°02.59'N, 141°45.29'E	Top <i>Sphelolithus</i>	3.54	89.9	91.56	Top <i>C. armaratus</i>	5.04	131.70	134.70	4.615	0.076	0.074	Y
Brönnimann et al. (1971)	DSDP 62	Eauripik Rise, Pac.	01°52.2'N, 141°56.3'E	Top <i>S. kochi</i>	4.49	102.00	103.00	Bottom <i>G. tumida</i> (Pac.)	5.57	143.99	145.49	4.682	0.040	0.039	Y
Kaushik et al. (2020)	ODP 807A	Ontong Java Plateau, Pac.	03°36.42'N, 156°37.49'E	Bottom <i>G. fistulosa</i>	3.85	66.00	66.00	Bottom <i>G. tumida</i> (Pac.)	5.57	136.17	136.47	4.606	0.006	0.006	Y
Chaisson and Leckie (1993)	ODP 806B	Ontong Java Plateau, Pac.	00°19.1'N, 159°21.7'E	Top <i>G. nepenthes</i>	4.38	111.00	112.80	Bottom <i>G. tumida</i> (Pac.)	5.57	171.29	172.79	4.877	0.031	0.031	Y
Expedition 320/321 Scientists (2010b); Wilkens et al. (2013); Drury et al. (2018)	IODP U1338A	Eastern equatorial Pac.	02°30.47'N, 117°58.16'W	Top tie	5.000	76.40	76.40	Bottom tie	5.237	82.200	82.200	5.135	0.089	0.089	Y

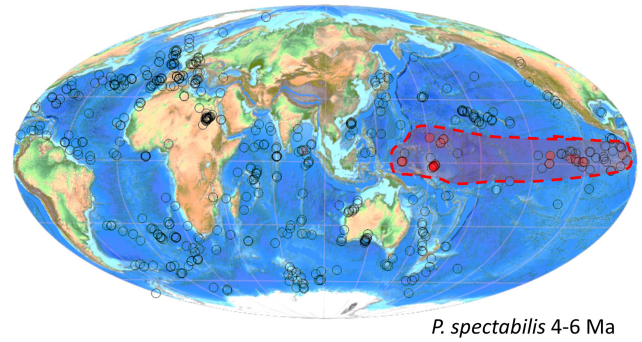


Figure 7. Biogeographic distribution of *Pulleniatina spectabilis* between 4 and 6 Ma from the Triton database. The dashed lines enclosing the shaded area were manually drawn around the known occurrences.

where the transition from *P. praespectabilis* was first described (Brönnimann and Resig, 1971). However, other studies have found the biohorizon at a lower level, most notably at Hole U1338A by Expedition 320/321 Scientists (2010b), where we have converted the shipboard data to an astronomical calibration using the tuning of Drury et al. (2018). While it is possible that the transition to the *P. spectabilis* morphospecies occurred in a time-transgressive manner, we think it more likely that discrepancies have arisen between authors in placing the arbitrary transition. We suggest a calibration age of 5.14 ± 0.1 Ma (pink band in Fig. 6) based on the record at Hole U1338A but record the bioevent as having low correlation potential, at least until morphometric data are available.

3.4.2 Evolution

The evolution of *P. spectabilis* appears to have been through continuation of the trend towards more acute peripheries among populations of *P. praespectabilis*, which eventually resulted in a more “advanced” pseudocarinate form that is conventionally described as *P. spectabilis*; nevertheless, populations containing *P. spectabilis* always contain specimens that are referable to *P. praespectabilis*, as would be the earlier ontogenetic stages of undoubted *P. spectabilis*. Only one record exists outside of the Pacific, namely at ODP Hole 758A in the tropical Indian Ocean where two occurrences are recorded in the supplementary data table of Podder et al. (2021), but there are no illustrations to support the reported occurrence. The species has not been reported from the South China Sea or Kuroshio Current region (Fig. 7). The ancestral form, *P. praespectabilis*, is rare in the Indian Ocean but has been described from DSDP Site 219 in the Arabian Sea (Fleisher, 1974, p. 1031) and on the northwestern Australian shelf at IODP Site U1482 (Rosenthal et al., 2018a). The evolution of *P. spectabilis* therefore seems to have been accompanied by a progressive geographic range restriction. Srinivasan and Sinha (1998, 2000) have argued that this may be related to the gradual restriction of the Indonesian

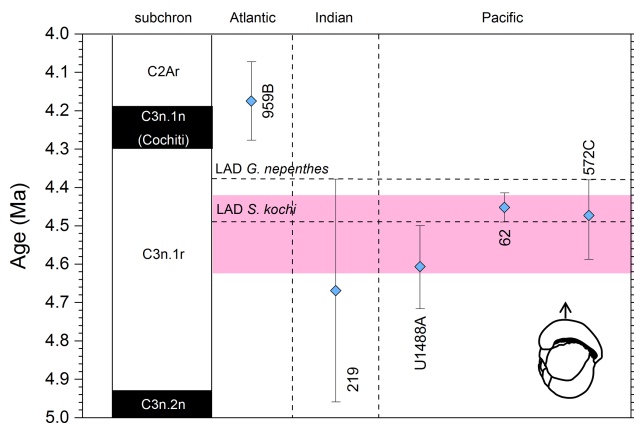


Figure 8. Biochronological constraints on the FAD of *Pulleniatina praecursor* in the Pacific Ocean. Blue diamonds represent biochronological calibrations. The much older calibration of Sinha and Singh (2008) is not shown. The pink band shows the suggested summary calibration of 4.52 ± 0.10 Ma.

Throughflow through the late Miocene and Pliocene associated with northward movement of the Australian plate and shallowing of the sills. This is an attractive idea because of the alleged deep-dwelling habitat of *P. spectabilis*. However, we note that *P. spectabilis* is isotopically similar to co-occurring *P. primalis* (data in Boscolo-Galazzo et al., 2022), which, like other deep-dwelling species, is not itself similarly restricted to the Pacific. Hence, there may also be an element of ecological specialization involved in the geographic restriction, reminiscent of the way in which the modern Type IIa genotype of *P. obliquiloculata* is restricted to the warmest areas of the Pacific (Ujiié et al., 2012; Ujiié and Ishitani, 2016).

3.5 FAD of *Pulleniatina praecursor*

3.5.1 Biochronology

We report eight recalibrations of this bioevent (Table 4, Fig. 8).

Between the FAD of *P. spectabilis* (~ 4.93 Ma) and the first major coiling change in the *Pulleniatina* lineage (see Sect. 3.8 below) there is an interval of ~ 850 kyr in which three *Pulleniatina* bioevents occurred (according to most records), namely the FAD of *P. praecursor* (this section), the FAD of *P. obliquiloculata* (Sect. 3.6) and the LAD of *P. spectabilis* (Sect. 3.7). Precise dating of these events is currently problematic because of a lack of good sections with palaeomagnetic age control. When Banner and Blow (1967) revised the taxonomy of *Pulleniatina*, they recognized a long-term chronocline from relatively small, trochospiral morphotypes (*Pulleniatina primalis*) to larger more irregularly coiled forms (*P. obliquiloculata* and *P. finalis*; see below for discussion) and designated an intermediate form as the subspecies *P. obliquiloculata praecursor*. Most modern

workers recognize this as a distinct morphospecies, *P. praecursor*, distinguished by an aperture that extends to the periphery, although some authors include it within an expanded concept of *P. primalis* (Parker, 1965; Kaneps, 1973; Orr and Jenkins, 1980), some within *P. obliquiloculata* (Chaisson and Leckie, 1993; Chaisson and Pearson, 1997) and others simply omit it from their taxonomy (e.g. Lam and Leckie, 2020; Groeneveld et al., 2021; Podder et al., 2021).

Although *P. praecursor* is characteristic of upper Pliocene to lower Pleistocene assemblages, its Bottom occurrence is of limited use for correlation because it appears by gradual transition. Banner and Blow (1967) placed the event in the lower Pliocene, about half way through the range of *P. spectabilis* and not far below the Bottom of *P. obliquiloculata* based on their unpublished data from Ecuador, Java and Borneo. Brönnimann and Resig (1971) and Brönnimann et al. (1971) placed it just above the Top of *Sphaeroidinellopsis kochi*, at a similar level to that implied by Banner and Blow (1967). Saito (1985) recorded a single rare occurrence at a correlative level in DSDP Hole 572C. Our own observations at IODP Hole U1488A, where the morphospecies is continuously present, are in good agreement with this level (Sect. 2 above). In contrast, however, Hays et al. (1969) placed the event below the Bottom of *P. spectabilis* in Piston Core V24-59 (extending its range to the bottom of the record in that core, so no calibration is possible). Singh (1995) and Sinha and Singh (2008) also placed the event at a much lower level, within the lower Gilbert reversed interval (Chron C3r) at ODP Hole 763A. The only Atlantic calibration is that of Norris (1998), who recorded it at a significantly younger level than the rest, but the occurrences are patchy at that site. Although the event may be diachronous (Singh et al., 2021), that is difficult to evaluate without assuming taxonomic consistency and repeatability between studies. From the combined information we tentatively suggest a “global” calibration of 4.52 ± 0.10 Ma. The biohorizon is, however, of limited utility because it is a subjective morphological transition.

3.5.2 Evolution

The FAD of *P. praecursor* appears to be another example of a pseudospeciation, with the morphospecies differentiated from *P. primalis* by arbitrary shape criteria (most importantly, an aperture that extends to the periphery). As yet there is no good evidence that it involved cladogenesis (lineage splitting) although no detailed morphometric work has yet been conducted to test this.

3.6 FAD of *Pulleniatina obliquiloculata*

3.6.1 Biochronology

We report seven recalibrations of this bioevent (Table 5, Fig. 9).

When Banner and Blow (1967) recognized a long-term *Pulleniatina* chronocline, which they divided into several

Table 4. Recalibrations of the FAD of *Pulleniatina praecursor*.

Reference	Location		Upper calibration event				Lower calibration event				Target event						
	Site	Physiographic feature	Grid reference	Event	Age (Ma)	Top con-straint (m)	Bottom con-straint (m)	Event	Age (Ma)	Top con-straint (m)	Bottom con-straint (m)	Top con-straint (m)	Bottom con-straint (m)	Age (Ma)	Calculated error + (Ma)	Calculated error - (Ma)	Plotted?
Norris (1998)	ODP 959B	Ivorian Basin, All.	03°37.70' N, 02°44.10' W	Top <i>G. margaritae</i>	3.83	51.09	52.54	Top <i>G. nepenthes</i>	4.38	59.09	60.59	56.09	57.59	4.174	0.102	0.102	Y
Gupta and Thomas (1999)	DSDP 219	Arabian Sea, Ind.	09°01.75' N, 75°52.67' E	Top <i>G. nepenthes</i>	4.38	48.45	49.95	Bottom <i>S. dehiscentes</i>	5.54	54.44	55.94	49.94	51.44	4.669	0.290	0.290	Y
Sinha and Singh (2008)	ODP 763A	Exmouth Plateau, Ind.	20°35.20' S, 112°12.50' E	C3n.4n	5.235	99.50	99.50	C3r	6.023	107.97	107.97	99.69	100.63	5.296	0.044	0.044	–
This study	IODP U1488A	Eauripik Rise, Pac.	02°02.59' N, 141°45.29' E	Top <i>Sphenolithus</i>	3.54	89.9	91.56	Top <i>G. nepenthes</i>	4.38	158.30	59.09	60.59	118.70	4.174	0.102	0.102	Y
Brönnimann et al. (1971)	DSDP 62	Eauripik Rise, Pac.	01°52.2' N, 141°56.3' E	Top <i>S. kochi</i>	4.49	102.00	103.00	Bottom <i>G. tumida</i> (Pac.)	5.57	143.99	145.49	100.00	102.000	4.452	0.038	0.038	Y
Perebo (1994)	ODP 832	Aoba Basin, Pac.	14°47.78' S, 167°34.35' E	C3n.4n	5.235	766.4	766.6	C3r	6.023	808.5	809.5	801.300	803.750	5.903	0.031	0.031	–
Premoli Silva et al. (1993); Sager et al. (1993)	ODP 810C	Shatsky Rise, Pac.	32°25.40' N, 157°50.74' E	C2r.2r	2.610	38	38	C2An.1n	3.032	46.300	46.300	45.15	47.00	3.021	0.047	0.047	–
Saito (1985)	DSDP 572C	Eastern equatorial Pac.	01°26.09' N, 113°50.52' W	Top <i>G. nepenthes</i>	4.38	63.60	65.10	Bottom <i>G. tumida</i> (Pac.)	5.57	86.53	93.4	65.10	67.590	4.473	0.114	0.093	Y

Table 5. Recalibrations of the FAD of *Pulleniatina obliquiculata*.

Reference	Site	Location Physiographic feature	Grid reference	Upper calibration event				Lower calibration event				Target event		Plotted?			
				Event	Age (Ma)	Top con- strait (m)	Bottom con- strait (m)	Event	Age (Ma)	Top con- strait (m)	Bottom con- strait (m)	Top con- strait (m)	Bottom con- strait (m)		Age (Ma)	Calculated error + (Ma)	Calculated error - (Ma)
Weaver and Raymo (1989)	ODP 667A	Sierra Leone Rise, Atl.	04°34.15' N, 21°54.68' W	Top D. <i>adlispira</i>	3.47	18.06	20.15	Top G. <i>nepenthes</i>	4.38	63.2	66.2	47.79	52.9	4.093	0.079	0.077	Y
Simha and Singh (2008)	ODP 763A	Exmouth Plateau, Ind.	20°35.20' S, 112°12.50' E	C2An.2r	3.330	67.80	67.80	C2An.3n	3.596	81.5	81.5	71.51	72.16	3.408	0.006	0.006	Y
This study	IODP U1488A	Eauripik Rise, Pac.	02°02.59' N, 141°45.29' E	Top <i>Sphenolithus</i>	3.54	89.9	91.56	Top C. <i>arnatus</i>	5.04	131.70	134.70	109.00	110.47	4.211	0.067	0.065	Y
Kaushik et al. (2020)	ODP 807A	Ontong Java Plateau, Pac.	03°36.42' N, 156°37.49' E	Top D. <i>adlispira</i>	3.47	56.15	56.59	Top G. <i>nepenthes</i>	4.38	92.91	93.22	85.0	85.3	4.184	0.008	0.008	Y
Pereumbo (1994)	ODP 832	Aoba Basin, Pac.	14°47.78' S, 167°34.35' E	C2r.2r	2.581	724.5	725.0	C2An.1n	3.032	740.6	740.8	733.0	734.0	2.828	0.019	0.019	Y
Hays et al. (1969)	Y24-59	Central equatorial Pac.	02°34' N, 145°32' W	C2r.2r	2.610	7.35	7.35	C2an.1n	3.032	8.69	8.69	8.50	8.50	2.972	0.000	0.000	-
Expedition 330/331 Scientists (2010a); Wilkens et al. (2013); Tian et al. (2018)	IODP U1337A	Eastern equatorial Pac.	03°50.01' N, 123°12.36' W	Top tie	1.966	28.99	28.99	Bottom tie	3.039	44.950	44.950	35.31	38.31	2.492	0.101	0.101	-

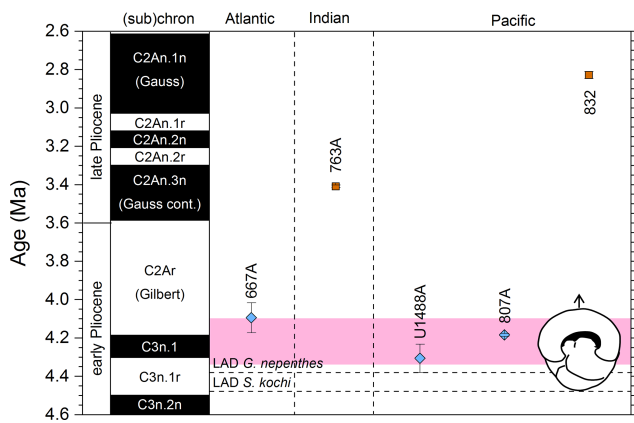


Figure 9. Biochronological constraints on the FAD of *Pulleniatina obliquiloculata*. Brown squares are magnetostratigraphic, and blue diamonds are biostratigraphic. The pink band shows the suggested summary calibration of 4.22 ± 0.12 Ma.

morphospecies, they necessarily restricted the concept of *P. obliquiloculata*; hence, to calibrate FAD *P. obliquiloculata* sensu stricto it is necessary to consider only those studies that recognize both *P. obliquiloculata* and its predecessor in the bioseries, *P. praecursor*, as distinct forms. Even in those circumstances, much subjectivity is required in separating the morphospecies. Banner and Blow (1967, fig. 14) placed the Bottom of *P. obliquiloculata* at around the same level as the Top of “*Globigerina*” (= *Globoturborotalita nepenthes*) in the middle of their Zone N19 (the biostratigraphic interval between the Bottom of *Sphaeroidinella dehiscens* and the Top of *Dentoglobigerina altispira*). They noted that this level was found in both the Caribbean–Atlantic province (Bowden Formation at Jamaica) and in the Indo-Pacific (Sarmi Formation of West Papua; Banner and Blow, 1967, p. 139), but they did not publish their biostratigraphic data, so no recalibration is possible. Our own calibration at IODP Hole U1488A (Sect. 2 above) accords with the level originally suggested by Blow and Banner (1967), although various other authors have recorded the biohorizon at higher levels. We attribute the substantial differences in calibration age in the various studies (Fig. 9) to subjectivity arising from the distinction of the two morphospecies and the patchy record at sites such as ODP Site 832. We suggest a global calibration of 4.22 ± 0.12 Ma for the original species concept based on harmonizing the records from in Holes 667A, U1488A and 807A (pink band in Fig. 9).

3.6.2 Evolution

The main distinguishing feature of the *P. obliquiloculata* morphospecies is the distinctly “streptospiral” (irregular) coiling mode (Banner and Blow, 1967). Although no morphometric studies have yet been conducted, our impression is that the degree of streptospirality increases up core, and thus

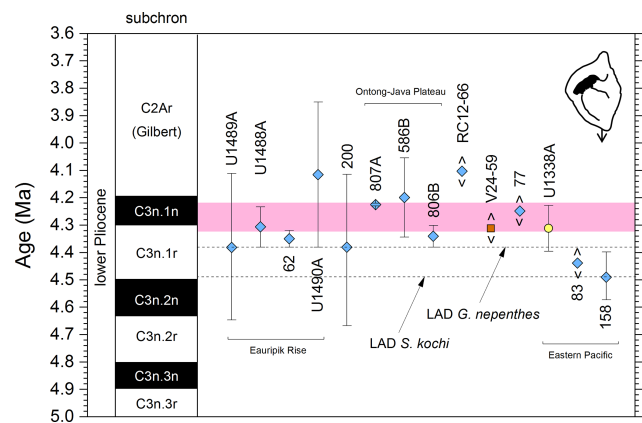


Figure 10. Biochronological constraints on the LAD of *Pulleniatina spectabilis* ordered from west to east across the Pacific: the gold circle is astrochronological, the brown square is magnetostratigraphic and the blue diamonds are biostratigraphic. Chevrons are for calibrations with no known sampling error. The pink band shows the suggested summary calibration of 4.27 ± 0.05 Ma based on harmonizing multiple sites.

the proportion of noticeably streptospiral tests assignable to the *P. obliquiloculata* morphospecies also increases. The change in spire height is accompanied by the development of larger more globular chambers and a reduction in the number of chambers per whorl, resulting in an overall more subspherical shape for the adult test. The possible ecological significance of these shape changes is unknown.

3.7 LAD of *Pulleniatina spectabilis*

3.7.1 Biochronology

We report 14 recalibrations of this bioevent (Table 6, Fig. 10).

The earliest calibration of this event is by Hays et al. (1969) from “Vema” Piston Core V24-59 as cited in the compilations of Berggren et al. (1985a, b) and Wade et al. (2011). This remains the only palaeomagnetic calibration because all other sites in the equatorial Pacific lack interpretable magnetostratigraphy through this interval. Berggren et al. (1995b) stated that the event is in the top of the Cochiti subchron (i.e. C3n.1n), but this appears to be an error because it is indicated by Hays et al. (1969) close to the top of the reversed interval below that (i.e. C3n.1r) at a level distinctly above the Top of *Globoturborotalita nepenthes*. However, like other early studies, there are no associated data, so the sampling interval is unknown and the recalibration is made here from the published figure (Hays et al., 1969, fig. 6) (see Table 6 and Fig. 9). It may be that the true level is indeed in lower C3n.1n.

Pulleniatina spectabilis was recorded and illustrated by Jenkins and Orr (1972) from DSDP Site 77 in the eastern equatorial Pacific, although it does not appear on the range chart for that site (Shipboard Scientific Party, 1972). Our

Table 6. Recalibrations of the LAD of *Pulleniatina spectabilis*.

Reference	Site	Location	Physiographic feature	Grid reference	Event	Upper calibration event				Lower calibration event				Target event				Protect?
						Age (Ma)	Top con-straint (m)	Bottom con-straint (m)	Event	Age (Ma)	Top con-straint (m)	Bottom con-straint (m)	Top con-straint (m)	Bottom con-straint (m)	Age (Ma)	Calculated error + (Ma)	Calculated error - (Ma)	
Rosenthal et al. (2018)	IODP U1489A	Eauripik Rise, Pac.		02°07.19' N, 141°01.67' E	Top G. <i>margaritae</i>	3.85	60.87	70.75	Top G. <i>nepenthes</i>	4.38	79.84	89.39	79.94	89.39	4.381	0.265	0.270	Y
This study	IODP U1488A	Eauripik Rise, Pac.		02°02.59' N, 141°45.29' E	Top <i>Sphenolithus</i>	3.54	89.9	91.56	Top G. <i>nepenthes</i>	4.38	110.47	112.70	109.00	110.47	4.305	0.075	0.073	Y
Brönimann et al. (1971)	DSDP 62	Eauripik Rise, Pac.		01°52.2' N, 141°56.3' E	Top G. <i>margaritae</i>	3.85	80.00	82.00	Top G. <i>nepenthes</i>	4.38	106.000	108.000	105.000	106.000	4.349	0.031	0.031	Y
Rosenthal et al. (2018)	IODP U1490A	Eauripik Rise, Pac.		05°48.95' N, 142°39.27' E	Top G. <i>margaritae</i>	3.85	52.02	61.60	Top G. <i>nepenthes</i>	4.38	70.97	80.52	61.60	70.97	4.115	0.265	0.265	Y
Krascheninnikov and Hoskins (1973)	DSDP 200	Caroline Abyssal Plain, Pac.		12°50.2' N, 156°47.0' E	Top G. <i>nepenthes</i>	4.38	20.50	22.00	Bottom S. <i>delisicens</i>	5.53	26.5	28.500	20.500	22.000	4.380	0.288	0.265	Y
Kaushtik et al. (2020)	ODP 807A	Ontong Plateau, Pac.	Java	03°36.42' N, 156°37.49' E	Bottom G. <i>fastuosus</i>	3.85	66.00	66.00	Top G. <i>nepenthes</i>	4.38	92.91	93.22	85	85.3	4.225	0.005	0.005	Y
Lam et al. (2022)	DSDP 586B	Ontong Plateau, Pac.	Java	00°29.84' S, 158°29' E	Top R. <i>pseudobombicus</i>	3.82	78.20	87.80	Top C. <i>acutus</i>	5.04	125.100	134.700	96.810	98.310	4.199	0.144	0.144	Y
Chassinon and Leckie (1993)	ODP 806B	Ontong Plateau, Pac.	Java	00°19.1' N, 159°21.7' E	Top G. <i>margaritae</i>	3.85	77.79	79.29	Top G. <i>nepenthes</i>	4.38	111	112.800	107.790	111.000	4.340	0.040	0.039	Y
Saito et al. (1975)	RC12-66	Central equatorial Pac.		02°36.06' N, 148°12.08' W	Top S. <i>semihilina</i>	3.59	11.15	11.15	Bottom S. <i>delisicens</i>	5.53	17.2	17.200	12.750	12.750	4.103	0.000	0.000	Y
Hays et al. (1969)	V24-59	Central equatorial Pac.		02°34' N, 145°32' W	C3n.1n	4.30	1049.00	1049.00	C3n.1r	4.493	1116	1116	1053	1053	4.312	0.000	0.000	Y
Orr and Jenkins (1980)	DSDP 77	Eastern equatorial Pac.		00°28.90' N, 133°13.70' W	Top S. <i>semihilina</i>	3.59	48.00	48.00	Top G. <i>nepenthes</i>	4.38	60	60	58.000	58.000	4.248	0.000	0.000	Y
Expedition 320/321 Scientists (2010b); Wilkens et al. (2013); Druy et al. (2018)	IODP U1338A	Eastern equatorial Pac.		02°30.47' N, 117°58.16' W	The top	4.177	57.63	57.63	The bottom	4.428	62.070	62.070	58.53	61.49	4.312	0.084	0.084	Y
Orr and Jenkins (1980)	DSDP 83	Eastern equatorial Pac.		04°02.08' N, 95°44.25' W	Top S. <i>semihilina</i>	3.59	66.00	66.00	Bottom S. <i>delisicens</i>	5.53	106	106.000	83.500	83.500	4.439	0.000	0.000	Y
Kanepps (1973)	DSDP 158	Cocos Ridge, Pac.		06°37.36' N, 85°14.16' W	Bottom G. <i>fastuosus</i>	3.85	32.21	37.76	Bottom G. <i>tumida</i>	5.72	87.840	87.120	52.220	53.710	4.490	0.082	0.093	Y

recalibration uses the range as depicted in Orr and Jenkins (1980, fig. 3) where Top *P. spectabilis* is placed midway between Top *Sphaeroidinellopsis seminulina* and Top *Globoturborotalita nepenthes* but without stated sampling errors. At DSDP Site 83 a single occurrence of *P. spectabilis* was noted by Orr and Jenkins (1980, fig. 3). The low level of this occurrence suggests that the species may have had a restricted range in the eastern equatorial Pacific, as was argued by Jenkins and Orr (1972) and Orr and Jenkins (1980). A similar situation occurs in the Panama Basin at DSDP Site 158, where just two occurrences were recorded by Kaneps (1973; note that the specimens recorded by Kaneps at DSDP Site 157 with “only a very weakly angled periphery” probably accord with the subsequently accepted concept of *P. praespectabilis*, meaning that level is not calibrated here). Another significant eastern Pacific record is from IODP Hole U1338A, for which we have recalibrated the shipboard data (Expedition 320/321 Scientists, 2010b) to the astronomical timescale of Drury et al. (2018). The species is rare and patchy at Site U1338 so this calibration may not record the global last occurrence; nevertheless, it is consistent with the western Pacific sites within the relatively broad sampling error.

Of the three calibrations on the Ontong Java Plateau, the best constraint is at ODP Hole 807A, where Kaushik et al. (2020) used very high-resolution post-expedition sampling to establish the ~ 120 kyr gap from Top *Globoturborotalita nepenthes* to Top *Pulleniatina spectabilis*. Our re-study of the event in Hole U1488A on Eauripik Rise (Sect. 2 above) is consistent with this, and we found that *P. spectabilis* in the higher part of its range have a larger proportion of dextral specimens than earlier. We suggest that the stratigraphically lower record of Brönnimann et al. (1971) at neighbouring Site 62 may be a highest common occurrence at that site that was incompletely recovered by rotary drilling. The data from Hole U1488A are also consistent with the much lower-resolution records from Holes U1489A and U1490A (Rosenthal et al., 2018f, g). Taking all these constraints into account, we suggest a global calibration of 4.27 ± 0.05 Ma (pink band in Fig. 10). The species may well have disappeared from the eastern Pacific before its final appearance in the west. The best prospect of improved calibration is from resampling the records at Sites U1488 and U1338 to compare the precise LADs against astrochronology and isotope stratigraphy.

3.7.2 Evolution

The LAD of *Pulleniatina spectabilis* is coincident with the LAD of *P. praespectabilis* in most records, including our own. We interpret both morphospecies to be part of the same evolving lineage which became extinct, possibly after being restricted to the core of its range in the Warm Pool. The extinction level is not remarkable in any way, and no other species seem to have been affected.

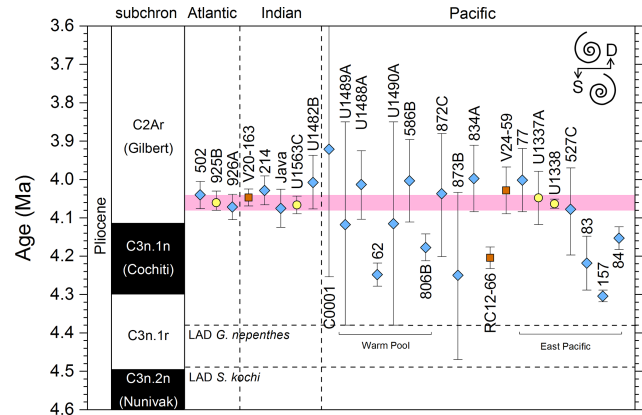


Figure 11. Biochronological constraints on the mid-Pliocene “L9” sinistral to dextral coiling reversal. Biohorizons LO *G. nepenthes* and LO *S. kochi* are shown for reference (dashed lines). Gold circles are astrochronological, brown squares are magnetochronological and blue diamonds are biochronological calibrations. The pink bands show the suggested summary calibration of 4.06 ± 0.02 Ma.

3.8 “L9” coiling event

3.8.1 Biochronology

We report 27 recalibrations of this prominent bioevent (Table 7, Fig. 11). The terminology “L9” is derived from the classic paper of Saito (1976) and is retained here as a useful name for the bioevent even though the wider alphanumeric scheme of Saito (1976) is no longer used as a whole (see Pearson and Penny, 2021, for discussion).

The earliest *Pulleniatina* are dominantly sinistrally coiled, although occasional dextral specimens occur (see Fig. 2). The lineage presumably inherited this characteristic from the ancestral population of *Neogloboquadrina acostaensis* from which it likely evolved. The *Pulleniatina praespectabilis* – *pectabilis* lineage is also sinistrally dominant, although our data suggest a significant increase in dextral specimens in the latter part of the range. Shortly after the extinction of *P. spectabilis* (in most records at least) the main lineage flipped to a dominantly dextral condition. This bioevent was recognized by Bandy (1963) and has been used for correlation since the early days of the DSDP. It was labelled “L9”, short for “left-coiling episode 9” by Saito (1976). In most records, the coiling change is from a strong sinistral to a strong dextral dominance and is rapid. In a small number of records (e.g. Kaneps, 1973, at DSDP Site 157 in the eastern equatorial Pacific) intermediate values occur. To avoid ambiguity, we define the bioevent as being from $> 80\%$ sinistral to $> 80\%$ dextral, and any intermediate values are recorded as being part of the transition interval.

Four astronomical calibrations exist from widely separated locations, and all are in remarkably tight agreement (see Fig. 11). These are the tuned records at ODP Hole 925B on Ceara Rise in the Atlantic (Chaisson and Pearson, 1997,

Table 7. Recalibrations of the L9 coiling reversal.

Reference	Site	Location		Upper calibration event				Lower calibration event				Target event		Plotted?			
		Physiographic feature	Grid reference	Event	Age (Ma)	Top con-straint (m)	Bottom con-straint (m)	Event	Age (Ma)	Top con-straint (m)	Bottom con-straint (m)	Top con-straint (m)	Bottom con-straint (m)		Age (Ma)	Calculated error + (Ma)	Calculated error - (Ma)
Kieigwin (1982)	DSDP 502	Caribbean Sea, Atl.	11°24.4' N, 79°22.7' W	Top S. <i>seminulina</i>	3.59	80.06	80.56	Top G. <i>neperthes</i>	4.380	115	117	99.7	101.55	4.040	0.036	0.035	Y
Chaisson and Pearson (1997)	ODP 925B	Ceara Rise, Atl.	04°12.25' N, 43°29.35' W											4.060	0.02	0.03	Y
Shipboard Scientific Party (1995a)	ODP 926A	Ceara Rise, Atl.	03°43.15' N, 42°54.51' W	Bottom G. <i>miocenica</i> (Atl.)	3.72	93.20	94.70	Top G. <i>neperthes</i>	4.38	123.20	124.70	109.18	110.68	4.072	0.033	0.033	Y
Saito (1976)	V20-163	Nineiy Ridge, Ind.	17°12' S, 88°41' E	C2An.3n	3.596	3.32	3.32	C2Ar	4.187	3.72	3.72	3.61	3.64	4.047	0.022	0.022	Y
Srinivasan and Sinha (1998)	DSDP 214	Nineiy Ridge, Ind.	11°20.21' S, 88°43.08' E	Bottom G. <i>fastiosa</i>	3.85	45.40	45.40	Bottom G. <i>tumida</i> (Pac.)	5.57	95.6	95.6	49.5	51.7	4.028	0.038	0.038	Y
Van Gorsel and Troelstra (1981)	Java	Solo River, Ind.	06°55' N, 111°14' E	Bottom G. <i>tumida</i> (Pac.)	5.57	510	520	S to D coiling in <i>N. acostensis</i>	6.37	655.0	665.0	240	248	4.075	0.050	0.050	Y
Shipboard Scientific Party (2000)	ODP 1143	South China Sea	09°21.72' N, 113°17.11' E	Bottom G. <i>rosensis</i>	3.35	142.37	152.46	Top G. <i>neperthes</i>	4.38	171.880	180.750	152.460	161.690	3.694	0.330	0.344	N
Groeneveld et al. (2021)	U1463C	NW Australian Margin, Ind.	18°57.92' S, 117°37.43' E											4.066	0.023	0.023	Y
Rosenthal et al. (2018a)	IODP U1482B	NW Australian Margin, Ind.	15°3.52' S, 120°26.10' E	Top D. <i>ditispra</i> (Pac.)	3.47	126.56	129.48	Bottom S. <i>deliscens</i>	5.53	265.84	268.28	160.96	167.60	4.007	0.070	0.070	Y
Hayashi et al. (2011)	IODP C0001	Nankai Trough, Pac.	33°14' N, 136°42' E	Top D. <i>ditispra</i> (Pac.)	3.47	199.29	200.98	Top G. <i>neperthes</i>	4.38	237.87	240.91	206.66	232.52	3.921	0.333	0.322	Y
Rosenthal et al. (2018)	IODP U1489A	Eauripik Rise, Pac.	02°07.19' N, 141°01.67' E	Top G. <i>margaritae</i>	3.85	60.87	70.75	Top G. <i>neperthes</i>	4.38	79.84	89.39	70.750	79.840	4.117	0.263	0.267	Y
Rosenthal et al. (2018c)	IODP U1488A	Eauripik Rise, Pac.	02°02.59' N, 141°45.29' E	Top <i>Sphenolithus</i>	3.54	89.9	91.56	Top C. <i>arnatus</i>	5.040	131.70	134.70	101.25	103.70	3.955	0.080	0.078	Y
Brommann et al. (1971)	DSDP 62	Eauripik Rise, Pac.	01°52.2' N, 141°56.3' E	Top G. <i>margaritae</i>	3.85	80.00	82.00	Top G. <i>neperthes</i>	4.380	106.00	108.00	100.05	101.00	4.248	0.030	0.030	Y
Rosenthal et al. (2018e)	IODP U1490A	Eauripik Rise, Pac.	05°48.95' N, 142°39.27' E	Top G. <i>margaritae</i>	3.85	52.02	61.60	Top G. <i>neperthes</i>	4.38	70.97	80.52	61.60	70.97	4.115	0.265	0.265	Y
Srinivasan and Sinha (1998)	ODP 586B	Ontong Java Plateau, Pac.	00°29.84' S, 158°29.89' E	Bottom G. <i>fastiosa</i>	3.85	96.00	96.00	Bottom G. <i>tumida</i>	5.72	157	157	97.500	104.50	4.003	0.107	0.107	Y
Chaisson and Leckie (1993)	ODP 806B	Ontong Java Plateau, Pac.	00°19.1' N, 159°21.7' E	Top <i>Sphaerolitholopsis</i>	3.59	74.79	76.29	Top G. <i>neperthes</i>	4.38	111.00	112.80	101.80	103.30	4.177	0.035	0.035	Y
Pearson (1995)	ODP 872C	Lo-En Guyot, Pac.	10°05.85' N, 162°51.96' E	Top D. <i>ditispra</i> (Pac.)	3.47	17.00	19.09	Top P. <i>spectabilis</i>	4.29	25.29	26.90	23.250	23.970	4.037	0.165	0.157	Y

Table 7. Continued.

Reference	Location			Upper calibration event			Lower calibration event			Target event					
	Site	Physiographic feature	Grid reference	Event	Age (Ma)	Top con-straint (m)	Bottom con-straint (m)	Event	Age (Ma)	Top con-straint (m)	Bottom con-straint (m)	Age (Ma)	Calculated error + (Ma)	Calculated error - (Ma)	Plotted?
Pearson (1995)	ODP 873B	Wodejebato Guyot, Pac.	11°53.80' N, 164°55.19' E	Top <i>D. altispira</i> (Pac.)	3.47	11.82	13.32	Top <i>P. spectabilis</i>	4.29	18.00	18.920	4.250	0.220	0.216	Y
Chaproniere and Nishi (1994)	ODP 834A	Lau Basin, Pac.	18°34.058' S, 177°51.735' W	Top <i>G. margaritae</i>	3.85	69.49	69.64	Bottom <i>S. delihscens</i>	5.53	112.54	112.900	3.997	0.087	0.087	Y
Saito et al. (1975)	RC12-66	Central equatorial Pac.	02°36.06' N, 148°12.08' W	C2Ar	4.187	3.72	3.72	C3n.1n	4.300	3.82	3.82	4.204	0.028	0.028	Y
Hays et al. (1969)	V24-59	Central equatorial Pac.	02°34' N, 145°32' W	C2An.3n	3.596	920.00	920.00	C2Ar	4.187	1017	1017	4.029	0.061	0.061	Y
Orr and Jenkins (1980)	DSDP 77	Eastern equatorial Pac.	00°28.90' N, 133°13.70' W	Top <i>S. seminulina</i> (Pac.)	3.59	48.00	48.00	Top <i>G. nepenthes</i>	4.38	60	60	4.001	0.082	0.082	Y
Expedition 320/321 Scientists (2010a); Wilkens et al. (2013); Tian et al. (2018)	IODP U1337A	Eastern equatorial Pac.	03°50.01' N, 123°12.36' W	Tie top	3.601	55.62	55.62	Tie bottom	4.190	70.030	70.030	4.048	0.069	0.069	Y
Expedition 320/321 Scientists (2010b); Hayashi et al. (2013); Wilkens et al. (2013)	IODP U1338	Eastern equatorial Pac.	02°30.47' N, 117°58.16' W	Tie top	3.686	50.17	50.17	Tie bottom	4.177	57.630	57.630	4.063	0.012	0.012	Y
Saito (1985)	DSDP 572C	Eastern equatorial Pac.	01°26.09' N, 113°50.52' W	Top <i>S. seminulina</i> (Pac.)	3.59	54.97	55.47	Top <i>G. nepenthes</i>	4.38	63.6	65.1	4.077	0.120	0.107	Y
Orr and Jenkins (1980)	DSDP 83	Eastern equatorial Pac.	04°02.08' N, 95°44.25' W	Top <i>S. seminulina</i> (Pac.)	3.59	66.00	66.00	Bottom <i>S. delihscens</i>	5.53	106	106.00	4.218	0.070	0.070	Y
Kaneps (1973)	DSDP 157	Cocos Ridge, Pac.	01°45.70' N, 85°14.16' W	Top <i>S. seminulina</i> (Pac.)	3.59	193.42	194.92	Top <i>G. nepenthes</i>	4.38	271.200	272.70	4.304	0.015	0.015	Y
Srinivasan and Sinha (1998)	DSDP 84	Eastern equatorial Pac.	05°44.92' N, 82°53.29' W	Top <i>S. seminulina</i> (Pac.)	3.59	127.00	127.00	Bottom <i>S. delihscens</i>	5.53	192.5	192.50	4.153	0.030	0.030	Y

updated according to Wilkens et al., 2017, and King et al., 2020); IODP Hole U1563C in the Indian Ocean on the north-western Australian margin (Groeneveld et al., 2021); and IODP Holes U1337A and U1338A in the eastern equatorial Pacific. The latter two sites are here calibrated from the data of Expedition 320/321 Scientists (2010a, b) and, in the case of additional data from Hole U1338B, from Hayashi et al. (2013) using the tuning of Tian et al. (2018) and Drury et al. (2017). These four tuned records strongly suggest that the bioevent is globally synchronous to within ~ 40 kyr or less (4.06 ± 0.02 Ma). Most of the other calibrations are consistent with this age, including the original palaeomagnetic calibration of Hays et al. (1969) from Vema core V24-59 in the central Pacific. Occasional records that disagree may be due to sedimentary complications, long calibration intervals or other issues. A possible exception is the far eastern Pacific where three sites record significantly older estimates. To these can be added the observation of Chaisson (1995), who suggested that the coiling reversal was more gradual in two other eastern Pacific sites, ODP Sites 847 and 852, than it is in the western Pacific, but the data from both those sites are too low resolution to provide useful calibrations here.

3.8.2 Evolution

No difference in size or shape between left- and right-coiling shells near the time of the L9 coiling bioevent has so far been observed, although no morphometric study has so far been attempted. We suggest that dextrally dominant populations first arose as an otherwise cryptic genotype, possibly in the eastern equatorial Pacific, and then rapidly replaced the predominantly sinistral genotypes worldwide. There is no evidence for a climatic linkage.

3.9 LAD of *Pulleniatina primalis*

3.9.1 Biochronology

We report 10 recalibrations of this bioevent (Table 8, Fig. 12).

This biohorizon is highly subjective because of the intergradation of the morphospecies *P. primalis* with *P. praecursor* and *P. obliquiloculata* and from the persistence of *primalis*-like morphotypes as part of the pre-adult life cycle of *P. obliquiloculata*. Because of the intergradation and to ensure consistent criteria, only studies that recognize all three morphospecies can be considered, which excludes for instance the studies of Krasheninnikov and Hoskins (1973), Keigwin (1982), Chaisson and Pearson (1997), Expedition 320/321 Scientists (2010a, b), Lam and Leckie (2020), Groeneveld et al. (2021), and Lam et al. (2022). A widely accepted early magnetostratigraphic calibration that has propagated through the literature was based on DSDP Site 502 (Colombian Basin) by combining the biostratigraphic data of Keigwin (1982) with the palaeomagnetic data of Kent and Spariosu (1982a). Berggren et al. (1985a) suggested an approximate age of 3.50 Ma based on this (recorded as

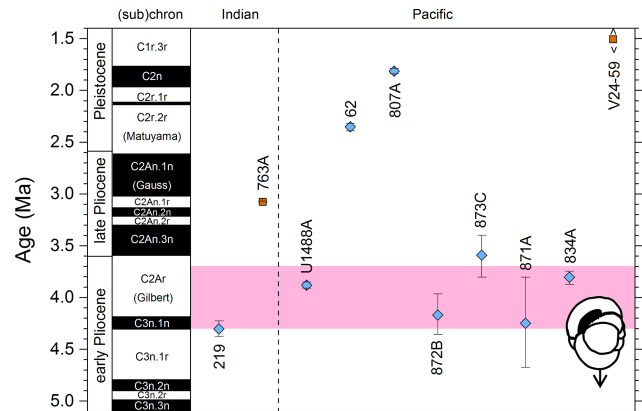


Figure 12. Biochronological constraints on the LAD of *P. primalis* arranged west to east. Brown squares are magnetostratigraphical, and blue diamonds are biochronological. The pink band shows the suggested summary calibration of 4.00 ± 0.60 Ma based on our new observations at IODP Hole U1488A and constraints from three sites from ODP Leg 144.

3.53 Ma by Keigwin, 1982). Berggren et al. (1995b) revised this to 3.65 Ma based on revised magnetostratigraphy (see also Wade et al., 2011). As an exercise, we recalibrated the event against the magnetostratigraphic timescale of Raffi et al. (2020) taking into account the original sampling errors reported by Keigwin (1982) and Kent and Spariosu (1982a), which yields an age estimate of 3.56 ± 0.04 Ma. However, we discount this as a valid recalibration because Keigwin (1982) did not recognize the morphospecies *P. praecursor*.

In their original subdivision of the genus, Banner and Blow (1967, fig. 14) indicated Top *P. primalis* as occurring slightly before Top *P. spectabilis* within their Zone N20 but did not publish the data on which this interpretation was based. Our new study at Hole U1488A places Top *P. primalis* at a somewhat higher level, approximately consistent with those recorded by Pearson (1995) at three Pacific guyot sites in the Marshall Islands region (ODP Holes 872B, 873C and 871A) and Chaproniere and Nishi (1994) and Chaproniere et al. (1994) at ODP Hole 834A in the eastern Pacific Lau Basin, but these are still far lower than the levels reported at several other sites, as shown in Fig. 12. We attribute the lack of consistency between biostratigraphic studies to being a result of problems in taxonomic discrimination, in particular that pre-adult *P. obliquiloculata* often resemble the *P. primalis* morphospecies when the streptospiral coiling arrangement has not fully asserted itself (Bolli and Saunders, 1985). This may be why some authors record *P. primalis* as occurring into the Quaternary (e.g. Hays et al., 1969; Bolli and Saunders, 1985; Premoli Silva et al., 1993; Hayashi et al., 2013; Lam and Leckie, 2020). Such forms have occasionally been recognized as a taxonomically distinct species, *Pulleniatina okinawaensis* of Natori (1976), but this is regarded here as pre-adult *P. obliquiloculata*. Based on these consid-

Table 8. Recalibrations of the LAD of *P. primalis*.

Reference	Location			Upper calibration event			Lower calibration event			Target event							
	Site	Physiographic feature	Grid reference	Event	Age (Ma)	Top constraint (m)	Bottom constraint (m)	Event	Age (Ma)	Top constraint (m)	Bottom constraint (m)	Top constraint (m)	Bottom constraint (m)	Age (Ma)	Calculated error + (Ma)	Calculated error - (Ma)	Plotted?
Gupta and Thomas (1999)	DSDP 219	Arabian Sea, Ind.	09°01.75' N, 75°52.67' E	Top D. <i>altispira</i> (Pac.)	3.47	30.45	31.95	Top G. <i>nepenthes</i>	4.38	48.45	49.95	46.91	48.41	4.302	0.076	0.076	Y
Sinha and Singh (2008)	ODP 763A	Exmouth Plateau, Ind.	20°35.20' S, 112°12.50' E	C2An.1n	3.032	52.30	52.30	C2An.1r	3.116	64.2	64.2	57.65	59.16	3.075	0.005	0.005	Y
This study	IODP U1488A	Eauripik Rise, Pac.	02°02.59' N, 141°45.29' E	Top G. <i>margaritae</i>	3.85	80.50	82.22	Top G. <i>nepenthes</i>	4.38	110.47	112.70	82.22	83.90	3.880	0.030	0.030	Y
Brönnimann et al. (1971)	DSDP 62	Eauripik Rise, Pac.	01°52.2' N, 141°56.3' E	Top D. <i>broweri</i>	1.930	42.00	42.00	Top D. <i>pentaradiatus</i>	2.390	59.000	61.000	58.000	59.000	2.352	0.038	0.034	Y
Kaushik et al. (2020)	ODP 807A	Ontong Java Plateau, Pac.	03°36.42' N, 156°37.49' E	Top G. <i>rosaensis</i>	0.610	10.20	10.50	Top G. <i>fistulosa</i>	1.880	26.74	27.04	25.83	26.22	1.814	0.026	0.026	Y
Premoli Silva et al. (1993); Sager et al. (1993)	ODP 810C	Shatsky Rise, Pac.	32°25.40' N, 157°50.74' E	Core top	0	0	0	C1n	0.773	18.100	18.100	1.90	3.40	0.113	0.032	0.032	-
Pearson (1995)	ODP 872B	Lo-En Guyot, Pac.	10°05.85' N, 162°51.96' E	Top D. <i>altispira</i> (Pac.)	3.47	17.00	19.09	Top G. <i>nepenthes</i>	4.38	24.56	25.29	22.66	23.97	4.167	0.188	0.202	Y
Pearson (1995)	ODP 873C	Wodejebato Guyot, Pac.	11°53.80' N, 164°55.19' E	Top D. <i>altispira</i> (Pac.)	3.47	11.82	13.32	Top G. <i>nepenthes</i>	4.38	18.92	20.42	12.72	14.28	3.589	0.213	0.192	Y
Pearson (1995)	ODP 871A	Limalok Guyot	05°33.43' N, 172°20.69' E	Top G. <i>fistulosa</i>	1.88	16.60	17.60	Top D. <i>altispira</i> (Pac.)	3.47	19.73	20.60	21.23	22.10	4.248	0.426	0.444	Y
Chaproniere and Nishi (1994)	ODP 834A	Lau Basin, Pac.	18°34.058' S, 177°51.735' W	C2An.3n	3.596	71.80	71.80	Top R. <i>pseudoumbilica</i>	3.82	76.2	77.300	75.49	77.28	3.803	0.071	0.057	Y
Hays et al. (1969)	V24-59	Central equatorial Pac.	02°34' N, 145°32' W	C1r.2n	1.221	570.00	570.00	C1r.3r	1.775	735	735	655	655	1.506	0.000	0.000	Y

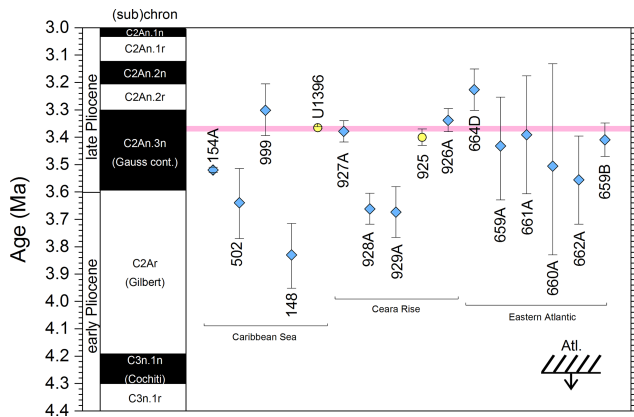


Figure 13. Biochronological constraints on the Pliocene disappearance of *Pulleniatina* from the Atlantic sector, arranged west to east. The gold circle is astrochronological, and blue diamonds are biochronological. The pink band shows the suggested summary calibration of 3.370 ± 0.005 Ma based on the tuned records at IODP Site U1396 and ODP Site 925. Earlier calibrations may be due to the patchy occurrence of *Pulleniatina* prior to its disappearance.

erations, we propose a LAD of 4.0 ± 0.6 Ma, as shown by the pink band in Fig. 12, and recommend that the taxonomic concept of *P. primalis* is restricted to demonstrably adult tests in tropical regions. The LAD of *P. primalis* has not been used as a biostratigraphic marker, but if it is to be used, it will need to be based on much improved taxonomic discrimination.

3.9.2 Evolution

We regard this bioevent as an example of a pseudoextinction caused by gradual evolution of the lineage away from the initial *P. primalis* morphology. Lam et al. (2022) have used it as an example of extra-tropical diachrony, but it is a highly subjective, and the lack of agreement between calibration ages is likely as much a function of taxonomic inconsistency as a true biogeographic pattern.

3.10 Atlantic Ocean disappearance

3.10.1 Biochronology

We report 16 recalibrations of this bioevent (Table 9, Fig. 13).

Lamb and Beard (1972), Saito (1976) and Bolli and Krasheninnikov (1977) observed that *Pulleniatina* was absent from several sites in the Caribbean and Gulf of Mexico for an extended interval in the late Pliocene, but their records are insufficient to provide a precise calibration for either the disappearance or reappearance. During DSDP Leg 15, Bolli and Premoli Silva (1973) recorded a stratigraphic gap in Holes 148 (Aves Ridge, eastern Caribbean) and 154A (Columbian Basin), finding *P. primalis* to be intermittent prior to its disappearance. The latter site was re-studied by Keigwin (1978), who found the disappearance at a slightly

higher level than previously reported, dating it to approximately 3.1 Ma based on interpolation between a few biostratigraphic datums. Our recalibration to the timescale of Raffi et al. (2020) using the level reported by Keigwin (1978) combined with the wider biostratigraphic constraints of Bolli and Premoli Silva (1973) indicates an age of ~ 3.52 Ma, but although the sampling is well constrained, the biostratigraphic framework is questionable because of anomalous reported ranges of some marker species, suggesting that the succession may be disturbed around the level of interest. Keigwin (1982) suggested an age of 3.3 Ma at DSDP Site 502, also in the Columbian Basin, again by indirect calibration to widely spaced biostratigraphic events (recalibrated here to 3.64 Ma).

Several relevant sites were drilled during ODP Leg 154 on Ceara Rise in the equatorial Atlantic Ocean. Chaisson and Pearson (1997) estimated the Atlantic disappearance at 3.41 ± 0.03 Ma at ODP Site 925 where there is an excellent orbital cyclostratigraphy. This is revised here to 3.40 ± 0.03 Ma following changes to the inter-hole splice and orbital solution as discussed in King et al. (2020). A similar level was found in Hole 926A and Hole 927A (Shipboard Scientific Party, 1995a, b). Slightly older calibrations in Holes 928A and 929A (Shipboard Scientific Party, 1995c, d) are probably due to sampling of the patchy distribution of *Pulleniatina* prior to its disappearance. Further data was provided by Chaisson and D'Hondt (2000) from ODP Site 999 in the Caribbean Sea, who found the event at a similar level to Site 925. A very high-resolution orbitally tuned record from near the island of Montserrat (IODP Site U1396) was provided by Fraass et al. (2017) that is consistent with the Ceara Rise age.

Several sites were drilled in the eastern Atlantic during ODP Legs 108 (Weaver and Raymo, 1989) and 159 (Norris, 1998). Most of these are consistent with the tight constraint of Fraass et al. (2017) except the equatorial record at ODP Hole 664D which is slightly younger, but that site is affected by a prominent hiatus at a slightly younger level and may be disturbed lower down the core. Given these considerations, we propose a summary calibration of 3.370 ± 0.005 Ma for the final Atlantic disappearance (pink band in Fig. 13) with the proviso that the disappearance in some places was preceded by an interval of stuttering occurrences and there may have been an element of diachrony between local refugia.

3.10.2 Evolution

The disappearance of *Pulleniatina* from the Atlantic is a good example of a temporary range contraction (local extinction). There was no prominent climatic cooling associated with the disappearance level, which seems to rule out a direct climate link such as has been hypothesized for the short-term disappearance during the Last Glacial Maximum (Prell and Damuth, 1978). There was increasing endemism of planktonic foraminifera in general between the Atlantic

Table 9. Recalibrations of the Atlantic Ocean disappearance.

Reference	Location			Upper calibration event				Lower calibration event				Target event					
	Site	Physiographic feature	Grid reference	Event	Age (Ma)	Top constraint (m)	Bottom constraint (m)	Event	Age (Ma)	Top constraint (m)	Bottom constraint (m)	Age (Ma)	Top constraint (m)	Bottom constraint (m)	Calculated error + (Ma)	Calculated error - (Ma)	Plotted?
Bolli and Premoli Silva (1973); Keigwin (1978)	DSDP 154A	Caribbean Sea, Atl.	11°05.07' N, 80°22.82' W	Bottom G. <i>truncatulinoides</i>	1.92	71.22	73.2	Top G. <i>mul-ticamerata</i>	2.97	106.00	106.10	3.519	123.00	124.50	0.009	0.010	Y
Keigwin (1982)	DSDP 502	Caribbean Sea, Atl.	11°24.4' N, 79°22.7' W	Top G. <i>fastulosa</i>	1.88	39.60	41.36	Bottom S. <i>dehiscens</i>	5.53	136.92	143.95	3.639	87.30	90.00	0.131	0.125	Y
Chaisson and D'Hondt (2000)	ODP 999	Caribbean Sea, Atl.	12°44.64' N, 78°44.36' W	Top D. <i>altispira</i>	3.11	95.02	99.52	Top G. <i>nepenthes</i>	4.38	137.55	140.58	3.301	102.58	104.52	0.093	0.096	Y
Bolli and Premoli Silva (1973)	DSDP 148	Caribbean Sea, Atl.	13°25.12' N, 63°43.25' W	Top G. <i>miocentica</i>	2.39	135.77	137.51	Top G. <i>margaritae</i>	3.83	223.70	231.16	3.830	223.70	231.16	0.122	0.115	Y
Fraass et al. (2017)	IODP U1396	Caribbean Sea, Atl.	16°30.49' N, 62°27.10' W									3.365			0.004	0.004	Y
Shipboard Scientific Party (1995b)	ODP 927A	Ceara Rise, Atl.	05°27.76' N, 44°28.84' W	Top D. <i>altispira</i> (Atl.)	3.000	103.20	104.36	Top G. <i>nepenthes</i>	4.38	141.20	143.20	3.378	113.91	114.70	0.040	0.039	Y
Shipboard Scientific Party (1995c)	ODP 928A	Ceara Rise, Atl.	05°27.32' N, 43°44.88' W	Top D. <i>altispira</i> (Atl.)	3.000	89.67	91.16	Top G. <i>nepenthes</i>	4.38	126.20	127.70	3.661	107.18	108.67	0.056	0.056	Y
Shipboard Scientific Party (1995d)	ODP 929A	Ceara Rise, Atl.	05°58.57' N, 43°44.39' W	Top D. <i>altispira</i> (Atl.)	3.000	85.70	87.20	Top G. <i>nepenthes</i>	4.38	115.47	117.15	3.673	99.80	102.23	0.093	0.093	Y
Chaisson and Pearson (1997)	ODP 925	Ceara Rise, Atl.	04°12.25' N, 43°29.35' W									3.40			0.03	0.03	Y
Shipboard Scientific Party (1995a)	ODP 926A	Ceara Rise, Atl.	03°43.15' N, 42°54.51' W	Top D. <i>altispira</i> (Atl.)	3.000	82.21	83.71	Top G. <i>nepenthes</i>	4.38	127.61	128.11	3.338	93.21	94.71	0.042	0.043	Y
Weaver and Raymo (1989)	ODP 664D	Eastern tropical Atl.	00°06.44' N, 23°13.65' W	Top D. <i>altispira</i> (Atl.)	3.000	125.8	135.3	Top G. <i>margaritae</i>	3.83	230.3	239.8	3.226	154.3	163.8	0.075	0.075	Y
Weaver and Raymo (1989)	ODP 659A	Cape Verde region, Atl.	18°04.63' N, 21°01.57' W	Top D. <i>altispira</i> (Atl.)	3.000	83.8	84.8	Top G. <i>nepenthes</i>	4.38	125.5	131.1	3.431	93.3	102.8	0.198	0.178	Y
Weaver and Raymo (1989)	ODP 661A	Eastern tropical Atl.	09°26.81' N, 19°23.17' W	Top D. <i>altispira</i> (Atl.)	3.000	41	44	Top G. <i>margaritae</i>	3.83	65.1	68.1	3.391	49.1	58.6	0.215	0.215	Y
Weaver and Raymo (1989)	ODP 660A	Eastern tropical Atl.	10°00.81' N, 19°14.74' W	Top D. <i>altispira</i> (Atl.)	3.000	53.8	56.8	Top G. <i>margaritae</i>	3.83	68.3	69.4	3.505	58.8	68.3	0.325	0.374	Y
Weaver and Raymo (1989)	ODP 662A	Eastern tropical Atl.	01°23.41' N, 11°44.35' W	Top D. <i>altispira</i> (Atl.)	3.000	165.8	168.4	Top G. <i>margaritae</i>	3.83	197.5	200.5	3.556	183.7	193.2	0.162	0.160	Y
Norris (1998)	ODP 959B	Ivorian Basin, Atl.	03°37.70' N, 02°44.10' W	Top D. <i>altispira</i> (Atl.)	3.000	35.59	37.09	Top G. <i>nepenthes</i>	4.38	59.09	60.59	3.409	43.01	43.59	0.061	0.061	Y

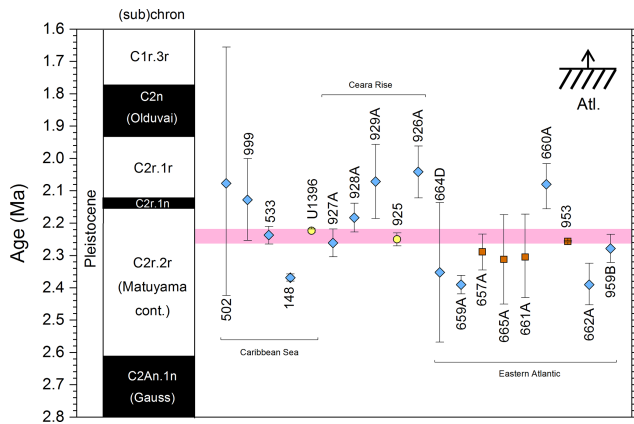


Figure 14. Biochronological constraints on the Pleistocene reappearance of *Pulleniatina* in the Atlantic sector, arranged west to east. Gold circles are astrochronological, brown squares are magnetostratigraphical and blue diamonds are biochronological. The pink band shows the suggested summary calibration of 2.24 ± 0.02 Ma.

and Pacific during the late Pliocene, which has been linked to the gradual closure of the Panama gateway (Schmidt, 2007). Nevertheless, populations have always been able to communicate via the Indian Ocean and the Agulhas Current around South Africa. The genus remained present in high abundance in the tropical Pacific and Indian oceans during the Atlantic disappearance, although there may have been a geographic range contraction in the South China Sea, as evidenced by very low abundances at this time (Li et al., 2005).

3.11 Atlantic Ocean reappearance

3.11.1 Biochronology

We report 19 recalibrations of this bioevent (Table 10, Fig. 14).

The highest-resolution record of this bioevent is the tuned age of Fraass et al. (2017) at IODP Site U1396 in the Caribbean Sea, which is in good agreement with the earlier astronomical calibration of Chaisson and Pearson (1997) at ODP Site 925 on Ceara Rise (revised here to 2.25 ± 0.03 Ma as discussed by King et al., 2020). A high-resolution magnetostratigraphic calibration was provided by Maniscalco and Brunner (1998) at ODP Site 953 (Canary Islands region) that places the event in the upper part of Subchron C2r.2r, albeit based on unpublished magnetostratigraphy. At that site the *Pulleniatina* reappearance occurs immediately above a short interval of poor recovery but the calibration is nevertheless in excellent agreement with the astronomical calibrations from the other side of the Atlantic. These calibrations are also consistent with the biostratigraphic records of Moullade (1983) at DSDP Site 533 on the Blake Outer Ridge, western North Atlantic, and Norris (1998) at ODP Site 959 in the eastern Ivorian Basin. Together these records suggest that *Pulleniatina* appeared across the tropical Atlantic at 2.24 ± 0.02 Ma.

The older calibration age at DSDP Site 148 in the Caribbean Sea (Bolli and Premoli Silva, 1973) can probably be discounted because of sedimentary complexities and anomalous reported stratigraphic ranges at that site, combined with a long calibration interval.

The eastern equatorial records from three Leg 108 sites (ODP Holes 661A, 665A and 657A) were herein calibrated by combining the fossil occurrence data of Weaver and Raymo (1989) with the magnetostratigraphy of Tauxe et al. (1989). All of these records are within error of the above stated age. However three other Leg 108 sites (Holes 659A, 660A and 662A) have anomalous calibrations (see Fig. 14). These have no reliable magnetostratigraphy through the calibration interval and thus rely on biostratigraphic calibrations. They may be unreliable because they are from relatively high-productivity environments and may have anomalous ranges of marker taxa. Because of this they are not considered good evidence for diachrony.

3.11.2 Evolution

The re-establishment of *Pulleniatina* in the Atlantic was presumably via Indian Ocean populations because the Panama Gateway was likely closed by that time. There is no obvious climatic link to the event, and the reason why the genus was able to thrive once again in the Atlantic is not known. An interesting question is to what extent *Pulleniatina* has experienced inter-ocean gene flow since the recolonization. Saito (1976) claimed that the coiling direction history diverged in the Atlantic compared to the Indo-Pacific (as discussed in Sect. 3.12, 3.15, and 3.16 below), at least from the period up to the “L1” shift at ~ 0.855 Ma. Since then, populations everywhere have been dominated by dextral specimens. Modern Atlantic and Indian Ocean populations of *P. obliquiloculata* are dominated by the Type I genotype, with rare examples of Type IIb, whereas the Pacific is dominated by Type IIb and Type IIa (Ujiié and Ishitani, 2016). It is currently unclear to what extent these genotypes represent discrete populations with deep divergence times in the past (see Ujiié and Ishitani, 2016, and Pearson and Penny, 2021, for discussion).

3.12 Bottom of the “L5” coiling interval

3.12.1 Biochronology

We report four recalibrations of this bioevent (Table 11; Fig. 15).

One of the most promising of the *Pulleniatina* coiling shifts located by Pearson and Penny (2021) at Site U1486 occurs at the bottom of Saito’s (1976) “L5” interval (depending on how it is defined) within the upper part of Matuyama Subchron C2r.1r (see also Rosenthal et al., 2018c). Data from earlier studies (Hays et al., 1969; Bolli and Premoli Silva, 1973; Saito, 1976; Thompson and Sciarillo, 1978)

Table 10. Recalibrations of the Atlantic Ocean reappearance.

Reference	Location		Upper calibration event				Lower calibration event				Target event						
	Site	Physiographic feature	Grid reference	Event	Age (Ma)	Top constraint (m)	Bottom constraint (m)	Event	Age (Ma)	Top constraint (m)	Bottom constraint (m)	Top constraint (m)	Bottom constraint (m)	Age (Ma)	Calculated error + (Ma)	Calculated error – (Ma)	Plotted?
Keigwin (1982)	DSDP 502	Caribbean Sea, Atl.	11°24.4' N, 79°22.7' W	Bottom <i>G. truncatulinoides</i> (Atl.)	1.93	41.46	48.80	Top <i>S. seminulina</i>	3.59	80.06	80.56	43.54	52.94	2.077	0.347	0.422	Y
Chaisson and D'Hondt (2000)	ODP 999	Caribbean Sea, Atl.	12°44.64' N, 78°44.36' W	Top <i>G. fistulosa</i>	1.88	66.52	71.02	Top <i>D. altispira</i> (Atl.)	3.00	95.02	99.02	74.02	76.02	2.128	0.126	0.128	Y
Moullade (1983)	DSDP 533	Blake Outer Ridge, Atl.	31°15.6' N, 74°52.2' W	Top <i>G. extremus</i>	1.970	143.5	143.82	Top <i>G. perrenius</i>	2.30	151.96	152.65	150.25	151.05	2.237	0.028	0.027	Y
Bolli and Premoli Silva (1973)	DSDP 148	Caribbean Sea, Atl.	13°25.12' N, 63°43.25' W	Bottom <i>G. truncatulinoides</i> (Atl.)	1.93	94.5	97.4	Top <i>G. miocenica</i>	2.39	135.77	137.51	134.66	134.86	2.369	0.011	0.011	Y
Fraass et al. (2017)	IODP U1396	Caribbean Sea, Atl.	16°30.49' N, 62°27.10' W											2.223	0.005	0.005	Y
Shipboard Scientific Party (1995b)	ODP 927A	Ceara Rise, Atl.	05°27.76' N, 44°28.84' W	Top <i>G. fistulosa</i>	1.88	70.20	71.20	Top <i>D. altispira</i> (Atl.)	3.00	103.2	104.36	81.2	82.7	2.261	0.043	0.043	Y
Shipboard Scientific Party (1995c)	ODP 928A	Ceara Rise, Atl.	05°27.32' N, 43°44.88' W	Top <i>G. fistulosa</i>	1.88	59.68	61.17	Top <i>D. altispira</i> (Atl.)	3.00	89.67	91.16	68.09	68.98	2.183	0.044	0.044	Y
Shipboard Scientific Party (1995d)	ODP 929A	Ceara Rise, Atl.	05°58.57' N, 43°44.39' W	Top <i>G. fistulosa</i>	1.88	63.70	65.20	Top <i>D. altispira</i> (Atl.)	3.00	85.7	87.2	66.7	69.7	2.071	0.115	0.115	Y
Chaisson and Pearson (1997)	ODP 925	Ceara Rise, Atl.	04°12.25' N, 43°29.35' W											2.25	0.02	0.02	Y
Shipboard Scientific Party (1995a)	ODP 926A	Ceara Rise, Atl.	03°43.15' N, 42°54.51' W	Bottom <i>T. truncatulinoides</i>	1.92	59.71	60.81	Top <i>D. altispira</i> (Atl.)	3.00	82.21	83.71	61.69	63.91	2.041	0.081	0.079	Y
Weaver and Raymo (1989)	ODP 664D	Eastern equatorial Atl.	00°06.44' N, 23°13.65' W	Bottom <i>G. truncatulinoides</i>	1.920	78.30	87.80	Top <i>D. altispira</i> (Atl.)	3.00	125.8	135.3	97.3	106.8	2.352	0.216	0.216	Y
Weaver and Raymo (1989); Tauxe et al. (1989)	ODP 659A	Cape Verde region, Atl.	18°04.63' N, 21°01.57' W	Top <i>G. miocenica</i>	2.39	64.80	65.70	Top <i>D. altispira</i> (Atl.)	3.00	83.8	84.8	64.8	65.7	2.390	0.029	0.029	Y
Weaver and Raymo (1989); Tauxe et al. (1989)	ODP 657A	Eastern tropical Atl.	21°19.89' N, 20°57.93' W	C1r.1n	1.076	36.20	36.20	C2r.2r	2.61	72.1	73.3	64.2	65.9	2.288	0.057	0.055	Y
Weaver and Raymo (1989); Tauxe et al. (1989)	ODP 665A	Eastern tropical Atl.	02°57.07' N, 19°40.07' W	C2n	1.934	36.40	36.40	C2r.2r	2.61	49.1	49.1	40.9	46.1	2.312	0.138	0.138	Y

Table 11. Recalibrations of the bottom of the “L5” colling interval.

Reference	Site	Location	Upper calibration event				Lower calibration event				Target event		Plotted?			
			Event	Age (Ma)	Top con-straunt (m)	Bottom con-straunt (m)	Event	Age (Ma)	Top con-straunt (m)	Bottom con-straunt (m)	Top con-straunt (m)	Bottom con-straunt (m)		Age (Ma)	Calculated error + (Ma)	Calculated error – (Ma)
Pearson and Penny (2021)	IODP U1483A	NW Australian Margin, Ind.	C2n	1.934	186.20	189.65	C2r:2r	2.610	224.200	228.100	193.391	196.538	2.058	0.059	0.059	Y
Pearson and Penny (2021)	IODP U1486	Mannus Basin, Pac.	C2n	1.934	124.46	124.46	C2r:2r	2.610	194.930	194.930	133.340	133.840	2.022	0.002	0.002	Y
Chuang et al. (2018)	ODP 1115B	Solomon Sea, Pac.											2.147	0.004	0.004	Y
Chaproniere and Nishi (1994)	ODP 834A	Lau Basin, Pac.	C2n	1.934	35.3	35.3	C2r:2r	2.610	45.50	45.50	36.37	37.05	2.027	0.023	0.023	Y

Table 10. Continued.

Reference	Site	Location	Upper calibration event				Lower calibration event				Target event		Plotted?			
			Event	Age (Ma)	Top con-straunt (m)	Bottom con-straunt (m)	Event	Age (Ma)	Top con-straunt (m)	Bottom con-straunt (m)	Top con-straunt (m)	Bottom con-straunt (m)		Age (Ma)	Calculated error + (Ma)	Calculated error – (Ma)
Weaver and Raymo (1989); Tauxe et al. (1989)	ODP 661A	Eastern tropical Atl.	C1r:3r	1.775	26.10	26.70	C2r:2r	2.61	36.8	36.8	31.5	34.5	2.305	0.126	0.133	Y
Weaver and Raymo (1989); Tauxe et al. (1989)	ODP 660A	Eastern tropical Atl.	C2n	1.934	38.40	38.40	Top D. <i>altispira</i> (Atl.)	3.00	53.8	56.6	39.8	41.6	2.080	0.076	0.064	Y
Maniscalco and Brunner (1998)	ODP 953	Canary Islands region, Atl.	C2r:1n	2.14	147.00	147.00	C2An:1n	2.61	177.7	177.7	154.49	154.71	2.256	0.002	0.002	Y
Weaver and Raymo (1989)	ODP 662A	Eastern tropical Atl.	Top G. <i>mitocentica</i>	2.39	137.50	140.50	Top D. <i>altispira</i> (Atl.)	3.00	166.8	168.4	137.5	140.5	2.390	0.062	0.066	Y
Norris (1998)	ODP 959B	Ivorian Basin, Atl.	Top D. <i>altispira</i> (Atl.)	3.00	35.59	37.09	Top G. <i>neperthes</i> (Atl.)	4.38	59.09	60.59	24.05	24.05	2.278	0.044	0.044	Y

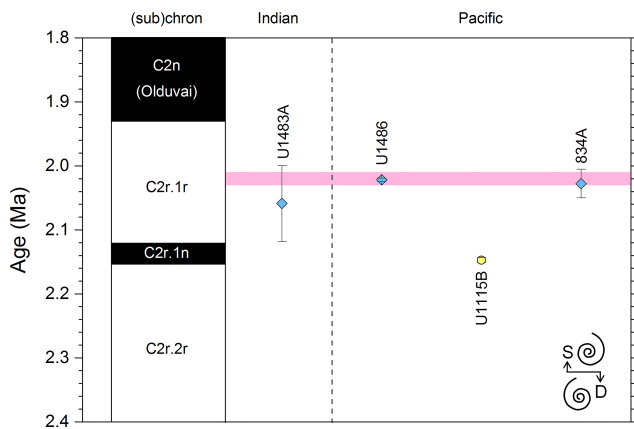


Figure 15. Biochronological constraints on the bottom of the “L5” coiling interval, arranged west to east. The gold circle is astrochronological calibration, while blue diamonds are biochronological. The pink band shows the suggested summary calibration of 2.02 ± 0.01 Ma.

were not sufficiently detailed to resolve this shift or are ambiguous. Nevertheless, it is a very sharp transition that can be calibrated precisely (Pearson and Penny, 2021). For maximum correlation potential it is defined here as a shift from $< 60\%$ dextral to $< 10\%$ dextral in the upper part of the Matuyama Chron and is calibrated palaeomagnetically to 2.022 ± 0.002 Ma at Pacific Ocean Site U1486 in the western Pacific Manus Basin, which is consistent with broader calibration intervals at IODP Hole U1483A in the eastern tropical Indian Ocean (Rosenthal et al., 2018b; Pearson and Penny, 2021) and ODP Hole 834A in the western Pacific Lau Basin (Chaproniere and Nishi, 1994).

An astronomical calibration at ODP Site 1115 in the Solomon Sea (Chuang et al., 2018) gives the significantly older age of 2.147 ± 0.004 Ma. The discrepancy is unlikely to be due to diachrony because it is in the same region as the other western Pacific sites; instead the sedimentary disturbance at Site 1115 (Resig et al., 2001) may be responsible for an age model error. Until more information is available, the calibration at Site U1486 is preferred here, and a “global” calibration of 2.02 ± 0.01 Ma is suggested.

3.12.2 Evolution

Pearson and Penny (2021) found that the coiling shift at IODP Site U1486 was characterized by a rapid decline of dextral specimens which only later re-established themselves. Single-specimen isotopic analysis of 100 left-coiling and 100 right-coiling shells just prior to the shift found no significant differences, and no size difference was detected. The cause of the bioevent may have been the extinction of a cryptic genotype characterized by predominantly dextral shells, leaving populations dominated by sinistral individuals.

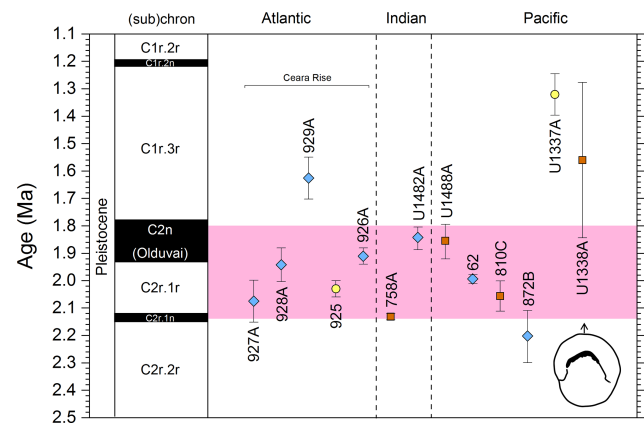


Figure 16. Biochronological constraints on the FAD of *Pulleniatina finalis*, arranged west to east. Gold circles are astrochronological, blue diamonds are biochronological, brown squares are magnetostratigraphical and blue diamonds are biochronological. The broad pink band shows the suggested summary calibration of 1.97 ± 0.17 Ma.

3.13 FAD of *Pulleniatina finalis*

3.13.1 Biochronology

We report 14 recalibrations of this bioevent (Table 12, Fig. 16).

The FAD of *P. finalis* is a pseudospeciation that depends on a taxonomist being confident that at least one specimen in an assemblage can be assigned to the *P. finalis* morphospecies. As such it depends on a somewhat arbitrary distinction between *P. obliquiloculata* and *P. finalis* relating to the perceived pseudo-planispirality of the adult shell. Banner and Blow (1967) originally placed the biohorizon in the lower part of their Zone N22 (Pleistocene) but did not publish the data on which this was based. Lamb and Beard (1972) placed the bioevent at a much higher level and used it to define an upper Pleistocene *Pulleniatina primalis* subzone for the Caribbean and Gulf of Mexico (see also the summary of DSDP Leg 10 by Smith and Beard, 1973), although stratigraphic constraints are too poor to attempt a modern recalibration. At ODP Hole 810C on Shatsky Rise in the northwestern Pacific, Premoli Silva et al. (1993) found the Bottom of a form they called “cf. *finalis*” within the lower part of the Olduvai Subchron Chron C2n followed by a gap in its range and the incoming of “*P. finalis sensu stricto*” at a higher level. Chaisson and Pearson (1997) estimated its age at ODP Site 925 on Ceara Rise in the tropical Atlantic at 2.04 ± 0.03 Ma based on cyclostratigraphy, revised by King et al. (2020) to 2.03 Ma. This is broadly consistent with other Ceara Rise sites except Site 929, which is in deeper water and may be affected by dissolution. At tropical Indian Ocean Hole 758A, Podder et al. (2021) recorded the FAD at a level that is calibrated here against the palaeomagnetic record of Farrell and Janecek (1991) to 2.13 Ma. That places it near to the short Feni Subchron C2r.1n, which unfortunately was not resolved

Table 12. Recalibrations of the FAD of *P. finialis*.

Reference	Site	Location	Physiographic feature	Grid reference	Upper calibration event				Lower calibration event				Target event		Plotted?			
					Event	Age (Ma)	Top con- strait (m)	Bottom con- strait (m)	Event	Age (Ma)	Top con- strait (m)	Bottom con- strait (m)	Top con- strait (m)	Bottom con- strait (m)		Age (Ma)	Calculated error + (Ma)	Calculated error - (Ma)
Moullade (1983)	DSDP 533	Blake Outer Ridge, Atl.		31°15.6' N, 74°52.2' W	Core top	0.000	0	0	Top G. <i>loxeuensis</i>	0.610	90.73	95.35	76.39	81.30	0.517	0.030	0.028	-
Shipboard Scientific Party (1995b)	ODP 927A	Ceara Rise, Atl.		05°27.76' N, 44°28.84' W	Top G. <i>finilosa</i>	1.880	70.20	71.20	Top D. <i>altispira</i> (Atl.)	3.000	103.2	104.36	74.7	78.2	2.075	0.077	0.076	Y
Shipboard Scientific Party (1995c)	ODP 928A	Ceara Rise, Atl.		05°27.32' N, 43°44.88' W	Top G. <i>finilosa</i>	1.880	59.68	61.17	Top D. <i>altispira</i> (Atl.)	3.000	89.67	91.16	61.17	62.99	1.942	0.062	0.062	Y
Shipboard Scientific Party (1995d)	ODP 929A	Ceara Rise, Atl.		05°58.57' N, 43°44.39' W	Top G. <i>finilosa</i>	1.880	63.70	65.20	Top D. <i>altispira</i> (Atl.)	3.000	85.7	87.2	58.7	60.2	1.625	0.076	0.076	Y
Chaisson and Pearson (1997)	ODP 925B	Ceara Rise, Atl.		04°12.25' N, 43°29.35' W											2.03	0.03	0.03	Y
Shipboard Scientific Party (1995e)	ODP 926A	Ceara Rise, Atl.		03°43.15' N, 42°54.51' W	Top G. <i>finilosa</i>	1.880	55.20	56.70	Bottom T. <i>truncat- truncat- ultriodes</i> (Atl.)	1.920	57.19	58.66	56.7	58.2	1.910	0.030	0.030	Y
Podder et al. (2021); Farrell and Janecek (1991)	ODP 758A	Ninety East Ridge, Ind.		05°23.05' N, 90°21.67' E	C2n	1.934	30.33	30.33	C2n-2r	2.610	38.530	38.530	32.580	32.870	2.131	0.012	0.012	Y
Rosenthal et al. (2018a)	IODP U1482A	NW Australian Margin, Ind.		15°33.27' S, 120°26.10' E	Top G. <i>finilosa</i>	1.880	88.91	91.07	Top D. <i>altispira</i> (Pac)	3.470	126.82	136.2	88.91	89.07	1.842	0.045	0.038	Y
This study	IODP U1488A	Eaunpik Rise, Pac.		02°02.59' N, 141°45.29' E	C1r-3r	1.775	39.50	39.53	C2n	1.934	43.23	43.55	40.00	42.90	1.855	0.066	0.061	Y
Brönimann et al. (1971)	DSDP 62	Eaunpik Rise, Pac.		01°52.2' N, 141°56.3' E	Top D. <i>browneri</i>	1.930	42.00	42.00	Top D. <i>pentaradiatus</i>	2.390	59.00	61.00	44.00	45.00	1.994	0.017	0.015	Y
Pernotti Silva et al. (1993); Sager et al. (1993)	ODP 810C	Shatsky Rise, Pac.		32°25.40' N, 157°50.74' E	C2n	1.934	28.6	28.6	C2n:1n (middle)	2.134	31.30	31.30	29.50	31.00	2.056	0.056	0.056	Y
Pearson (1995)	ODP 872B	Lo-En Guyot, Pac.		10°05.85' N, 162°51.96' E	Top G. <i>finilosa</i>	1.880	7.06	7.60	Bottom G. <i>finilosa</i>	3.33	19.09	20.15	9.58	10.54	2.202	0.097	0.093	Y
Expedition 320/321 Scientists (2010a); Wilkens et al. (2013); Tian et al. (2018)	IODP U1337A	Eastern equatorial Pac.		03°50.01' N, 123°12.36' W	The top	1.069	15.00	15.00	The bottom	1.781	27.330	27.330	18.04	20.66	1.320	0.076	0.076	Y
Expedition 320/321 Scientists (2010b); Wilkens et al. (2013)	IODP U1338A	Eastern equatorial Pac.		02°30.47' N, 117°58.16' W	C1r:1n	1.076	13.60	13.60	C2n-2r	2.610	34.800	34.800	16.37	24.21	1.560	0.284	0.284	Y

in Hole 758A. Our new record from IODP Hole U1488A (see Sect. 2 and Rosenthal et al., 2018e) yields a palaeomagnetic calibration within the Olduvai Subchron C2n of 1.86 Ma. We note that the *P. finalis* morphospecies becomes rare up section and has a second reappearance at a considerably higher level. The record at Hole U1337A (Expedition 320/321 Scientists, 2010a) has been tuned here to the astronomical age model of Tian et al. (2018) to yield a much younger age estimate of 1.32 Ma, which may be a function of the rarity of *Pulleniatina* in the higher-productivity environments of the eastern Pacific. There is little close agreement between the various calibrations but no clear geographic pattern that might suggest diachrony. The scatter is instead interpreted as more likely being a function of the high ecophenotypic variability of the genus and the rather subjective criteria for distinguishing *P. finalis* from *P. obliquiloculata*. We therefore propose a broad “global” calibration of 1.97 ± 0.17 Ma (pink band in Fig. 16).

3.13.2 Evolution

We regard the bioevent as a pseudospeciation caused by ongoing trends in the evolution of the *P. obliquiloculata* lineage relating to increasing size, involution, and streptospirality. Specimens attributed to the *P. finalis* morphotype are usually at the large end of the size range of populations, and it may well be that the shape change is largely accounted for by the addition of one or two extra chambers in the adult streptospiral (possibly a case of hypermorphosis or extended development), causing the test to be virtually planispiral in outward appearance.

3.14 LAD of *Pulleniatina praecursor*

3.14.1 Biochronology

We report five recalibrations of this bioevent (Table 13; Fig. 17) on the timescale of Raffi et al. (2020).

This bioevent is extremely subjective because of difficulties distinguishing the somewhat arbitrary and intergrading morphospecies *Pulleniatina praecursor* and *P. obliquiloculata*, especially given that sub-adult specimens of the latter can resemble the former, even in the modern ocean. Moreover, some authors do not include *P. praecursor* in their taxonomy, as discussed above in Sect. 3.6. When they first described *P. praecursor*, Banner and Blow (1967) suggested a disappearance level within the middle part of their “Zone N21” (i.e. around 2 Ma on modern timescales) based on their knowledge of spot samples and exploration boreholes around the world. At DSDP Site 62 on Eauripik Rise, western equatorial Pacific Ocean, Brönnimann et al. (1971) located the biohorizon in the interval between the Top of nannofossil *Discoaster brouweri* and the Top of *D. pentaradiatus*, which yields an indirect calibration of 1.99 Ma. Our own palaeomagnetic recalibration from IODP Hole U1488A points to a slightly higher level within the Olduvai Subchron C2n. In

Table 13. Recalibrations of the LAD of *P. praecursor*.

Reference	Location		Upper calibration event			Lower calibration event			Target event							
	Site	Physiographic feature	Grid reference	Event	Age (Ma)	Top con-straint (m)	Bottom con-straint (m)	Event	Age (Ma)	Top con-straint (m)	Bottom con-straint (m)	Age (Ma)	Calculated error + (Ma)	Calculated error – (Ma)	Plotted?	
Gupta and Thomas (1999)	DSDP 219	Arabian Sea, Ind.	09°01.75' N, 75°52.67' E	Top <i>D. aldispira</i> (Pac.)	3.47	30.45	31.95	Top <i>G. nepenthes</i>	4.38	48.45	49.95	33.74	3.560	0.076	0.076	Y
This study	IODP U1488A	Eauripik Rise, Pac.	02°02.59' N, 141°45.29' E	Clr.3r	1.775	39.50	39.53	C2n	1.934	43.23	43.55	42.90	1.855	0.066	0.061	Y
Brönnimann et al. (1971)	DSDP 62	Eauripik Rise, Pac.	01°52.2' N, 141°56.3' E	Top <i>D. brouweri</i>	1.930	42.00	42.00	Top <i>D. pentaradiatus</i>	2.390	59.000	61.000	44.000	1.994	0.017	0.015	Y
Hays et al. (1969)	V24-59	Central equatorial Pac.	02°34' N, 145°32' W	Clr.1n	1.076	445.00	445.00	Clr.2r	1.221	540	540	465	1.107	0.000	0.000	Y
Chaproniere and Nishi (1994)	ODP 834A	Lau Basin, Pac.	18°34.058' S, 177°51.735' W	C2An.2r	3.330	64.20	64.20	C2An.3n	3.596	71.9	71.900	68.59	3.497	0.016	0.016	Y

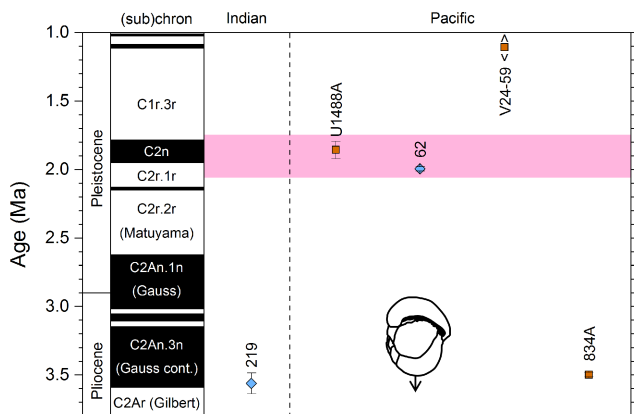


Figure 17. Biochronological constraints on the LAD of *Pulleniatina praecursor* arranged west to east. Brown squares are magnetostratigraphic, and blue diamonds are biochronological. The broad pink band shows the suggested summary calibration of 1.90 ± 0.15 Ma.

contrast, Hays et al. (1969) indicated the event at a much higher level in central Pacific Piston Core V24-59, within Subchron C1r.2r, which gives an approximate age (recalibrated here) of 1.11 Ma but with no known sampling error. Two much older calibrations are also available, one from DSDP Site 219 in the Indian Ocean and one from ODP Hole 834A in the Lau Basin (see Fig. 17). Without detailed morphometric data or descriptions, we cannot use this as evidence for diachrony, and thus we attribute it to divergent taxonomic concepts. We suggest a “global” calibration age of 1.90 ± 0.15 Ma to encompass the records at Site U1488 and 62, but stress the high level of subjectivity involved.

3.14.2 Evolution

We regard this bioevent as an example of pseudoextinction caused by ongoing evolutionary changes in the *P. obliquiloculata* lineage. For a short interval there are populations which can be divided arbitrarily between the *P. praecursor*, *P. obliquiloculata* and *P. finalis* morphospecies. As yet there is no evidence that these taxa are anything other than arbitrary and convenient subdivisions within an extended chronocline.

3.15 Top of “L5” coiling interval

3.15.1 Biochronology

We report 11 recalibrations of this bioevent (Table 14, Fig. 18).

A prominent coiling shift from sinistral to dextral dominance near the top of the Olduvai subchron has significant potential for recognition and correlation. It was first found by Hays et al. (1969) in central equatorial Pacific Piston Core V24-58. Kaneps (1973) found the event in several DSDP sites in the eastern equatorial Pacific although

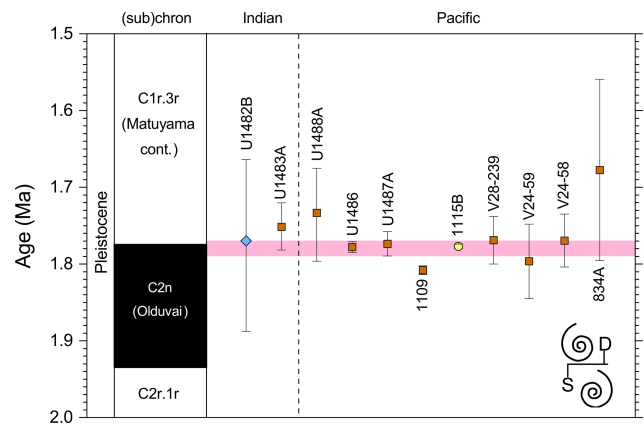


Figure 18. Biochronological constraints on the sinistral to dextral coiling shift (top “L5”) near the top of the Olduvai subchron, arranged from west to east. The gold circle is astrochronological, brown squares are magnetostratigraphic and the blue diamond is biochronological. The pink band shows the suggested summary calibration of 1.78 ± 0.01 Ma.

the data counts in that study are too low for precise correlation. Saito (1976) labelled the event “L5” in some records, although in others it is apparently labelled as “L4” or is ambiguous. Oda (1977, fig. 12) located the event to near the top of the Olduvai subchron in outcropping succession in Japan, but the magnetic polarity data are difficult to interpret in that study. The bioevent is defined here as an up-core shift from populations with $> 50\%$ sinistral specimens (usually $> 80\%$) to populations with consistently $< 20\%$ sinistral specimens that occur close to the top of Subchron C2n in the Indian and Pacific oceans. The high-resolution record of Pearson and Penny (2021) at IODP Site U1486 north of Papua New Guinea shows a run of intermediate values through the coiling transition from dominantly sinistral to dextral specimens and also reveals the existence of a short sinistrally dominant interval within the upper part of Subchron C2n that could be mistaken for the event in low-resolution records with spotty sampling. An astronomical calibration of 1.777 ± 0.003 Ma was provided by Chuang et al. (2018) based on the data of Chiang et al. (2018) and Resig et al. (2001) from ODP Site 1115 in the Woodlark Basin east of Papua New Guinea. This is within error of the palaeomagnetic calibration at IODP Site U1486, and also within error of the top of the Olduvai subchron itself (1.775 Ma; Raffi et al., 2020) (Fig. 4). Lower-resolution records are mostly in agreement. The only suspected diachrony is at ODP Site 1109, but that is probably a problem with the age model, which may have been affected by sedimentary disturbance, incompleteness or problems with magnetostratigraphy at that site (as discussed by Resig et al., 2001). The “global” calibration preferred here is 1.78 ± 0.01 Ma based on the high-resolution records at Sites 1115 and U1486.

Table 14. Recalibrations of the top of the “L5” coiling interval.

Reference	Location			Upper calibration event				Lower calibration event				Target event					
	Site	Physiographic feature	Grid reference	Event	Age (Ma)	Top con-straint (m)	Bottom con-straint (m)	Event	Age (Ma)	Top con-straint (m)	Bottom con-straint (m)	Top con-straint (m)	Bottom con-straint (m)	Age (Ma)	Calculated error + (Ma)	Calculated error – (Ma)	Plotted?
Rosenthal et al. (2018a)	IODP 1482B	NW Australian Margin, Ind.	15°03.31' S, 120°26.10' E	Core top	0.000	0.00	0.00	Top <i>G. fistulosa</i>	1.88	88.19	98.07	86.79	88.55	1.770	0.118	0.106	Y
Pearson and Penny (2021)	IODP U1483A	NW Australian Margin, Ind.	13°05.24' S, 121°48.25' E	C1r.3r	1.775	167.40	171.60	C2n	1.934	186.200	189.650	165.402	168.218	1.752	0.030	0.031	Y
Rosenthal et al. (2018e)	IODP U1488A	Eauripik Rise, Pac.	02°02.59' N, 141°45.29' E	C1r.3r	1.775	39.50	39.53	C2n	1.934	43.225	43.550	37.000	40.000	1.733	0.063	0.058	Y
Pearson and Penny (2021)	IODP U1486	Manus Basin, Pac.	02°22.34' S, 144°36.08' E	C1r.3r	1.775	109.74	109.74	C2n	1.934	124.460	124.460	109.360	110.670	1.778	0.007	0.007	Y
Rosenthal et al. (2018d)	IODP U1487A	Manus Basin, Pac.	02°19.99' S, 144°49.16' E	C1r.3r	1.775	53.18	53.80	C2n	1.934	63.200	64.030	52.700	54.100	1.774	0.016	0.016	Y
Resig et al. (2001)	ODP 1109	Woodlark Basin, Pac.	09°30.39' S, 151°34.39' E	C1r.3r	1.775	206.40	206.40	C2n	1.934	251.600	251.600	214.200	217.400	1.808	0.006	0.006	Y
Resig et al. (2001); Chuang et al. (2018)	ODP 1115B	Woodlark Basin, Pac.	09°11.38' S, 151°34.44' E											1.777	0.003	0.003	Y
Thompson and Sciarillo (1978)	V28-239	Central equatorial Pac.	03°15' N, 158°11' E	C1r.3r	1.775	1.78	1.78	C2n	1.934	1.934	1.934	1.738	1.800	1.769	0.031	0.031	Y
Saito (1976)	V24-59	Central equatorial Pac.	02°34' N, 145°32' W	C1r.3r	1.775	1.78	1.78	C2n	1.934	1.934	1.934	1.748	1.845	1.797	0.049	0.049	Y
Hays et al. (1969); Saito (1976)	V24-58	Central equatorial Pac.	02°16' N, 141°40' W	C1r.3r	1.775	1.78	1.78	C2n	1.934	1.934	1.934	1.735	1.804	1.770	0.035	0.035	Y
Chaproniere and Nishi (1994)	ODP 834A	Lau Basin, Pac.	18°34.058' S, 177°51.735' W	C1r.3r	1.775	32.60	32.60	C2n	1.934	35.3	35.3	28.94	32.95	1.678	0.118	0.118	Y

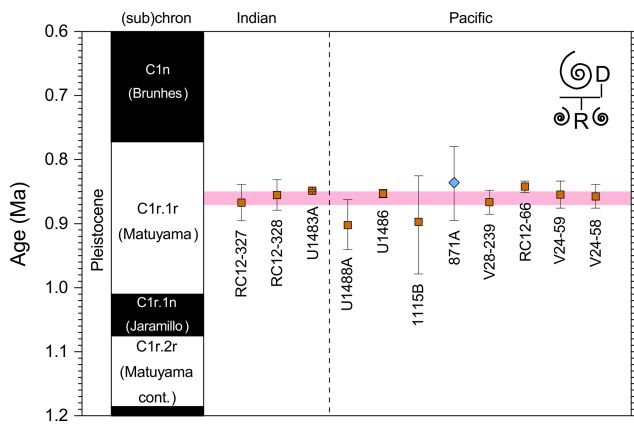


Figure 19. Biochronological constraints on the top of the “L1” coiling shift to sinistral dominance within Subchron C1r.1r, arranged west to east. Brown squares are magnetochronological calibrations, and the blue diamond is biochronological. The pink band shows the suggested summary calibration of 0.86 ± 0.01 Ma based on harmonizing all these records.

It is possible the same reversal occurs in the Atlantic sector, although records there are difficult to correlate. Bolli and Premoli Silva (1973) described a sinistral to dextral shift at a similar stratigraphic level at ODP Site 148 in the Caribbean Sea, followed by a switch to dextral and back to sinistral, and Saito (1976) also recorded two such events in three piston cores from the central and south Atlantic, labelling them “AL1” and “AL2” (for Atlantic left coiling intervals 1 and 2). More work is needed to determine if these events align with the Indo-Pacific (as we suspect) or are specific to the Atlantic Ocean as proposed by Saito (1976).

3.15.2 Evolution

The rapidity of the event suggests it is probably an example of a genetic sweep in which a cryptic population typified by dextral shells largely replaced the incumbent sinistral population, although without any other noticeable change in size or shape (Pearson and Penny, 2021).

3.16 “L1” coiling event

3.16.1 Biochronology

We report 11 recalibrations of this bioevent (Table 15, Fig. 19) on the timescale of Raffi et al. (2020).

This event is defined here as an up-core shift from populations with consistently $> 10\%$ sinistral specimens (usually around 50%) to populations with consistently $< 10\%$ sinistral specimens that occurs within the Matuyama Subchron C1r.1r in the Indian and Pacific oceans. Saito (1976) described it as the top of his “L1” coiling interval and recorded it in several piston cores across the Indian and Pacific oceans. The event was not included in the compilations of Berggren

et al. (1985a) and Berggren et al. (1995b), but Wade et al. (2011) proposed an indirect biostratigraphic calibration of 0.80 Ma on the timescale of Cande and Kent (1995) based on the record at ODP Hole 871A (Pearson, 1995). A total of 10 of the local events recalibrated here are palaeomagnetic calibrations, although many are old records estimated from published figures rather than replotted from data. Currently, the most precise calibrations are palaeomagnetic interpolations in the composite splice at IODP Site U1486 and in IODP Hole U1483A (North Australian Shelf, Indian Ocean) (Pearson and Penny, 2021). Tuned astronomical calibrations of these records can be expected in due course. Overall there is no evidence for diachrony; the shift could have occurred within ~ 20 kyr across the entire Indo-Pacific. The “global” Indo-Pacific calibration preferred here is 0.86 ± 0.01 Ma (pink band on Fig. 19).

3.16.2 Evolution

Pearson and Penny (2021) found that in both a Pacific Ocean site (IODP Site U1486) and Indian Ocean site (IODP Site U1483) the bioevent seems to have been caused by the reduction or near disappearance of sinistrally coiled shells. Single-shell stable isotope data suggest that sinistral and dextral populations occupied different but overlapping ecological niches prior to the bioevent. In both sites the sinistral forms have significantly more negative $\delta^{18}\text{O}$ values, which may indicate a preference for shallower or warmer-water conditions, while the carbon isotopes are significantly more negative in the Pacific site and more positive in the Indian Ocean site. There is also a significant size difference at the Pacific site, with sinistral shells being smaller on average. Pearson and Penny (2021) suggested that the evolution involved the extinction or near extinction of a largely cryptic sinistral genotype that was already restricted to the Indo-Pacific. Occasional sinistral shells are found from younger sediments at many sites across that region, but never in large numbers, and modern populations of *Pulleniatina* appear to be entirely dextral everywhere.

4 Summary and conclusions

We have conducted a thorough survey of bioevents in the history of the *Pulleniatina* clade using new data from IODP Hole U1488A in the equatorial Pacific and recalibrations of many published biohorizons worldwide using a consistent methodology and the timescale of Raffi et al. (2020) (Table 16). Events with the greatest potential for correlation are referred to as primary events. These are generally objective, such as the first appearance of the genus, the terminal extinction of the *spectabilis* lineage, biogeographic expansions and contractions in and out of the Atlantic, and widespread shifts in the dominant coiling direction. The latter events in particular are proving to be remarkably rapid and potentially near synchronous either globally or spanning

Table 15. Recalibrations of the “LJ” coiling event.

Reference	Location			Upper calibration event				Lower calibration event				Target event					
	Site	Physiographic feature	Grid reference	Event	Age (Ma)	Top con-straint (m)	Bottom con-straint (m)	Event	Age (Ma)	Top con-straint (m)	Bottom con-straint (m)	Top con-straint (m)	Bottom con-straint (m)	Age (Ma)	Calculated error + (Ma)	Calculated error – (Ma)	Plotted?
Saito (1976)	RC12-327	Western equatorial Ind.	01°44' N, 57°50' E	ClIn	0.773	0.77	0.77	Clr.Ir	1.008	0.990	0.990	0.834	0.886	0.867	0.028	0.028	Y
Saito (1976)	RC12-328	Western equatorial Ind.	03°57' N, 60°36' E	ClIn	0.773	0.77	0.77	Clr.Ir	1.008	0.990	0.990	0.827	0.871	0.855	0.024	0.024	Y
Pearson and Penny (2021)	IODP U1483A	NW Australian Margin, Ind.	13°05.24' S, 121°48.25' E	Clr.Ir	1.008	96.04	96.04	Clr.In	1.076	103.125	103.125	79.223	79.613	0.848	0.002	0.002	Y
Rosenthal et al. (2018e)	IODP U1488A	Eauripik Rise, Pac.	02°02.59' N, 141°45.29' E	ClIn	0.773	18.58	18.75	Clr.Ir	1.008	23.780	23.830	20.690	22.290	0.902	0.039	0.039	Y
Pearson and Penny (2021)	IODP U1486	Manus Basin, Pac.	02°22.34' S, 144°36.08' E	ClIn	0.773	51.20	51.20	Clr.Ir	1.008	59.995	59.995	53.950	54.450	0.853	0.007	0.007	Y
Resig et al. (2001)	ODP 1115B	Woodlark Basin, Pac.	09°11.38' S, 151°34.44' E	ClIn	0.773	17.50	18.00	Clr.Ir	1.008	21.500	22.500	19.000	21.000	0.897	0.081	0.072	Y
Pearson (1995)	ODP 871A	Limalok Guyo, Pac.	05°33.43' N, 172°20.69' E	Core top	0.000	0.00	0.00	Top G. <i>fastulosa</i>	1.880	17.000	17.600	7.300	8.090	0.836	0.058	0.056	Y
Thompson and Sciarrillo (1978)	V28-239	Central equatorial Pac.	03°15' N, 158°11' E	ClIn	0.773	0.77	0.77	Clr.Ir	1.008	0.990	0.990	0.842	0.877	0.867	0.019	0.019	Y
Saito et al. (1975); Saito (1976)	RC12-66	Central equatorial Pac.	02°36.6' N, 148°12.8' W	ClIn	0.773	0.77	0.77	Clr.Ir	1.008	0.990	0.990	0.829	0.845	0.842	0.009	0.009	Y
Saito (1976)	V24-59	Central equatorial Pac.	02°34' N, 145°32' W	ClIn	0.773	0.77	0.77	Clr.Ir	1.008	0.990	0.990	0.829	0.868	0.855	0.021	0.021	Y
Hays et al. (1969); Saito (1976)	V24-58	Central equatorial Pac.	02°16' N, 141°40' W	ClIn	0.773	0.77	0.77	Clr.Ir	1.008	0.990	0.990	0.834	0.868	0.857	0.018	0.018	Y

Table 16. Summary of bioevents.

Primary bioevent	Secondary bioevent	Interpretation	Age (Ma), Raffi et al. (2020)	Age (Ma), this study	Error \pm (Ma)	Main reference(s)
"L1" coiling shift		Population sweep	0.79	0.86	0.01	Saito (1976); Pearson and Penny (2021)
Top "L5" coiling shift		Population sweep		1.78	0.01	Chuang et al. (2018); Pearson and Penny (2021)
	LAD <i>P. praecursor</i>	Pseudoextinction		1.90	0.15	Brönnimann and Resig (1971); this study
	FAD <i>P. finalis</i>	Pseudospeciation	2.04	1.97	0.17	Chaisson and Pearson (1997); this study
Bottom "L5" coiling shift		Population sweep		2.02	0.01	Chaproniere and Nishi (1994); Pearson and Penny (2021)
Atlantic reappearance		Dispersal	2.26	2.24	0.02	Chaisson and Pearson (1997); Maniscalco and Brunner (1998); Fraass et al. (2017)
Atlantic disappearance		Contraction	3.41	3.37	0.005	Chaisson and Pearson (1997); Fraass et al. (2017)
	LAD <i>P. primalis</i>	Pseudoextinction	3.66	4.00	0.60	Chaproniere and Nishi (1994); Pearson (1995); this study
"L9" coiling shift (Pacific Ocean)		Population sweep	4.08	4.06	0.02	Chaisson and Pearson (1997); Groeneveld et al. (2021); Expedition 320/321 Scientists (2010a, b); this study
LAD <i>P. spectabilis</i>		Extinction	4.21	4.27	0.05	Hays et al. (1969); Chaisson and Leckie (1993); Expedition 320/321 Scientists (2010b); Kaushik et al. (2020); this study
	FAD <i>P. obliquiloculata</i>	Pseudospeciation		4.22	0.12	Weaver and Raymo (1986); Kaushik et al. (2020); this study
	FAD <i>P. praecursor</i>	Pseudospeciation		4.52	0.10	Brönnimann and Resig (1971); Saito (1985); this study
	FAD <i>P. spectabilis</i>	Pseudospeciation		5.14	0.10	Expedition 320/321 Scientists (2010b); this study
FAD <i>P. primalis</i> (Atlantic Ocean)		Dispersal		5.33	0.25	Chaisson and Pearson (1997)
	FAD <i>P. praespectabilis</i>	Pseudospeciation		5.98	0.05	Brönnimann and Resig (1971); this study
FAD <i>P. primalis</i> (tropical Indo-Pacific)		Speciation	6.57	6.50	0.10	Jenkins (1978); Keigwin (1982); Chaisson and Leckie (1993); Expedition 320/321 Scientists (2010a); Lam et al. (2022); this study.

the Indo-Pacific. The secondary events are all apparently gradual, caused by gradual evolutionary change producing pseudospeciations or pseudoextinctions that rely on subjective boundaries between morphospecies. Because most of the literature is site or expedition specific, very few studies have involved direct comparison of assemblages between sites. The bioevents are nevertheless useful for providing general constraints, and their future use will benefit from

improved taxonomic discrimination between morphospecies and/or morphometric studies to ensure greater consistency between workers.

The evolutionary history of the *Pulleniatina* clade is summarized in Fig. 20. This includes an interpretation of the genus as consisting of two main lineages, one of which (the *spectabilis* lineage) became extinct around 4.27 Ma. Gradual evolution caused the lineages to track through areas of mor-

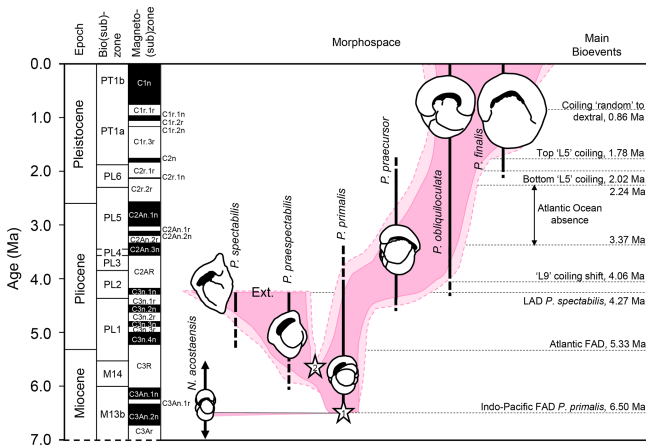


Figure 20. Summary of *Pulleniatina* evolution and biochronology as currently understood. The shaded field is an interpretation of the way the genus has evolved through morphospace, as divided into six named morphospecies. Lighter shading represents age uncertainty. Cartoons are based on the holotype specimens and are approximately to scale. Cladogenetic events are shown in stars: (1) split between the *N. acostaensis* and *Pulleniatina* lineages and (2) split between the *spectabilis* and main lineages. “Ext.” represents the one genuine extinction in the group. Modified from Pearson and Penny (2021).

phospace delineated as six named morphospecies. Within the lineages there has been a great deal of evolution, sometimes involving rapid global changes in the coiling ratio.

Data availability. Data are available in the NERC EDS Geoscience Data Centre at <https://doi.org/10.5285/14fb1745-00ed-4a0d-922b-d2c94157d17f> (Pearson, 2023).

Author contributions. BSW and PNP conceptualized the research and developed the methods. PNP conducted the investigation and prepared the manuscript with contributions from all authors. JY enabled the map plotting via the mikrotax web portal.

Competing interests. The contact author has declared that none of the authors has any competing interests.

Disclaimer. Publisher’s note: Copernicus Publications remains neutral with regard to jurisdictional claims made in the text, published maps, institutional affiliations, or any other geographical representation in this paper. While Copernicus Publications makes every effort to include appropriate place names, the final responsibility lies with the authors.

Acknowledgements. We used data provided by the International Ocean Discovery Program and samples from IODP Expedition 363,

Site U1488. We thank Anna Joy Drury and Alessio Fabbrini for commenting on the manuscript. We thank the reviewers for their insightful comments.

Financial support. This research has been supported by the Natural Environment Research Council (grant nos. NE/P019013/1 and NE/P016375/1).

Review statement. This paper was edited by Sev Kender and reviewed by Hiroki Hayashi and Raphael Morard.

References

- An, Y. and Jian, Z.: *Pulleniatina* Minimum Event during the last deglaciation in the southern South China Sea, Chinese Sci. Bull., 54, 4514–4519, <https://doi.org/10.1007/s11434-009-0290-4>, 2009.
- André, A., Quillevère, F., Morard, R., Ujjié, Y., Escarguel, G., De Vargas, C., de Garidel-Thoron, T., and Douady, C. J.: SSU rDNA divergence in planktonic foraminifera: molecular taxonomy and biogeographic implications, PLoS One, 9, e104641, <https://doi.org/10.1371/journal.pone.0104641>, 2014.
- Azibeiro, L. A., Kučera, M., Jonkers, L., Cloke-Hayes, A., and Sierro, F. J.: Nutrients and hydrography explain the composition of recent Mediterranean planktonic foraminiferal assemblages, Mar. Micropaleontol., 179, 10220, <https://doi.org/10.1016/j.marmicro.2022.102201>, 2023.
- Bandy, O. L.: Miocene-Pliocene boundary in the Philippines as related to late Tertiary stratigraphy of deep-sea sediments, Science, 142, 1290–1292, 1963.
- Banner, F. T. and Blow, W. H.: Progress in the planktonic foraminiferal biostratigraphy of the Neogene, Nature, 208, 1164–1166, 1965.
- Banner, F. T. and Blow, W. H.: The origin, evolution and taxonomy of the foraminiferal genus *Pulleniatina* Cushman, 1927, Micropaleontology, 13, 133–162, 1967.
- Barton, C. E. and Bloemendal, J.: Paleomagnetism of sediments collected during Leg 90, southwest Pacific, Init. Repts DSDP, 90, 1273–1316, <https://doi.org/10.2973/dsdp.proc.90.136.1986>, 1986.
- Bé, A. W. and Hutson, W. H.: Ecology of planktonic foraminifera and biogeographic patterns of life and fossil assemblages in the Indian Ocean, Micropaleontology, 23, 369–414, 1977.
- Beckmann, J. P.: The foraminifera of Sites 68 to 75, Initial Rep. Deep Sea, 8, 713–725, <https://doi.org/10.2973/dsdp.proc.8.111.1971>, 1971.
- Beckmann, J. P.: The foraminifera and some associated microfossils of Sites 135 to 144, Initial Rep. Deep Sea, 14, 389–420, <https://doi.org/10.2973/dsdp.proc.14.113.1972>, 1972.
- Belyea, P. R. and Thunell, R. C.: Fourier shape analysis and planktonic foraminiferal evolution: the *Neogloboquadrina-Pulleniatina* lineages, J. Paleontol., 1026–1040, 1984.
- Berggren, W. A., Kent, D. V., and Van Couvering, J. A.: The Neogene: Part 2. Neogene geochronology and chronostratigraphy, in: The Chronology of the Geological Record, edited by:

- Snelling, N. J., Geological Society Memoir 10, Blackwell, 211–260, 1985a.
- Berggren, W. A., Kent, D. V., Flynn, J. J., and Van Couvering, J. A.: Cenozoic geochronology, *Geol. Soc. Am. Bull.*, 96, 1407–1418, 1985b.
- Berggren, W. A., Hilgen, F. J., Langereis, C. G., Kent, D. V., Obradovich, J. D., Raffi, I., Raymo, M. E., and Shackleton, N. J.: Late Neogene chronology: new perspectives in high-resolution stratigraphy, *Geol. Soc. Am. Bull.*, 107, 1272–1287, 1995a.
- Berggren, W. A., Kent, D. V., Swisher, C. C., and Aubry, M.-P.: A revised Cenozoic geochronology and chronostratigraphy, in: *Geochronology, Time Scales and Global Stratigraphic Correlation*, edited by: Berggren, W. A., Kent, D. V., Aubry, M.-P., and Hardenbol, J., SEPM Society for Sedimentary Geology, <https://doi.org/10.2110/pec.95.04>, 1995b.
- Blow, W. H.: Late Middle Eocene to Recent planktonic foraminiferal biostratigraphy, *Proceedings of the First International Conference on Planktonic Microfossils (Geneva, 1967)*, Vol. 1, E. J. Brill, Leiden, 199–422, 1969.
- Blow, W. H.: *The Cainozoic Globigerinida*, E. J. Brill, Leiden, 3 Volumes, 1413 pp., 1979.
- Bolli, H. M. and Krasheninnikov, V. A.: Problems in Paleogene and Neogene correlations based on planktonic foraminifera, *Micropaleontology*, 23, 436–452, 1977.
- Bolli, H. M. and Premoli Silva, I.: Oligocene to Recent planktonic foraminifera and stratigraphy of the Leg 15 sites in the Caribbean Sea, *Initial Rep. Deep Sea*, 15, 475–497, <https://doi.org/10.2973/dsdp.proc.15.110.1973>, 1973.
- Bolli, H. M. and Saunders, J. B.: Oligocene to Holocene low latitude planktic foraminifera, in: *Plankton stratigraphy: volume 1*, edited by: Bolli, H. M., Saunders, J. B., and Perch-Nielsen, K., Cambridge University Press, Cambridge, 155–262, 1985.
- Bolli, H. M., Loeblich, A. R., and Tappan, H.: Planktonic foraminiferal families Hantkeninidae, Orbulinidae, Globorotaliidae and Globotruncanidae, in: *Studies in Foraminifera*, edited by: Loeblich, A. R., Tappan, H., Beckmann, J. P., Bolli, H. M., Montanaro Gallitelli, E., and Troelsen, J. C., U.S. Government Printing Office, United States National Museum Bulletin, 215, 3–50, 1957.
- Bolli, H. M., Saunders, J. B., and Perch-Nielsen, K. (Eds.): *Plankton stratigraphy: volume 1, Planktic Foraminifera, Calcareous Nanofossils and Calpionellids*, Cambridge University Press, Cambridge, 1985.
- Boscolo-Galazzo, F., Jones, A., Dunkley Jones, T., Crichton, K. A., Wade, B. S., and Pearson, P. N.: Late Neogene evolution of modern deep-dwelling plankton, *Biogeosciences*, 19, 743–762, <https://doi.org/10.5194/bg-19-743-2022>, 2022.
- Bown, P., Coe, A., Cope, J., Edgar, K., Harper, D., Marshall, J., Wakefield, M., Pearson, P. N., and Zalasiewicz, J.: Biostratigraphy – using fossils to date and correlate rock, in: *Deciphering Earth's History: the Practice of Stratigraphy*, edited by: Coe, A. L., Geological Society of London, ISBN: 9781786205742, 2022.
- Brönnimann, P. and Resig, J.: A Neogene globigerinacean biochronologic time-scale of the southwestern Pacific, *Initial Rep. Deep Sea*, 7, 1235–1469, <https://doi.org/10.2973/dsdp.proc.7.128.1971>, 1971.
- Brönnimann, P., Martini, E., Resig, J., Riedel, W. R., Sanfilippo, A., and Worsley, T.: Biostratigraphic synthesis: Late Oligocene and Neogene of the Western Tropical Pacific, *Initial Rep. Deep Sea*, 7, 1723–1745, <https://doi.org/10.2973/dsdp.proc.7.136.1971>, 1971.
- Brummer, G.-J. A. and Kučera, M.: Taxonomic review of living planktonic foraminifera, *J. Micropaleontol.*, 41, 29–74, <https://doi.org/10.5194/jm-41-29-2022>, 2022.
- Cande, S. C. and Kent, D. V.: Revised calibration of the geomagnetic polarity timescale for the Late Cretaceous and Cenozoic, *J. Geophys. Res.*, 100, 6093–6095, 1995.
- Casalbore, D., Romagnoli, C., Chiocci, F., and Frezza, V.: Morpho-sedimentary characteristics of the volcanoclastic apron around Stromboli volcano (Italy), *Mar. Geol.*, 269, 132–148, <https://doi.org/10.1016/j.margeo.2010.01.004>, 2010.
- Chaisson, W. P.: Planktonic foraminiferal assemblages and palaeoceanographic change in the transtropical Pacific Ocean: a comparison of west (Leg 130) and east (Leg 138), latest Miocene to Pleistocene, *Proc. ODP Sci. Res.*, 555–597, <https://doi.org/10.2973/odp.proc.sr.138.129.1995>, 1995.
- Chaisson, W. P. and D'Hondt, S. L.: Neogene planktonic foraminifer biostratigraphy at Site 999, western Caribbean Sea, *Proc. ODP Sci. Res.*, 165, 19–56, <https://doi.org/10.2973/odp.proc.sr.165.010.2000>, 2000.
- Chaisson, W. P. and Leckie, R. M.: High-resolution Neogene planktonic foraminifer biostratigraphy of Site 806, Ontong Java Plateau (Western Equatorial Pacific), *Proc. ODP Sci. Res.*, 130, 137–178, <https://doi.org/10.2973/odp.proc.sr.130.010.1993>, 1993.
- Chaisson, W. P. and Pearson, P. N.: Planktonic foraminifer biostratigraphy at Site 925: Middle Miocene–Pleistocene, *Proc. ODP Sci. Res.*, 154, 3–32, <https://doi.org/10.2973/odp.proc.sr.154.104.1997>, 1997.
- Chaproniere, G. H. and Nishi, H.: Miocene to Pleistocene planktonic foraminifer biostratigraphy of the Lau Basin and Tongan Platform, Leg 135, *Proc. ODP Sci. Res.*, 135, 207–229, <https://doi.org/10.2973/odp.proc.sr.135.117.1994>, 1994.
- Chaproniere, G. H., Styzen, M., Sager, W., Nishi, H., Quinterno, P., and Abrahamsen, N.: Late Neogene biostratigraphic and magnetostratigraphic synthesis, Leg 135, *Proc. ODP Sci. Res.*, 135, 857–877, <https://doi.org/10.2973/odp.proc.sr.135.116.1994>, 1994.
- Chiang, M., Wei, K.-Y., Chuang, C.-K., and Lo, L.: Two left-coiling events of planktonic foraminifer genus *Pulleniatina* during the early Pleistocene: Insights from population dynamics observed from foraminiferal assemblages in Core ODP 1115B, western equatorial Pacific, *Western Pacific Earth Sciences*, 15–18, 53–82, 2018.
- Chuang, C.-K., Lo, L., Zeeden, C., Chou, Y.-M., Wei, K.-Y., Shen, C.-C., Mii, H.-S., Chang, Y.-P., and Tung, Y.-H.: Integrated stratigraphy of ODP Site 1115 (Solomon Sea, southwestern equatorial Pacific) over the past 3.2 Ma, *Mar. Micropaleontol.*, 144, 25–37, <https://doi.org/10.1016/j.marmicro.2018.09.003>, 2018.
- Cifelli, R.: Radiation of Cenozoic planktonic foraminifera, *Syst. Zool.*, 18, 154–168, 1969.
- Cushman, J. A.: An outline of a reclassification of the Foraminifera, *Contributions from the Cushman Laboratory for Foraminiferal Research*, 3, 1–105, 1927.
- Dang, H., Jian, Z., Wu, J., Bassinot, F., Wang, T., and Kissel, C.: The calcification depth and Mg/Ca thermometry of *Pulleniatina obliquiloculata* in the tropical Indo-

- Pacific: A core-top study, *Mar. Micropaleontol.*, 145, 28–40, <https://doi.org/10.1016/j.marmicro.2018.11.001>, 2018.
- Drury, A. J., Westerhold, T., Frederichs, T., Tian, J., Wilkens, R., Channell, J. E., Evans, H., John, C. M., Lyle, M., and Röhl, U.: Late Miocene climate and time scale reconciliation: Accurate orbital calibration from a deep-sea perspective, *Earth Planet Sc. Lett.*, 475, 254–266, <https://doi.org/10.1016/j.epsl.2017.07.038>, 2017.
- Drury, A. J., Lee, G. P., Gray, W. R., Lyle, M., Westerhold, T., Shevenell, A. E., and John, C. M.: Deciphering the state of the Late Miocene to Early Pliocene Equatorial Pacific, *Paleoceanogr. Paleocl.*, 33, 246–263, <https://doi.org/10.1002/2017PA003245>, 2018.
- Dunhill, A., Renaudie, J., Young, J. R., Fenton, I. S., Saupe, E. E., Woodhouse, A., Aze, T., and Lazarus, D.: Triton, a new database of Cenozoic Planktonic Foraminifera, FigShare [data set], <https://doi.org/10.6084/m9.figshare.c.5242154>, 2021.
- Expedition 320/321 Scientists: Site U1337, Proceedings of the International Ocean Discovery Program, 320/321, <https://doi.org/10.2204/iodp.proc.320321.109.2010>, 2010a.
- Expedition 320/321 Scientists: Site U1338, Proceedings of the International Ocean Discovery Program, 320/321, <https://doi.org/10.2204/iodp.proc.320321.110.2010>, 2010b.
- Farrell, J. W. and Janecek, T. R.: Late Neogene paleoceanography and paleoclimatology of the Northeastern Indian Ocean (Site 758), *Proc. ODP Sci. Res.*, 121, 297–355, <https://doi.org/10.2973/odp.proc.sr.121.124.1991>, 1991.
- Fenton, I. S., Baranowski, U., Boscolo-Galazzo, F., Cheales, H., Fox, L., King, D. J., Larkin, C., Latas, M., Liebrand, D., Miller, C. G., Nilsson-Kerr, K., Piga, E., Pugh, H., Rimmelzwaal, S., Roseby, Z. A., Smith, Y. M., Stukins, S., Taylor, B., Woodhouse, A., Worne, S., Pearson, P. N., Poole, C. R., Wade, B. S., and Purvis, A.: Factors affecting consistency and accuracy in identifying modern macroperforate planktonic foraminifera, *J. Micropalaeontol.*, 37, 431–443, <https://doi.org/10.5194/jm-37-431-2018>, 2018.
- Fenton, I. S., Woodhouse, A., Aze, T., Lazarus, D., Renaudie, J., Dunhill, A. M., Young, J. R., and Saupe, E. E.: Triton, a new species-level database of Cenozoic planktonic foraminiferal occurrences, *Sci. Data*, 8, 1–9, <https://doi.org/10.1038/s41597-021-00942-7>, 2021.
- Fleisher, R. L.: Cenozoic planktonic foraminifera and biostratigraphy, Arabian Sea Deep Sea Drilling Project, Leg 23A, Initial Rep. Deep Sea, 23, 1001–1072, <https://doi.org/10.2973/dsdp.proc.23.139.1974>, 1974.
- Fraass, A. J., Wall-Palmer, D., Leckie, R. M., Hatfield, R. G., Burns, S. J., Le Friant, A., Ishizuka, O., Ajahdali, M., Jutzeler, M., Martinez-Colon, M., Palmer, M. R., and Talling, P. J.: A revised Plio-Pleistocene age model and paleoceanography of the northeastern Caribbean Sea: IODP Site U1396 off Montserrat, Lesser Antilles, *Stratigraphy*, 13, 183–203, <https://doi.org/10.29041/strat.13.3.183-203>, 2017.
- Groeneveld, J., De Vleeschouwer, D., McCaffrey, J. C., and Gallagher, S. J.: Dating the northwest shelf of Australia since the Pliocene, *Geochem. Geophys. Geosy.*, 22, e2020GC009418, <https://doi.org/10.1029/2020GC009418>, 2021.
- Gupta, A. K. and Thomas, E.: Latest Miocene-Pleistocene Productivity and Deep-sea Ventilation in the Northwestern Indian Ocean (Deep Sea Drilling Project Site 219), *Paleoceanography*, 14, 62–73, 1999.
- Hayashi, H., Asano, S., Yamashita, Y., Tanaka, T., and Nishi, H.: Data report: late Neogene planktonic foraminiferal biostratigraphy of the Nankai Trough, IODP Expedition 315, Proceedings of the International Ocean Discovery Program, 314/315/316, <https://doi.org/10.2204/iodp.proc.314315316.206.2011>, 2011.
- Hayashi, H., Idemitsu, K., Wade, B. S., Idehara, Y., Kimoto, K., Nishi, H., and Matsui, H.: Middle Miocene to Pleistocene planktonic foraminiferal biostratigraphy in the eastern equatorial Pacific Ocean, *Paleontol. Res.*, 17, 91–109, <https://doi.org/10.2517/1342-8144-17.1.91>, 2013.
- Hays, J. D., Saito, T., Opdyke, N. D., and Burckle, L. H.: Pliocene-Pleistocene sediments of the equatorial Pacific: their paleomagnetic, biostratigraphic, and climatic record, *Geol. Soc. Am. Bull.*, 80, 1481–1514, 1969.
- Jenkins, D. G.: Neogene planktonic foraminifera from DSDP Leg 40 Sites 360 and 362 in the southeastern Atlantic, Initial Rep. Deep Sea, 40, 723–739, <https://doi.org/10.2973/dsdp.proc.40.116.1978>, 1978.
- Jenkins, D. G. and Orr, W. N.: Planktonic Foraminiferal Biostratigraphy of the Eastern Equatorial Pacific–DSDP Leg 9, Initial Rep. Deep Sea, 9, 1059–1193, <https://doi.org/10.2973/dsdp.proc.9.125.1972>, 1972.
- Jenkins, D. G. and Srinivasan, M. S.: Cenozoic planktonic foraminifera from the equator to the subantarctic of the southwest Pacific, Initial Rep. Deep Sea, 90, 795–834, <https://doi.org/10.2973/dsdp.proc.90.113.1986>, 1986.
- Jenkins, D. G., Whittaker, J. E., and Carlton, R.: On the age and correlation of the St. Erth Beds, S.W. England, based on planktonic foraminifera, *J. Micropalaeontol.*, 5, 25, <https://doi.org/10.1144/jm.5.2.93>, 1986.
- Jonkers, L. and Kučera, M.: Global analysis of seasonality in the shell flux of extant planktonic Foraminifera, *Biogeosciences*, 12, 2207–2226, <https://doi.org/10.5194/bg-12-2207-2015>, 2015.
- Kaneps, A. G.: Cenozoic planktonic foraminifera from the eastern equatorial Pacific Ocean, Initial Rep. Deep Sea, 16, 713–745, <https://doi.org/10.2973/dsdp.proc.16.127.1973>, 1973.
- Kaushik, T., Singh, A. K., and Sinha, D. K.: Late Neogene–Quaternary Planktic Foraminiferal Biostratigraphy and Biochronology from ODP Site 807A, Ontong Java Plateau, Western Equatorial Pacific, *J. Foraminin. Res.*, 50, 111–127, <https://doi.org/10.2113/gsjfr.50.2.111>, 2020.
- Keigwin, L. D.: Pliocene closing of the Isthmus of Panama, based on biostratigraphic evidence from nearby Pacific Ocean and Caribbean Sea cores, *Geology*, 6, 630–634, 1978.
- Keigwin, L. D.: Neogene Planktonic Foraminifera from Deep Sea Drilling Project Sites 502 and 503, Initial Rep. Deep Sea, 68, 269–288, <https://doi.org/10.2973/dsdp.proc.68.105.1982>, 1982.
- Kennett, J. P.: Middle and Late Cenozoic planktonic foraminiferal biostratigraphy of the Southwest Pacific – DSDP Leg 21, Initial Rep. Deep Sea, 21, 575–639, <https://doi.org/10.2973/dsdp.proc.21.117.1973>, 1973.
- Kennett, J. P. and Srinivasan, M. S.: Neogene Planktonic Foraminifera, a Phylogenetic Atlas, Hutchinson Ross, Stroudsburg, Pennsylvania, 265 pp., 1983.
- Kent, D. V. and Spariosu, D. J.: Magnetostratigraphy of equatorial Pacific Site 502 hydraulic piston cores, Initial Rep. Deep Sea, 68, 435–440, <https://doi.org/10.2973/dsdp.proc.68.117.1982>, 1982a.

- Kent, D. V. and Spariosu, D. J.: Magnetostratigraphy of Caribbean Site 503 hydraulic piston cores, Initial Rep. Deep Sea, 68, 419–434, <https://doi.org/10.2973/dsdp.proc.68.116.1982>, 1982b.
- King, D. J., Wade, B. S., Liska, R. D., and Miller, C. G.: A review of the importance of the Caribbean region in Oligo-Miocene low latitude planktonic foraminiferal biostratigraphy and the implications for modern biogeochronological schemes, Earth-Sci. Rev., 202, 102968, <https://doi.org/10.1016/j.earscirev.2019.102968>, 2020.
- King, D. J., Wade, B. S., and Miller, C. G.: Biostratigraphic utility of coiling direction in Miocene planktonic foraminiferal genus *Paragloborotalia*, Newsl. Stratigr., 56, 331–355, <https://doi.org/10.1127/nos/2023/0681>, 2023.
- Krashennikov, V. A. and Hoskins, R. H.: Late Cretaceous, Paleogene and Neogene planktonic Foraminifera, Initial Rep. Deep Sea, 20, 105–203, <https://doi.org/10.2973/dsdp.proc.20.110.1973>, 1973.
- Lam, A. R. and Leckie, R. M.: Subtropical to temperate late Neogene to Quaternary planktic foraminiferal biostratigraphy across the Kuroshio Current Extension, Shatsky Rise, northwest Pacific Ocean, PLoS ONE, 15, e0234351, <https://doi.org/10.1371/journal.pone.0234351>, 2020.
- Lam, A. R., Crundwell, M. P., Leckie, R. M., Albanese, J., and Uzel, J. P.: Diachroneity rules the mid-latitudes: A test case using Late Neogene planktic foraminifera across the Western Pacific, Geosciences, 12, 190, <https://doi.org/10.3390/geosciences12050190>, 2022.
- Lamb, J. L. and Beard, J. H.: Late Neogene planktonic foraminifera in the Caribbean, Gulf of Mexico, and Italian stratotypes, The University of Kansas Paleontological Contributions, 57 (Protozoa 8), 1972.
- Laskar, J., Robutel, P., Joutel, F., Gastineau, M., Correia, A. C. M., and Levrard, B.: A long-term numerical solution for the insolation quantities of the Earth, Astron. Astrophys., 428, 261–285, <https://doi.org/10.1051/0004-6361:20041335>, 2004.
- Laskar, J., Fienga, A., Gastineau, M., and Manche, K.: La2010: a new orbital solution for the long-term motion of the Earth, Astron. Astrophys., 532, A89, <https://doi.org/10.1051/0004-6361/201116836>, 2011.
- Lastam, J., Griesshaber, E., Yin, X., Rupp, U., Sánchez-Almazo, I., Heß, M., Walther, P., Checa, A., and Schmahl, W. W.: The unique fibrillar to platy nano- and microstructure of twinned rotaliid foraminiferal shell calcite, Sci. Rep., 13, 2189, <https://doi.org/10.1038/s41598-022-25082-9>, 2023.
- Li, B., Jian, Z., Li, Q., Tian, J., and Wang, P.: Paleooceanography of the South China Sea since the middle Miocene: evidence from planktonic foraminifera, Mar. Micropaleontol., 54, 49–62, <https://doi.org/10.1016/j.marmicro.2004.09.003>, 2005.
- Lin, Y. S., Wei, K. Y., Lin, I. T., Yu, P. S., Chiang, H. W., Chen, C. Y., Shen, C. C., Mii, H. S., and Chen, Y. G.: The Holocene *Pulleniatina* Minimum Event revisited: Geochemical and faunal evidence from the Okinawa Trough and upper reaches of the Kuroshio current, Mar. Micropaleontol., 59, 153–170, <https://doi.org/10.1016/j.marmicro.2006.02.003>, 2006.
- Lirer, F., Foresi, L. M., Iaccarino, S., Salvatorini, G., Turco, E., Cosentino, C., Sierro, F. J., and Caruso, A.: Mediterranean Neogene planktonic foraminifer biozonation and biochronology, Earth Sci. Rev., 196, 102869, <https://doi.org/10.1016/j.earscirev.2019.05.013>, 2019.
- Lourens, L. J., Hilgen, F. J., Shackleton, N. J., Laskar, J., and Wilson, D.: The Neogene Period, in: Geological Time Scale 2004, edited by: Gradstein, F. M., Ogg, J. G., and Smith, A. G., Cambridge University Press, 409–440, 2004.
- Maniscalco, R. and Brunner, C. A.: Neogene and Quaternary planktonic foraminiferal biostratigraphy of the Canary Island Region, Proc. ODP Sci. Res., 157, 115–124, <https://doi.org/10.2973/odp.proc.sr.157.109.1998>, 1998.
- Moullade, M.: Upper Neogene and Quaternary planktonic foraminifera from the Blake Outer Ridge and Blake-Bahama Basin (Western North Atlantic), Deep Sea Drilling Project Leg 76, Sites 533 and 534, Initial Rep. Deep Sea, 76, 511–535, <https://doi.org/10.2973/dsdp.proc.76.119.1983>, 1983.
- Nathan, S. A. and Leckie, R. M.: Miocene planktonic foraminiferal biostratigraphy of Sites 1143 and 1146, ODP Leg 184, South China Sea, Proc. ODP Sci. Res., 184, 1–43, <https://doi.org/10.2973/odp.proc.sr.184.219.2003>, 2003.
- Natori, H.: Planktonic foraminiferal biostratigraphy and datum planes in the Late Cenozoic sedimentary sequence in Okinawa-jima, Japan, Progress in Micropaleontology, edited by: Takayanagi, Y. and Saito, T., Micropaleontology Press, 214–248, 1976.
- Norris, R. D.: Parallel evolution in the keel structure of planktonic foraminifera, J. Foramin. Res., 21, 319–331, 1991.
- Norris, R. D.: Planktonic foraminifer biostratigraphy: Eastern Equatorial Atlantic, Proc. ODP Sci. Res., 159, 445–479, <https://doi.org/10.2973/odp.proc.sr.159.036.1998>, 1998.
- Oda, M.: Planktonic foraminiferal biostratigraphy of the Late Cenozoic sedimentary sequence, central Honshu, Japan, Tohoku Univ. Sci. Rep. 2nd Ser. (Geol.), 48, 1–72, 1977.
- Ogg, J. G., Ogg, G. M., and Gradstein, F. M.: Neogene, in: A Concise Geologic Time Scale, edited by: Ogg, J. G., Ogg, G. M., and Gradstein, F. M., Elsevier, Amsterdam, 201–203, 2016.
- Orr, W. N. and Jenkins, D. G.: Eastern Equatorial Pacific Pliocene-Pleistocene Biostratigraphy, in Studies in Marine Micropaleontology and Paleocology, a Memorial Volume to Orville L. Bandy, edited by: Sliter, W. V., Cushman Foundation Special Publication, 19, 278–286, 1980.
- Parker, F. L.: A new planktonic species (Foraminiferida) from the Pliocene of Pacific Deep-Sea cores, Contributions from the Cushman Foundation for Foraminiferal Research, 16, 151–153, 1965.
- Pearson, P. N.: Planktonic foraminifer biostratigraphy and the development of pelagic caps on guyots in the Marshall Islands group, Proc. ODP Sci. Res., 144, 21–59, <https://doi.org/10.2973/odp.proc.sr.144.013.1995>, 1995.
- Pearson, P. N.: Evolutionary concepts in biostratigraphy, in: Unlocking the Stratigraphical Record, edited by: Doyle, P. and Bennett, M. R., John Wiley and Sons, Ltd., 123–144, 1998.
- Pearson, P. N.: Age model tie points and micropalaeontological data for International Ocean Discovery Program Hole U1488A, southern part of the Eauripik Rise, Pacific Ocean, NERC EDS National Geoscience Data Centre [data set], <https://doi.org/10.5285/14fb1745-00ed-4a0d-922b-d2c94157d17f>, 2023.
- Pearson, P. N. and Penny, L.: Coiling directions in the planktonic foraminifer *Pulleniatina*: A complex eco-evolutionary dynamic spanning millions of years, PLoS one, 16, e0249113, <https://doi.org/10.1371/journal.pone.0249113>, 2021.

- Perembo, R. B.: Miocene to Pliocene planktonic foraminifers from the North Aoba Basin, Site 832, Proc. ODP Sci. Res., 134, 247–263, <https://doi.org/10.2973/odp.proc.sr.134.010.1994>, 1994.
- Podder, R. S. I. S., Gupta, A. K., and Clemens, S.: Surface paleoceanography of the eastern equatorial Indian Ocean since the latest Miocene: Foraminiferal census and isotope records from ODP Hole 758A, Palaeogeogr. Palaeoclimatol., 579, 110617, <https://doi.org/10.1016/j.palaeo.2021.110617>, 2021.
- Poole, C. R. and Wade, B. S.: Systematic taxonomy of the *Trilobatus sacculifer* plexus and descendant *Globigerinoidesella fistulosa* (planktonic foraminifera), J. Syst. Palaeontol., 17, 1989–2030, <https://doi.org/10.1080/14772019.2019.1578831>, 2019.
- Prell, W. L. and Damuth, J. E.: The climate-related diachronous disappearance of *Pulleniatina obliquiloculata* in late Quaternary sediments of the Atlantic and Caribbean, Mar. Micropaleontol., 3, 267–277, 1978.
- Premoli Silva, I., Castradori, D., and Spezzaferri, S.: Calcareous nannofossil and planktonic foraminifer biostratigraphy of Hole 810C (Shatsky Rise, Northwestern Pacific), Proc. ODP Sci. Res., 132, 15–36, <https://doi.org/10.2973/odp.proc.sr.132.305.1993>, 1993.
- Raffi, I., Wade, B., and Pälike, H.: The Neogene Period, in: Geologic Time Scale 2020, edited by: Gradstein, F. M., Ogg, J. G., Scmitz, M. D., and Ogg, G. M., Elsevier, 1141–1215, <https://doi.org/10.1016/B978-0-12-824360-2.00029-2>, 2020.
- Resig, J. M., Frost, G. M., Ishikawa, N., and Perembo, R. C.: Micropalaeontological and palaeomagnetic approaches to stratigraphic anomalies in rift basins: ODP Site 1109, Woodlark Basin, Geol. Soc. Lond. Spec. Publ., 187, 389–404, 2001.
- Ride, W. D. L., Cogger, H. G., Dupuis, C., Kraus, O., Minelli, A., Thompson, F. C., and Tubbs, P. K. (Eds.): The International Code of Zoological Nomenclature, 4th Edn., International Commission on Zoological Nomenclature, ISBN 0 85301 006 4, 2000.
- Romer, A. S.: Darwin and the fossil record, in: A Century of Darwin, edited by: Barnett, S. A. and Gosner, K. L., American Museum of Natural History, 1959.
- Romine, K.: Planktonic foraminifers from Oligocene to Pleistocene sediments, Deep-sea Drilling Project Leg-92, Initial Rep. Deep Sea, 92, 291–297, <https://doi.org/10.2973/dsdp.proc.92.111.1986>, 1986.
- Rosenthal, Y., Holbourn, A. E., Kulhanek, D. K., Aiello, I. W., Babilala, T. L., Bayon, G., Beaufort, L., Bova, S. C., Chun, J.-H., Dang, H., Drury, A. J., Dunkley Jones, T., Eichler, P. P. B., Fernando, A. G. S., Gibson, K., Hatfield, R. G., Johnson, D. L., Kumagai, Y., Li, T., Linsley, B. K., Meinicke, N., Mountain, G. S., Opdyke, B. N., Pearson, P. N., Poole, C. R., Ravelo, A. C., Sagawa, T., Schmitt, A., Wurtzel, J. B., Xu, J., Yamamoto, M., and Zhang, Y. G.: Site U1482, in: Western Pacific Warm Pool, edited by: Rosenthal, Y., Holbourn, A. E., and Kulhanek, D. K., Proceedings of the International Ocean Discovery Program, 363, <https://doi.org/10.14379/iodp.proc.363.103.2018>, 2018a.
- Rosenthal, Y., Holbourn, A. E., Kulhanek, D. K., Aiello, I. W., Babilala, T. L., Bayon, G., Beaufort, L., Bova, S. C., Chun, J.-H., Dang, H., Drury, A. J., Dunkley Jones, T., Eichler, P. P. B., Fernando, A. G. S., Gibson, K., Hatfield, R. G., Johnson, D. L., Kumagai, Y., Li, T., Linsley, B. K., Meinicke, N., Mountain, G. S., Opdyke, B. N., Pearson, P. N., Poole, C. R., Ravelo, A. C., Sagawa, T., Schmitt, A., Wurtzel, J. B., Xu, J., Yamamoto, M., and Zhang, Y. G.: Site U1483, in: Western Pacific Warm Pool, edited by: Rosenthal, Y., Holbourn, A. E., and Kulhanek, D. K., Proceedings of the International Ocean Discovery Program, 363, <https://doi.org/10.14379/iodp.proc.363.104.2018>, 2018b.
- Rosenthal, Y., Holbourn, A. E., Kulhanek, D. K., Aiello, I. W., Babilala, T. L., Bayon, G., Beaufort, L., Bova, S. C., Chun, J.-H., Dang, H., Drury, A. J., Dunkley Jones, T., Eichler, P. P. B., Fernando, A. G. S., Gibson, K., Hatfield, R. G., Johnson, D. L., Kumagai, Y., Li, T., Linsley, B. K., Meinicke, N., Mountain, G. S., Opdyke, B. N., Pearson, P. N., Poole, C. R., Ravelo, A. C., Sagawa, T., Schmitt, A., Wurtzel, J. B., Xu, J., Yamamoto, M., and Zhang, Y. G.: Site U1486, in: Western Pacific Warm Pool, edited by: Rosenthal, Y., Holbourn, A. E., and Kulhanek, D. K., Proceedings of the International Ocean Discovery Program, 363, <https://doi.org/10.14379/iodp.proc.363.107.2018>, 2018c.
- Rosenthal, Y., Holbourn, A. E., Kulhanek, D. K., Aiello, I. W., Babilala, T. L., Bayon, G., Beaufort, L., Bova, S. C., Chun, J.-H., Dang, H., Drury, A. J., Dunkley Jones, T., Eichler, P. P. B., Fernando, A. G. S., Gibson, K., Hatfield, R. G., Johnson, D. L., Kumagai, Y., Li, T., Linsley, B. K., Meinicke, N., Mountain, G. S., Opdyke, B. N., Pearson, P. N., Poole, C. R., Ravelo, A. C., Sagawa, T., Schmitt, A., Wurtzel, J. B., Xu, J., Yamamoto, M., and Zhang, Y. G.: Site U1487, in: Western Pacific Warm Pool, edited by: Rosenthal, Y., Holbourn, A. E., and Kulhanek, D. K., Proceedings of the International Ocean Discovery Program, 363, <https://doi.org/10.14379/iodp.proc.363.108.2018>, 2018d.
- Rosenthal, Y., Holbourn, A. E., Kulhanek, D. K., Aiello, I. W., Babilala, T. L., Bayon, G., Beaufort, L., Bova, S. C., Chun, J.-H., Dang, H., Drury, A. J., Dunkley Jones, T., Eichler, P. P. B., Fernando, A. G. S., Gibson, K., Hatfield, R. G., Johnson, D. L., Kumagai, Y., Li, T., Linsley, B. K., Meinicke, N., Mountain, G. S., Opdyke, B. N., Pearson, P. N., Poole, C. R., Ravelo, A. C., Sagawa, T., Schmitt, A., Wurtzel, J. B., Xu, J., Yamamoto, M., and Zhang, Y. G.: Site U1488, in: Western Pacific Warm Pool, edited by: Rosenthal, Y., Holbourn, A. E., and Kulhanek, D. K., Proceedings of the International Ocean Discovery Program, 363, <https://doi.org/10.14379/iodp.proc.363.109.2018>, 2018e.
- Rosenthal, Y., Holbourn, A. E., Kulhanek, D. K., Aiello, I. W., Babilala, T. L., Bayon, G., Beaufort, L., Bova, S. C., Chun, J.-H., Dang, H., Drury, A. J., Dunkley Jones, T., Eichler, P. P. B., Fernando, A. G. S., Gibson, K., Hatfield, R. G., Johnson, D. L., Kumagai, Y., Li, T., Linsley, B. K., Meinicke, N., Mountain, G. S., Opdyke, B. N., Pearson, P. N., Poole, C. R., Ravelo, A. C., Sagawa, T., Schmitt, A., Wurtzel, J. B., Xu, J., Yamamoto, M., and Zhang, Y. G.: Site U1489, in: Western Pacific Warm Pool, edited by: Rosenthal, Y., Holbourn, A. E., and Kulhanek, D. K., Proceedings of the International Ocean Discovery Program, 363, <https://doi.org/10.14379/iodp.proc.363.110.2018>, 2018f.
- Rosenthal, Y., Holbourn, A. E., Kulhanek, D. K., Aiello, I. W., Babilala, T. L., Bayon, G., Beaufort, L., Bova, S. C., Chun, J.-H., Dang, H., Drury, A. J., Dunkley Jones, T., Eichler, P. P. B., Fernando, A. G. S., Gibson, K., Hatfield, R. G., Johnson, D. L., Kumagai, Y., Li, T., Linsley, B. K., Meinicke, N., Mountain, G. S., Opdyke, B. N., Pearson, P. N., Poole, C. R., Ravelo, A. C., Sagawa, T., Schmitt, A., Wurtzel, J. B., Xu, J., Yamamoto, M., and Zhang, Y. G.: Site U1490, in: Western Pacific Warm Pool, edited by: Rosenthal, Y., Holbourn, A. E., and Kulhanek, D. K., Proceedings of the International Ocean Discovery Program, 363, <https://doi.org/10.14379/iodp.proc.363.111.2018>, 2018g.

- Routledge, C., Kulhanek, D. K., Tauxe, L., Singh, A. D., Steinke, S., Griffith, E., and Saraswat, R.: A revised chronostratigraphic framework for International Ocean Discovery Program Expedition 355 sites in Laxmi Basin, eastern Arabian Sea, *Geol. Mag.*, 157, 961–978, <https://doi.org/10.1017/s0016756819000104>, 2020.
- Sager, W. W., Polgreen, E.K., and Rack, F. R.: Magnetic polarity reversal stratigraphy of Hole 810C, Shatsky Rise, Western Pacific Ocean, *Proc. ODP Sci. Res.*, 132, 47–55, <https://doi.org/10.2973/odp.proc.sr.132.304.1993>, 1993.
- Saito, T.: Geologic significance of coiling direction in the planktonic foraminifera *Pulleniatina*, *Geology*, 4, 305–309, 1976.
- Saito, T.: Planktonic foraminiferal biostratigraphy of Eastern Equatorial Pacific sediments, Deep-sea Drilling Project Leg-85, Initial Rep. Deep Sea, 85, 621–653, <https://doi.org/10.2973/dsdp.proc.85.116.1985>, 1985.
- Saito, T., Burckle, L. H., and Hays, J. D.: Late Miocene to Pleistocene biostratigraphy of equatorial Pacific sediments, in: Late Neogene epoch boundaries, edited by: Saito, T. and Burckle, L. H., American Museum of Natural History, New York, 226–244, 1975.
- Salvador, A.: International Stratigraphic Guide: A Guide to Stratigraphic Classification, Terminology, and Procedure, Geological Society of America, 1994.
- Schiebel, R. and Hemleben, C.: Planktic foraminifers in the Modern Ocean, Berlin, Springer, 358 pp., ISBN 978-3-662-50297-6, 2017.
- Schmidt, D. N.: The closure history of the Central American seaway: evidence from isotopes and fossils to models and molecules, in: Deep-Time Perspectives on Climate Change: Marrying the Signal from Computer Models to Biological Proxies, edited by: Williams, M., Haywood, A. M., Gregory, F. J., and Schmidt, D. N., The Micropalaeontological Society, 429–444, 2007.
- Serrano, F., González-Donoso, J. M., Palmqvist, P., Guerra-Merchán, A., Linares, D., and Pérez-Claros, J. A.: Estimating Pliocene sea-surface temperatures in the Mediterranean: An approach based on the modern analogs technique, *Palaeogeogr. Palaeoclimatol.*, 243, 174–188, <https://doi.org/10.1016/j.palaeo.2006.07.012>, 2007.
- Shackleton, N. J., Berger, A., and Peltier, W. R.: An alternative astronomical calibration of the lower Pleistocene timescale based on ODP Site 677, *T. Roy. Soc. Edin.-Earth*, 81, 251–261, 1990.
- Shackleton, N. J., Crowhurst, S., Hagelberg, T., Pisias, N. G., and Schneider, D. A.: A new late Neogene time scale: application to Leg 138 sites. *Proc ODP Sci Res*, 138, 73–101, <https://doi.org/10.2973/odp.proc.sr.138.106.1995>, 1995.
- Shipboard Scientific Party: Site 62, Initial Rep. Deep Sea, 7, 49–322, <https://doi.org/10.2973/dsdp.proc.7.104.1971>, 1971.
- Shipboard Scientific Party: Site 77, Initial Rep. Deep Sea, 9, 43–208, <https://doi.org/10.2973/dsdp.proc.7.104.1971>, 1972.
- Shipboard Scientific Party: Site 926, Proc. ODP Init. Repts., 154, 153–232, <https://doi.org/10.2973/odp.proc.ir.154.105.1995>, 1995a.
- Shipboard Scientific Party: Site 927, Proc. ODP Init Repts., 154, 233–279, <https://doi.org/10.2973/odp.proc.ir.154.106.1995>, 1995b.
- Shipboard Scientific Party: Site 928, Proc. ODP Init Repts., 154, 281–336, <https://doi.org/10.2973/odp.proc.ir.154.107.1995>, 1995c.
- Shipboard Scientific Party: Site 929, Proc. ODP Init Repts., 154, 337–471, <https://doi.org/10.2973/odp.proc.ir.154.108.1995>, 1995d.
- Shipboard Scientific Party: Site 1143, Proc. ODP Init Repts., 184, 1–103, <https://doi.org/10.2973/odp.proc.ir.184.104.2000>, 2000.
- Siccha, M. and Kucera, M.: ForCenS, a curated database of planktonic foraminifera census counts in marine surface sediment samples, *Sci. Data*, 4, 1–12, 2017.
- Sijinkumar, A. V., Nagender Nath, B., Possnert, G., and Aldahan, A.: *Pulleniatina* Minimum Events in the Andaman Sea (NE Indian Ocean): Implications for winter monsoon and thermocline changes, *Mar. Micropaleontol.*, 81, 88–94, 2011.
- Singh, A. D.: *Neoglobobulimina*, *Pulleniatina* and *Sphaeroidinella-Sphaeroidinellopsis* lineages in the northern Indian Ocean: Their Paleooceanographic relations and biostratigraphic significance, *J. Geol. Soc. Ind.*, 46, 163–175, 1995.
- Singh, A., Sinha, D., Mallick, K., Singh, P., and Shrivastava, A.: Diachronism in Late Neogene-Quaternary planktic foraminiferal events in Northern and Eastern Indian Ocean: Palaeoceanographic implications, *J. Paleaeontol. Soc. Ind.*, 66, 357–374, 2021.
- Sinha, D. K. and Singh, A. K.: Late Neogene planktic foraminiferal biochronology of the ODP Site 763A, Exmouth Plateau, south-east Indian Ocean, *J. Foramin. Res.*, 38, 251–270, 2008.
- Smith, L. A. and Beard, J. H.: The Late Neogene of the Gulf of Mexico, Initial Rep. Deep Sea, 10, 643–667, <https://doi.org/10.2973/dsdp.proc.10.125.1973>, 1973.
- Srinivasan, M. S. and Kennett, J. P.: A review of Neogene planktonic foraminiferal biostratigraphy: applications in the equatorial and south Pacific, in: The Deep Sea Drilling Project: A Decade of Progress, edited by: Warne, J. E., Douglas, R. G., and Winterer, E. L., SEPM Special Publication 32, <https://doi.org/10.2110/pec.81.32.0395>, 1981.
- Srinivasan, M. S. and Sinha, D. K.: Improved correlation of the late Neogene planktonic foraminiferal datums in the equatorial to cool subtropical DSDP sites, southwest Pacific: application of the graphic correlation method, *Geol. Soc. Ind. Mem.*, 20, 55–93, 1991.
- Srinivasan, M. S. and Chaturvedi, S. N.: Neogene planktonic foraminiferal biochronology of the DSDP sites along the Ninetyeast Ridge, northern Indian Ocean, in: Centenary of Japanese Micropaleontology, edited by: Ishizaki, K. and Daito, T., Terra Scientific, 175–178, 1992.
- Srinivasan, M. S. and Sinha, D. K.: Late Neogene planktonic foraminiferal events of the southwest Pacific and Indian Ocean: a comparison, in: Pacific Neogene: Environment, Evolution and Events, edited by: Tsuchi, R. and Ingle Jr., J. C., University of Tokyo Press, 203–220, 1992.
- Srinivasan, M. S. and Sinha, D.: Early Pliocene closing of the Indonesian Seaway: evidence from north-east Indian Ocean and Tropical Pacific deep sea cores, *J. Asian Earth Sci.*, 16, 29–44, 1998.
- Srinivasan, M. S. and Sinha, D.: Ocean circulation in the tropical Indo-Pacific during early Pliocene (5.6–4.2 Ma): Paleobiogeographic and isotopic evidence, *Proc. Ind. Acad. Sci.*, 109, 315–328, 2000.

- Subbotina, N.: Iskopaemye foraminifery SSSR (Globigerinidy, Khantkeninidy i Globorotaliidy) [Fossil foraminifera of the USSR, Globigerinidae, Hantkeninidae and Globorotaliidae], Trudy Vsesoyuznogo Neftyanogo Nauchno-Issledovatel'skogo Geologo-Razvedochnogo Instituta (VNIGRI), 76, 1–296, 1953.
- Tang, C.: Paleomagnetism of Cenozoic sediments in Holes 762B and 763A, central Exmouth Plateau, Northwest Australia, Proc. ODP Sci. Res., 122, 717–733, <https://doi.org/10.2973/odp.proc.sr.122.153.1992>, 1992.
- Tauxe, L., Valet, J.-P., and Bloemendal, J.: Magnetostratigraphy of Leg 108 Advanced Hydraulic Piston Cores, Proc. ODP Sci. Res., 108, 429–439, <https://doi.org/10.2973/odp.proc.sr.108.154.1989>, 1989.
- Thompson, P. R. and Sciarrillo, J. R.: Planktonic foraminiferal biostratigraphy in the equatorial Pacific, Nature, 276, 29–33, 1978.
- Thunell, R. C.: Pliocene-Pleistocene paleotemperature and paleosalinity history of the Mediterranean Sea: Results from DSDP Sites 125 and 132, Mar. Micropaleontol., 4, 173–187, 1979.
- Tian, J., Ma, X., Zhou, J., Jiang, X., Lyle, N., Shackford, J., and Wilkens, R.: Paleoceanography of the east equatorial Pacific over the past 16 Myr and Pacific–Atlantic comparison: High resolution benthic foraminiferal $\delta^{18}\text{O}$ and $\delta^{13}\text{C}$ records at IODP Site U1337, Earth Planet. Sc. Lett., 499, 185–196, <https://doi.org/10.1016/j.epsl.2018.07.025>, 2018.
- Toue, R., Fujita, K., Tsuchiya, M., Chikaraishi, Y., Sasaki, Y., and Ohkouchi, N.: Trophic niche separation of two non-spinose planktonic foraminifera *Neogloboquadrina dutertrei* and *Pulleniatina obliquiloculata*, Prog. Earth Planet. Sc., 9, 1–11, <https://doi.org/10.1186/s40645-022-00478-3>, 2022.
- Ujjié, Y. and Ishitani, Y.: Evolution of a planktonic foraminifer during environmental changes in the tropical oceans, PLoS One, 11, e0148847, <https://doi.org/10.1371/journal.pone.0148847>, 2016.
- Ujjié, Y., Asami, T., de Garidel-Thoron, T., Liu, H., Ishitani, Y., and de Vargas, C.: Longitudinal differentiation among pelagic populations in a planktic foraminifer, Ecol. Evol., 2, 1725–1737, <https://doi.org/10.1002/ece3.286>, 2012.
- Van Gorsel, J. T. and Troelstra, S. R.: Late Neogene planktonic foraminiferal biostratigraphy and climatostratigraphy of the Solo River section (Java, Indonesia), Mar. Micropaleontol., 6, 183–209, [https://doi.org/10.1016/0377-8398\(81\)90005-0](https://doi.org/10.1016/0377-8398(81)90005-0), 1981.
- Wade, B. S., Pearson, P. N., Berggren, W. A., and Pälike, H.: Review and revision of Cenozoic tropical planktonic foraminiferal biostratigraphy and calibration to the geomagnetic polarity and astronomical time scale, Earth-Sci. Rev., 104, 111–142, <https://doi.org/10.1016/j.earscirev.2010.09.003>, 2011.
- Wade, B. S., Premek Fucek, V., Kamikuri, S., Bartol, M., Luciani, V., and Pearson, P. N.: Successive extinctions of muricate planktonic foraminifera (*Morozovelloides* and *Acarinina*) as a candidate for marking the base Priabonian, Newsl. Stratigr., 45, 245–262, <https://doi.org/10.1127/0078-0421/2012/0023>, 2012.
- Wang, J., Chang, F., Li, T., Sun, H., Cui, Y., and Liu, T.: The evolution of the Kuroshio Current over the last 5 million years since the Pliocene: Evidence from planktonic foraminiferal faunas, Sci China Earth Sci., 63, 1714–1729, <https://doi.org/10.1007/s11430-019-9641-9>, 2020.
- Weaver, P. P. E. and Raymo, M. E.: Late Miocene to Holocene planktonic foraminifera from the Equatorial Atlantic, Leg 108, Proc. ODP Sci. Res., 108, 71–91, <https://doi.org/10.2973/odp.proc.sr.108.130.1989>, 1989.
- Wilkens, R. H., Dickens, G. R., Tian, J., Backman, J., and the Expedition 320/321 Scientists: Data Report: revised composite depth scales for Sites U1336, U1337, and U1338, Proceedings of the International Ocean Discovery Program, 320/321, <https://doi.org/10.2204/iodp.proc.320321.209.2013>, 2013.
- Wilkens, R. H., Westerhold, T., Drury, A. J., Lyle, M., Gorgas, T., and Tian, J.: Revisiting the Ceara Rise, equatorial Atlantic Ocean: isotope stratigraphy of ODP Leg 154 from 0 to 5 Ma, Clim. Past, 13, 779–793, <https://doi.org/10.5194/cp-13-779-2017>, 2017.
- Zenetos, A., Meriç, E., Verlaque, M., Galli, P., Boudouresque, C.-F., Giangrande, A., Çinar, M. E., and Bilecenoglu, M.: Additions to the annotated list of marine alien biota in the Mediterranean with special emphasis on Foraminifera and Parasites, Mediterr. Mar. Sci., 9, 119–166, <https://doi.org/10.12681/mms.146>, 2008.